DESIGN AND DEVELOPMENT OF A CONTINUOUS PRECAST PRESTRESSED CONCRETE BRIDGE SYSTEM FOR THE MULTIMODAL FREIGHT SHUTTLE PROJECT

A Thesis

by

ANAGHA SURESHKUMAR PARKAR

Submitted to the Office of Graduate Studies of
Texas A&M University
in partial fulfillment of the requirements for the degree of

MASTER OF SCIENCE

May 2011

Major Subject: Civil Engineering

DESIGN AND DEVELOPMENT OF A CONTINUOUS PRECAST PRESTRESSED CONCRETE BRIDGE SYSTEM FOR THE MULTIMODAL FREIGHT SHUTTLE PROJECT

A Thesis

by

ANAGHA SURESHKUMAR PARKAR

Submitted to the Office of Graduate Studies of
Texas A&M University
in partial fulfillment of the requirements for the degree of

MASTER OF SCIENCE

Approved by:

Co-Chairs of Committee,	John Mander
	Luciana Barroso
Committee Member,	Mohammed Haque
Head of Department,	John Niedzwecki

May 2011

Major Subject: Civil Engineering

ABSTRACT

Design and Development of a Continuous Precast Prestressed Concrete Bridge System for the Multimodal Freight Shuttle Project. (May 2011)

Anagha Sureshkumar Parkar, B.E., Mumbai University, Mumbai

Co- Chairs of Advisory Committee: Dr. John Mander
Dr. Luciana Barroso

The growth of freight transportation within the United States and across borders is tremendous, and it is expected to double over the next decade. The congestion due to increasing pressure of the freight, mainly transported by truck, is affecting the safety and serviceability of the existing transportation system. The proposed Multimodal Freight Shuttle (MFS) system offers a cost-effective and environmentally friendly method to transport containerized, intercity or port-to-terminal freight, and it alleviates the problem of severe deterioration of the outgrown capacity of existing highways. The Multimodal Freight Shuttle (MFS) system requires a continuous elevated guideway to be constructed for the freight shuttle. This research investigates the viability of a continuous precast bridge system for the freight shuttle. A number of design alternatives for the various bridge components are provided, and the merits of the different types are assessed from design, construction, in-service performance and life-cycle cost points-of-view.

Based on the comparative designs, it was found that a bridge system built of fully precast components is the most promising. This included a combination of precast prestressed concrete trough-girders, with a modular precast concrete sub-structure. Due

to the significant length of the proposed structural system, the construction sequence is important so that the progress can be made to enable the work force to advance by one span per day. Thus, the steps for construction of the bridge have been schematically presented and sequentially explained.

DEDICATION

I dedicate this thesis to my parents, Sureshkumar Parkar and Sunita Parkar.

ACKNOWLEDGEMENTS

I would like to gratefully acknowledge the invaluable guidance and support received from my advisor, Dr. John Mander. I would also like to thank Dr. Steve Roop from Texas Transportation Institute for giving me the opportunity to work on this prestigious project and for providing all the necessary funding, data and specifications of the project.

This project is a joint effort by me and my research partner, Ms. Subha Lakshmi Roy. I would like to acknowledge her contribution towards this project and thank her for making the work experience more enjoyable and balanced.

I would like to thank Dr. Luciana Barroso from the Civil Engineering Department and Dr. Mohammad Haque from the Construction Science Department, for serving on my committee and providing their support and professional advice. I take this opportunity to thank the Department faculty and staff for making my time at Texas A&M University an enriching experience.

Finally, I would like to thank all of my family and friends for their constant moral support and love, making this whole journey enjoyable and successful.

NOMENCLATURE

AASHTO	American Association of State Highway Transportation Officials
ACI	American Concrete Institute
AREMA	American Railway Engineering and Maintenance-of-Way Association
ASTM	American Society for Testing and Materials
CARD	Control and Repairability Damage
CIP	Cast-in-place
DAD	Damage Avoidance Design
DBE	Design Basis Earthquake
DC	Dead load of structural components and nonstructural attachments
E_c	Modulus of Elasticity of concrete
E_s	Modulus of Elasticity of steel
FHWA	Federal Highway Administration
f'_c	Concrete Compressive Strength
f_y	Reinforcement Yield Stress
IM	Vehicular dynamic load allowance
LL	Vehicular Live Load
LRFD	Load and Resistance Factor Design
PCBT	Pretensioned Precast Bulb T
PCI	Precast Concrete Institute

SIP	Stay-in-place
TTI	Texas Transportation Institute
TxDOT	Texas Department of Transportation
MFS	Multimodal Freight Shuttle
NCHRP	National Cooperative Highway Research Program
NU	University of Nebraska

TABLE OF CONTENTS

CHAPTER Page

Page

LIST OF FIGURES

Page

LIST OF TABLES

CHAPTER I

INTRODUCTION

1.1 Background

The nation's highways of present day world are becoming increasingly congested with short to medium haul trucking activities. It is not feasible to transport most of this tonnage by the railroads for two reasons. First, their network is not extensive enough to alleviate this congestion, and second rail transport is most economical over long distances. An alternative medium haul transportation system has been proposed by TTI called the *Multimodal Freight Shuttle System (MFS)*.

The 21st century faces a large amount of crisis in the transportation sector due to the increased demand for transportation services. An enormous quantity of goods and freight flow occurs from the manufacturers to the customers between the three trading partners, Canada, Mexico and United States across the borders. This amplified amount of container trucks on the highways is causing deterioration in the highway infrastructure by increasing the wear and tear, congestion and environmental pollution (Roop et al., 2005).

Highway expansion does not prove to be an effective solution for these problems since this expanded capacity will again add more trucks on the highways and boost the deteriorating conditions. To meet the high-reliability demands of the transportation

---

This thesis follows the style of *Journal of Structural Engineering*.

sector, Texas Transportation Institute (TTI) proposes to build a cost-effective and green solution- The Multimodal Freight Shuttle (MFS) system. The MFS addresses the constraints of the existing railroad and trucking system and aims to build a more technologically and environmentally efficient system giving simultaneous attention to the reduction of wear, increased safety and capacity. The MFS offers a new method to transport containerized, intercity or port-to-terminal freight. It consists of electrically powered vehicles propelled by linear induction motors that run on a specialized, derailment-proof elevated guide way from ports to terminals at highway speeds with the use of an automated control system. This will help in separating freight traffic from the passenger traffic on existing highways. The system could potentially run for several thousand miles across Texas and neighboring areas (Roop et al., 2005).

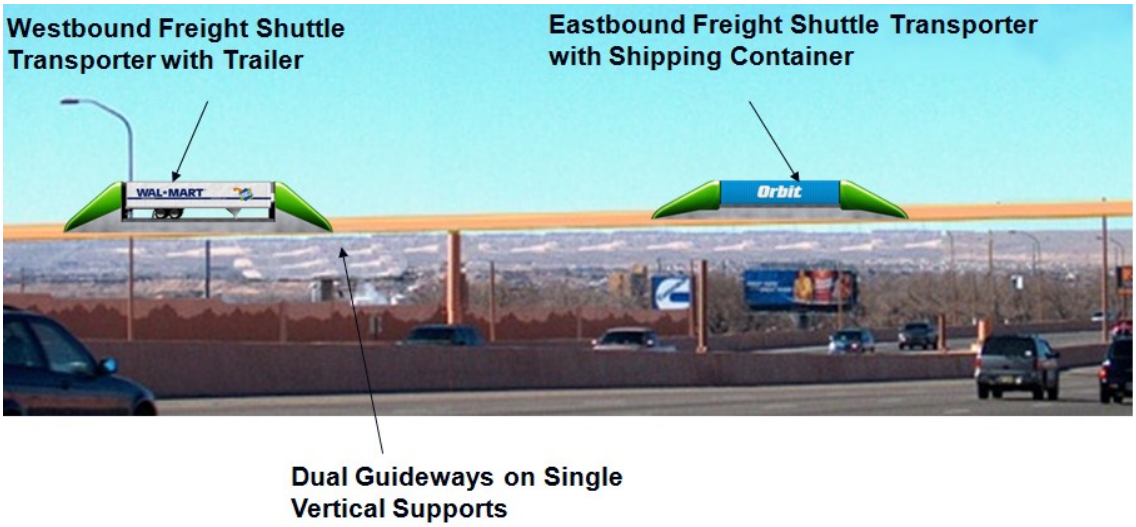

Figure 1 - Multimodal Freight Shuttle System by TTI (Roop et al., 2005)

The major reasons for choosing an elevated guideway system:-

- The concept will enable a smaller footprint on the ground
- Can be run along or near an existing right-of-way, such as a highway or railway.
- Allow movement beneath it. The guideway can be built over privately owned land with farmers able to continue their operations unimpeded.
- The elevated system will also ensure a greater security control.

Figure 2 shows a view of the proposed elevated guideway system.

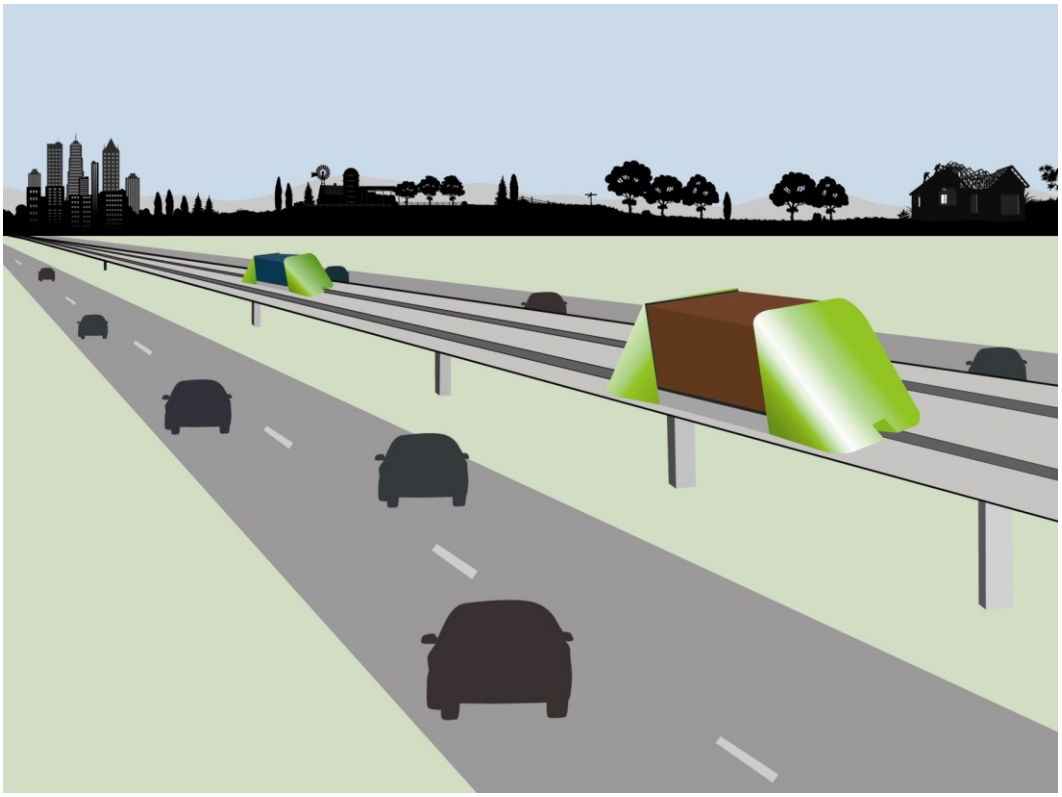

Figure 2 - Elevated Guideway System on Existing Rights-of-way
(Roop et al., 2005)

A key to the success of the MFS is the development of a very long continuous viaduct system. Bridge construction has evolved over the years from cast-in-place structures to precast concrete structures. Construction techniques have also improved through increased mechanization and refined to meet the growing needs of the present infrastructure. Prestressed concrete bridges have become the most popular due to their low maintenance, durability, long span capability and their general life cycle cost effectiveness. While there are many different approaches to constructing concrete bridges, the type required for MFS project needs to permit rapid construction over a very long work face. Thus a fully precast modular system is a natural choice for this project.

1.2 Research Objective and Scope

The goal of the Multimodal Freight Shuttle (MFS) project is to develop an elevated, continuous precast prestressed concrete bridge system for the known loadings and operational dynamics of the freight shuttle vehicles.

The main goals are:

- Overall low life cycle cost
- Provide a cost effective solution for mass construction over thousands of spans of bridge extent
- Easy and rapid construction over a variety of different terrain types.
- Modular simplicity
- Limited impact on surrounding infrastructure
- High durability and long term serviceability

- Ability to easily repair, dismantle and reuse- if necessary

1.3 Research Methodology

The research methodology has been based on the following conceptual framework:

(a) Literature review - A literature review has been done on the various existing methodologies of bridge design and construction. They have been studied from a perspective to integrate the conventional practices with the proposed method of design and construction.

(b) Formulation of critical design parameters

(c) Formulation of critical design issues including adoption of new techniques

(d) Formulation of critical construction issues including the expansive massive construction

(e) Detailed design calculations and drawings – The detailed design calculations have been presented for the proposed design and are further illustrated using detailed drawings of the bridge design.

1.4 Organization of Thesis

The thesis have been organized in several chapters discussing the analysis, design and comparison of design methodologies of the various bridge components consisting of the precast deck slab, the prestressed concrete girders and the pier design.

Chapter I presents the background of this research, the research objectives and methodology and also what particularly is new to this research.

Chapter II gives a literature review of the previous research and the conventional design practices being practiced for the design of the various bridge components.

Chapter III gives the analysis and design approach of the precast deck slab panels for long and continuous spans.

Chapter IV presents the analysis and design approach of the precast prestressed concrete girders and the truss modeling approach for design of shear connectors.

Chapter V presents the analysis and design of precast concrete bridge piers.

Chapter VI shows light on the construction steps and sequences for the design presented.

Chapter VII presents conclusions drawn from this work and some recommendations for future work.

1.5 What Particularly Is New in This Thesis?

The primary aim of this research is to develop a pioneer methodology for the design and construction of a very long multi-span continuous precast, prestressed concrete viaduct system for the Multimodal Freight Shuttle project. This project aims to build a bridge system which may extend to several thousand miles of area across Texas crossing national borders making it to be one of the longest bridges in the world. To facilitate this large-scale construction, it is of prime importance to optimize the various bridge components to economize the manufacture of the repetitive units. Thus, the

superstructure and the substructure designs have been aimed at a viable economical solution integrating the design requirements with the constructability options.

The Freight Shuttle System is an automated control system which will help in separating freight traffic from the passenger traffic on existing highways. The requirement of this project is a deviation from the conventional railways and highways design and construction. Thus the best practices and design specifications provided by the AASHTO (*American Association of State Highway Transportation Officials*), AREMA (*American Railway Engineering and Maintenance-of-Way Association*) and ACI (*American Concrete Institute*) Committee 318 (2008) have been aptly chosen and combined to suit the needs of this project.

Yield line theory has been used for the analysis of the continuous precast bridge deck slab which is based on the concept of determining the ultimate load capacity of the reinforced concrete slab by assuming a collapse mechanism defined by a pattern of yield lines depicting the yielding of the reinforcement in the slab. The conventional elastic method of analysis of a slab does not determine the ultimate load carrying capacity of a slab. The traditional TxDOT U54 girders have a maximum span of 120 ft. (Hueste et al., 2006) whereas the optimal cross section of the trough girder has been designed for span lengths of 140 ft. taking into account all serviceability criteria. The continuous spliced precast prestressed concrete trough girder sections have been designed using a modified design approach for the extended span length.

External post-tensioning is used to strengthen the trough girders. It helps in easy installation of the tendons and reduced or no interruptions to the regular function of the

structure. This is a deviation from the commonly used practices in Texas where post tensioning is done using internally bonded tendons. This allows for ease in inspection of loss of stress and damage in tendons due to impact or corrosion and also allows for replacement of tendons if required due to creep, relaxation or corrosion. The tendons can also be replaced in future for additional strengthening if necessary. Moreover the friction losses with external tendons will be less than internal bonded tendons, thus these external tendons can be provided in greater lengths and greater deviation angles. Anchorages and deviators can be easily installed.

The Damage Avoidance Design (DAD) by Mander and Cheng (1997) based on the dissipation of seismic energy by rocking of the pier is found to be a more effective solution compared to the conventional pier design. The joints have been specially detailed eliminating the formation of the plastic hinge. The post-tensioning contributes to the moment capacity of the columns and thus reduces the requirement of longitudinal mild steel reinforcement than if it was designed using the conventional method of design practice. Moreover the Dywidag bars provide stiffness and as a means of anchoring the structure to the ground and thus increasing its lateral capacity in earthquakes. The energy dissipation devices used provided additional lateral resistance. A DAD pier is recommended to be used for the particular bridge structure since it reduces a major financial loss due to repair and replacement of the damaged pier and closure time of traffic during the repair. Thus the damage caused to the plastic hinge zone during a severe earthquake which cannot be repaired in a conventional pier is overcome in a Damage Avoidance Design (Solberg et al., 2009).

CHAPTER II

LITERATURE REVIEW

2.1 Motivation for Constructing Precast Prestressed Concrete Bridges

Enormous amount of traffic and congestion across the urban areas as well as waterways demands for the employment of long span bridges. Precast prestressed concrete bridges are one of the most common solutions to bridge construction because of their durability, relatively low cost, modular construction method and general availability of materials. A large number of bridges in the United States and particularly in Texas have been constructed over the years using cast-in-place and precast prestressed concrete. The construction of bridges using precast or prefabricated elements facilitates ease of construction by minimizing traffic disruption and the on-site time to completion of project delivery. Less on-site labor increases the safety in the work area and also reduces the environmental impact. The precast concrete elements are manufactured in a quality controlled environment in the precasting plant which facilitates the repetition of the elements for mass production. Moreover, steel formwork can be retained and reused over a long duration. Excellent durability of precast elements also minimizes life cycle costs. The major job site constraints like the high elevations, stretches over water bodies, heavy traffic in and around the area, can be overcome by using the prefabricated precast prestressed concrete construction.

This chapter addresses the current state-of-the-art and practice for precast deck panels, continuous precast prestressed concrete girders and precast prestressed piers. The

planning, design and construction techniques used by different researchers revised and refined with period of time in order to suit several parameters such as feasibility, ease of construction, safety, maintainability and economy are presented to provide background knowledge of advantages and disadvantages of different systems. Design and construction issues that can be instructive in improving the components of the bridge system are evaluated in this research.

2.2 State-of-the-art and Practice for Precast Concrete Deck Slabs

Cast-in-place (CIP) reinforced concrete has been the most common form of bridge deck construction. The major disadvantage of CIP construction is the slow speed of construction. Since the 1970's, efforts have been made to speed up bridges deck construction. For example stay-in-place (SIP) forms can be used, mesh placed and the deck concrete poured. Such stay-in-place (SIP) precast panels were first used in the 1950s on large scale bridge projects in Illinois, and became incorporated for use in other states in the late 1960s and early 1970s (Goldberg, 1987). The panels became incorporated into bridge construction in other states in the US between the 1960s and 1970s, and first used in Texas in 1963 (Merrill, 2002). Contractors showed diminutive interest in adapting to a new system until the early 1980s after which SIP panels became increasingly popular. They are now the preferred method of construction in the state of Texas and are used in approximately 85 percent of new concrete bridge decks (Merrill, 2002). One of the main difficulties with this system was forming the deck overhang to cast a full depth (8 in. thick) deck section, which can be time consuming and potentially

unsafe. Corrugated galvanized steel is one SIP form type commonly used but mostly with steel girder bridges. For prestressed concrete girder bridges, half depth (4 in. thick) precast prestressed concrete panels are commonly used. This method is common in Texas, and recently efforts have been made to incorporate precast overhangs (Mander et al. 2009, 2010).

Significant utilization of the precast prestressed elements has been popular in North America in the late sixties and early seventies to increase bridge deck construction speed. Inconvenience to the movement of public and economic loss during construction of the bridge lead to the motivation of exploring new methods of construction. This was achieved by the use of full-depth precast panels in the areas of high traffic volumes for deck replacement projects. Full-depth precast panels were first used in the United States in 1965 by Biswas (1986). Bridges were originally used for non-composite construction, which resulted in the deck slab cracking. Composite action between full depth panels and girders was addressed in 1973 (Biswas, 1986) which improved the performance of the structures. Yamane et al. (1998) and Fallaha et al. (2004) investigated full-depth, 8-in. thick, precast deck panels used in both interior and exterior bays. Badie et al. (2008) developed and investigated full-depth precast concrete bridge deck panel systems. Durability of panel connections and quality of ride was accounted by them without using post-tensioning and overlays. The bridge can be opened for traffic operation faster by excluding the use of overlays and field post-tensioning. This is very useful in case of a deck replacement project since CIP concrete is usually needed at the prefabricated panel joints (Badie et al., 2008). For the rapid construction of a very long bridge system, it is

essential that bridge decks be fully precast. The designs presented herein extend the work of Mander et al. (2010) to incorporate a full-depth precast deck system. To keep the design simple, effective and efficient yield line theory is adopted.

The connection of the precast deck panels with the supporting girders is an important aspect to ensure deck-girder integrity with respect to longitudinal shear. Composite action between the deck and girder is achieved by using shear connectors. Shear pockets are cast in the precast deck panels to provide discrete locations for shear connectors to be located. A shear pocket system requires a large volume of grout and careful site placement to avoid unwanted voids from forming in the haunch. Excessive negative moments lead to cracks around shear pockets, allowing for chloride and moisture ingress, reducing the durability of the deck system. The full depth precast panels have considerable merit but have been used on a few occasions. For precast panel to precast concrete girders, shear connectors that consist of high strength reinforcing bars with or without couplers at the deck level are used (Mander et al., 2010). Experiments on the shear connection capacity have been conducted (Trejo et al. 2008, Henley 2008, Brey 2010). The testing investigated in their research study included the structural capacity of the precast overhang system and the corresponding deck joints; the interface shear capacity of the connectors, grout materials, and performance parameters; and the development of a haunch form system. Mander et al. (2009) investigated the performance of a new full-depth precast overhang panel system for concrete bridge decks, eliminating the need for onsite formwork and falsework at the overhang. Brey

(2010) proposed a truss modeling approach to evaluate the strength and interaction of the deck-haunch-girder system using both coil-rod and threaded-rod shear connectors.

For the SIP panel deck construction, continuity is achieved at interior transverse panel to-panel seams through a reinforced concrete CIP deck pour. The full-depth panels utilize a partial-depth seam. Experiments conducted by Mander et al. (2009) on exterior overhang precast deck panels indicated a mixed failure mode when the wheel load was placed immediately adjacent to the seam. In the reduced depth (4 in. thick) instead of the normal full slab (8 in. thick) region that constituted the panel-to-panel seam, high shear developed and led to partial shear failure along the seam line. Longitudinal displacement profiles were plotted to show the relative displacement between panels when loading on the edge of the seam between precast panels. Results indicated that the seam provides sufficient strength transfer under normal loads. Full flexural failure in both the loaded and adjacent panel would need to develop to increase the failure load capacity. This would require an increased shear capacity of the seam, which can be achieved by increasing the depth of the seam (to 6 in. in this case), or by providing a roughened surface or shear key (Mander, 2009).

In contrast to bridge deck construction using SIP panels, there is no second stage onsite reinforced concrete pour for full-depth panels. This requires a new means to achieve continuity at the transverse panel-to-panel seam that exists. Transverse panel edges are finished with shear keys to provide continuity so a loaded panel can distribute impact load to the adjacent panel. Shear keys are provided between transverse panel edges for continuity. Shear keys are typically either non-grouted male-to-female

connections, or grouted female-to-female connections. Spalling of concrete has been observed after bridges had been in service for a short time (Badie et al., 2008). Female-to-female joints provide inclined surfaces at the shear key to enhance shear strength. It is for this reason that female-to-female grouted connections are primarily used at transverse joints of full-depth precast panels. A full gap exists between the panels to allow for irregularities at the shear face of the panel and to increase the bearing area (Issa et al., 1995). Coil inserts are cast in select locations of full-depth panels to house leveling bolts. These bolts are used to level the deck at each girder to achieve the correct grade. Once the bolt, and therefore deck, is at the correct height, the haunch is formed and grouted. In some cases steel shims are used for the haunch, or once the deck is leveled to the correct height foam backer rods are put in place (Badie et al., 2008). This requires access from under the bridge which reduces the efficiency of the system. Leveling bolts are removed once the grout has cured to reduce the likelihood of a stress concentration forming on the girder flange (Hieber et al., 2004). The removal of the bolt also eliminates durability concerns and reduces material costs as bolts can be reused on other panels that will be constructed.

2.3 State-of-the-art and Practice for Precast Prestressed Concrete Girders

Precast, prestressed concrete girders are perhaps the predominant girder type for bridge construction of bridges in the United States and particularly in Texas. The use of precast prestressed concrete girders has facilitated the use of long span girder segments which can be easily hauled and constructed and presents a cost-effective solution with

good serviceability and minimal maintenance. In 1949, the first use of prestressing to bridges was applied to Walnut Lane Bridge in Philadelphia, Pennsylvania where high-strength steel wires were used (Aktan et al., 2000). From 1950 to the early 1990s, the count of prestressed concrete bridges went over to 50 percent of all bridges built in the United States. Early applications of the prestressed concrete to bridges involved development of different ideas of the best suitable girder sections for every project by designers. It became costly to design and fabricate different girder shapes used by different contractors for each project. Consequently, the Federal Highway Administration (FHWA), the American Association of State Highway and Transportation Officials (AASHTO) and Prestressed Concrete Institute (PCI) began work to standardize bridge girder sections for widespread utilization of prestressed concrete for bridges and reduction in the overall cost. The AASHTO-PCI standard girder sections Types I through IV were developed in the late 1950s and Types V and VI in the early 1960s to create a standardization of the girders and thus to reduce the cost of bridge construction. The AASHTO girders are lacking in sufficient compression area at the bottom of the girder and the width of the webs is too less to carry out continuity post-tensioning. Thus longer continuous spans are difficult to achieve with the AASHTO girders (Beacham and Derrick, 1999).

Many states over the years have developed their own alternatives to the standard AASHTO and PCI I-girders. In the late 1970s, FHWA sponsored a study evaluating existing standard girder sections and concluded that the bulb-tees were the most efficient sections (Aktan et al., 2000). For equal spans, these sections proved to reduce the girder

weights of up to 35 percent compared with the AASHTO Type VI and cost savings up to 17 percent compared with the AASHTO-PCI girders. As a result of this study, PCI developed the PCI bulb-tee standard, which was endorsed by bridge engineers at the 1987 AASHTO annual meeting and then adopted for usage in different states. For example, Florida State Department of Transportation has developed the Florida Bulb-Tee-girder bridges (Corven and Moreton, 2002). Washington State Department of Transportation developed the W95PTG "supergirder" sections. The NU I-girder series, developed by the Nebraska Department of Roads have depths ranging from 30 to 95 in., with constant top and bottom flange dimensions (Beacham and Derrick, 1999). Their new haunched girder shape (NU2000 I-girder) offers the advantage of allowing longer spans up to 300-ft. TxDOT developed the double tee girders which best suited the projects with short spans and imperative speed of construction. The most unique standard sections developed by TxDOT in the mid-1980s were the U48 and U54 for maximum span lengths of 105-ft and 120-ft respectively (TxDOT, 2004). The U-beams were expensive compared to the I-girders but with their high structural efficiency for long spans with shallower depth and a pleasing appearance, they gained an economic advantage. Some of the commonly used TxDOT standard shapes for the large number of bridges they build every year include: prestressed box beams, prestressed double tee beams, prestressed slab beams, deck slab beams, pretopped U beams and AASHTO prestressed standard girders.

Economic, aesthetic and environmental demands often result in the need for longer span range, fewer girder lines and minimum number of substructure units in the

bridge system. The designers, fabricators and contractors on successful collaboration can grab the advantage of applying continuous construction to standard precast, pretensioned girders developed by different states meeting specific requirements. Continuity in precast, prestressed concrete girders will aid them to present cost-effective, easily constructible and high performance alternatives against the custom used steel plate or steel box girders for longer spans. The development of continuity between precast prestressed concrete girders is not a new concept. Tests carried out by Kaar et al. (1960) investigated the development of continuity in precast, prestressed concrete bridge girders used in the conventional designs for extending span lengths. The conventional design used deformed reinforcement in the cast-in-place deck slab over the girders to provide continuity designed for resisting the live loads. The width of the diaphragms extending laterally between the girders was greater than the spacing between the ends of the girders which helped to provide lateral restraint to strengthen the concrete in compression. The results from this study found that this continuity connection detail was desirable as it permits sufficient redistribution of moment based upon the limit state and is simple to construct and relatively economical.

Mattock and Kaar (1960) carried out additional tests on the continuity connection for the precast, prestressed bridge girders with introduction of details for positive moment resistance. They carried out static and dynamic load tests on half scale component specimens of a two-span continuous connection between girders with cast-in-place deck and diaphragm. The results from the static tests confirmed the results determined by Kaar et al. (1960). From the dynamic test using repeated pulsating loads

applied to the free ends of the girders, it was found that the connection can potentially resist indefinite number of applications of design loads without failure. However, the width of the cracks and the resulting flexibility of the connection are found to increase. They tested two connection details for positive moment resistance: (i) fillet welding the projecting ends of the reinforcement bars to a structural steel angle, and (ii) bending the projecting ends of the reinforcement to form right angle hooks and lapping them with the longitudinal diaphragm reinforcement. Results from this tests showed that the performance of the welded detail was satisfactory compared to the hooked detail both at service load and ultimate strength with careful attention to the welding. Brittle fractures in the reinforcing bars were observed in the hooked detail.

Tadros and Baishya (1998) developed a threaded rod continuity system for the precast concrete I-girders at the University of Nebraska and this was further extended by Tadros (2007). This continuity detail used 1-3/8 in. high strength (150-ksi) threaded bars embedded in the top flange of the girder and connected using steel block and nuts. After the continuity diaphragm is cast, these bolts are tightened into position. A notable span-to-depth ratio of 36 from this threaded rod spliced system can be achieved by using it in combination with a splice haunch block on the piers. The longest spans achieved using this arrangement were 148-ft and 151-ft on a four span unit employing 50-in deep NU 1100 I-Girders (Standard girder section developed by Nebraska Department of Roads) which is a significant feature of this non-post-tensioned continuity system.

Sun et al. (2004) further refined and investigated this system at the University of Nebraska. Two systems were tested under this study: (i) using high strength bars in line

and cross-connecting with the high strength threaded rods or transverse rebar, and (ii) using high strength bars in line and welding transverse bars to longitudinal 50 ksi straps in form of an open box member. The major advantage of this system is that the high strength bars are connected before casting of the deck slab and therefore are subjected to permanent negative moment at the support on application of the deck load which eliminates the cracking of the bottom flange of the girders due to the positive thermal gradient effects.

Newhouse et al. (2005) carried out an analytical study on a continuity connection over the support at the Virginia Polytechnic and State University. The goal of this research was to recommend appropriate continuity details for the PCBT girder sections. They developed and tested three continuity details on PCBT-45 girder sections. The first two continuity details consisted of a full continuity diaphragm with a cast-in-place deck. Test 1 was carried out on specimens with prestressing strands extending out from the ends of the girders and bent to form a 90 degree hook. Test 2 involved specimens with #6 U bars bent into a 180 degree hook extending out from the bottom of the girders. Test 3 was carried out on a third continuity connection detail consisted of the slab only which was cast continuous over the girders. It was found from the tests that the Test 2 specimen with 180 degree bent U-bars was slightly stiffer with very small crack openings at the bottom interface as compared to the Test 1 specimen under the static and dynamic loads. The results from this investigation showed that the thermal restrain moments were significant than the restrain moments due to creep and shrinkage.

The types of methods used in different states for extending span ranges using incremental variations in the materials and conventional design procedures often result in relatively small increases in span range for the precast prestressed concrete girders. One of the techniques adopted in the current state of art and practice is spliced girder technology which has the potential to extend the simple spans by approximately 50 percent. In this technique, precast prestressed concrete girders are fabricated in several relatively long segments and are assembled into the final bridge structure. Post-tensioning is generally used to provide continuity between the girder segments. For example, the bridge along US 231 over the White River, Indiana constructed in the early 1990s is a multi-span spliced concrete girder bridge with constant depth, full span girders spliced at interior piers and post-tensioned for continuity. This spliced girder design was bid as an alternative to steel plate girder option. The bridge had three continuous spans. The provision of semilightweight concrete reduced the dead weight of the structure and continuity allowed for a very wide girder spacing resulting in an economic solution.

Ficenec J.A. et al. (1993) presented an article in the PCI journal describing the project phases and implementation of new girder continuity technology for two bridge structures in Nebraska. The continuous spliced, prestressed concrete I-girder option was selected with an estimated cost of $30,000 less than the steel plate girder. In this new girder continuity system, the girder segments are made continuous by splicing and coupling and tensioning the pre-tensioning strand extensions at the adjacent ends of the girder segments. The main viaduct bridge consists of six spans with 86-ft and 114-ft

exterior spans employing 4-ft 6-in deep Nebraska Type 4-A girders and 172-ft interior spans employing 6-ft 3-in deep Nebraska Type BT-1A girders. A combination of straight and harped strands is used for the pre-tensioned girders. The pre-tensioned strands are extended and positioned and then spliced and pretensioned to fully withstand the service stresses and ultimate strength conditions providing the same structural benefits as full-length post-tensioning (Tadros et al., 1993).

Ronald H.D. (2001) in an article in the PCI Journal highlights the use of post-tensioning splicing system coupled with high performance concrete to build longer spans ranging up to 320-ft in Florida. This article focused on the various factors to be accounted for in the analysis, design and construction of prestressed, post-tensioned bulb tee girders. In this design approach, the Bulb Tee girders were pre-cast, pretensioned and the spliced using post-tensioning performed in two stages on the construction site. The precast, prestressed Bulb Tee girders were fabricated as short segments and spliced on the construction site. Stage 1 post-tensioning allowed for girders to become continuous before casting of the deck. Stage 2 post-tensioning results in residual compression in the deck for serviceability and deflection control. This system of post-tensioning allows for wider spacing between the girders and the high cost of post-tensioning is compensated by fewer number of piers. Another advantage of this system is elimination of intermediate diaphragms. High strength concrete of f'c = 8500 psi for girder design and 0.6 in diameter strands for post-tensioning in this system helped to increase the capacity and span length of the girders. Since, lateral stability becomes an important issue for long and slender girders, it was recommended to use sections with wide top and bottom

flanges. The construction process for this spliced structural system was found to be simple and cost-effective compared to span-by-span and balanced cantilever construction.

The focus of the research presented in the NCHRP Report 517 (Castrodale and White, 2004) was to develop LRFD design procedures, standard details and design examples for long span continuous precast prestressed concrete bridge girders. It was noted in this report that the precast prestressed concrete bridge girders were rarely used for spans exceeding 160-ft. due to material limitations, hauling size and weight limitations and lack of design aids for the design of long span prestressed concrete girders. This report identified around 250 proven, spliced, precast prestressed concrete girder bridges built around the nation but the experience and information on these job specific projects was not available widely for use on similar proposed bridge projects. This report provided the needed documentation on all the known technologies for extending the span lengths of the prestressed concrete girders to 300-ft. From the assessment of all these methodologies, this study concluded that the splicing of precast, prestressed concrete girders had the potential to significantly increase the span lengths to achieve the desired span range. The use of splicing with multiple means and locations within the span and a list of similarities and differences between the spliced girder construction and the segmental bridge construction was identified in this report. This report summarized both material related options and design enhancements for extending the span lengths. The material related options included: (i) high strength concrete, (ii) specified density concrete, (iii) increased strand size, (iv) increased strand strength, and

(v) decks of composite materials. The alternatives for design enhancements included: (i) modified standard girder sections, (ii) creating new standard girder sections, (iii) modifying strand pattern or utilization, (iv) enhanced structural systems, and (v) enhanced analysis and design methods. The multiple design examples presented in this report guide in the comparison of the potential alternatives to extend span lengths.

2.4 State-of-the-art and Practice for Precast Concrete Piers

Several analytical and experimental studies are proposed for the bridge pier systems by various transportation agencies and research institutes. Traditional cast-in-place construction of bridge piers normally cause delay in the construction speed due to the process of placing, casting and curing of concrete at the job site and also causes traffic closure. A number of alternative designs and methods of construction are in practice like precast columns with precast cap beams or either component precast and the other cast-in-place.

LoBuono, Armstrong, & Associates (1996) investigated the viability, advantages and disadvantages of using precast concrete substructure systems in the State of Florida. Billington et al. (1999) presented a precast segmental pier system developed for the Texas Department of Transportation (TxDOT). This system could be used as an option for the cast-in-place concrete in non-seismic regions. It consisted of three major column components, a column component, a template component, and an inverted-T cap-beam component. In this system, a number of partial-height columns segments are stacked one over the other and then the template component is placed on the top of the columns with

the cap beam on top of that. The joints were matched by epoxy to minimize onsite construction time but this delayed the construction time due to prolonged fabrication time and thus increased labor. A more standardized method was developed to maintain quality control and mass production. Matsumoto et al. (2002) summarized research conducted for the TxDOT related to the design and construction of column-to-cap-beam connections. They carried out four full scale single column and cap beam assembly tests and they found that four types of connections like a single-line grout pocket, double line grout pocket, grouted vertical duct, and a bolted connection were adequate to develop required connection in the non- seismic regions. They provided recommendations for material properties, development lengths and construction tolerances for these four connections. Hieber et al. (2004) and Shahawy (2003) presented summaries of precast concrete bridge substructure systems developed for use in non-seismic regions.

The research conducted by Blakeley and Park (1971), Meek (1978), Aslam et al. (1980), Stanton et al. (1986), French et al. (1989a), French et al. (1989b), Priestley and Tao (1993), Priestley and MacRae (1996), El-Sheikh et al. (1999), and Hewes and Priestley (2002) on post-tensioned precast concrete columns and piers is discussed in detail in Roy (2011).

This research was extended by Mander and Cheng (1997) and Mander (2000) on a scaled bridge pier with an armored interface plates subjected to quasi-static and pseudo-dynamic bi-directional loading patterns. The results were compared with the performance of a conventional pier and it was found that the damage to Damage Avoidance Design (DAD) pier was minor. Bidirectional Pseudo dynamic tests of bridge

piers designed to different standards was conducted by Dhakal et al. (2007). Based on the physical testing of a DAD bridge pier by Solberg et al. (2009) it was concluded that the DAD pier will not undergo severe damage from a design basis earthquake. Concentrated axial loads were resisted by special detailing at the column-foundation interface. This concentration was resisted by a combination of reinforcing steel and high strength fiber-reinforced concrete. No stiffness degradation or residual displacement was observed. This was shown to be due to the rocking, bi-linear elastic hysteretic behavior of the pier. The lack of severe damage was found to potentially reduce the life-cycle operating and repair costs of the structure. Moreover negligible residual displacements ensured higher serviceability after an earthquake. Special attention was given to large concentrated forces which must be transmitted through a small region the specimen due to bi-directional rocking behavior. They investigated the damage classification according to an established indexing system and compared to that of a conventional bridge pier.

Pekcan and Mander et al. (2000) investigated research on balancing lateral loads using tendon based supplemental damping system. The system was based on the idea of prestressed load-balancing and used a combination of tendons, fuse-bars, and dampers. The strengthening, stiffening, or ductility improvements are not always desirable due to high cost and other constructional complexities and the ductile design philosophy suffers from the inability to avoid damage in high seismic activities. They suggested that supplemental damping systems are a desirable solution to take care of these deficits. The overall seismic design objective lies in the following inequality: seismic capacity $\geq$ seismic demand. Thus the ductile design targets in improving the left hand side of the

equation, the seismic capacity whereas by providing supplementary energy dissipation devices the seismic demand (the right hand side of the equation) on the structural system can be reduced. Eberhard et al. (2005) gave systems for precast concrete pier for rapid construction of bridges in seismic regions.

Cheng and Mander (1997) termed a design philosophy called the Control and Repairability Damage (CARD) in which they used specially designed plastic hinge zones. They concluded that the severe damage due to large seismic displacements can be localized and repaired after an earthquake. Plastic hinges are an extension of the ductile design concept in building seismically resistant structures. The collapse of the structure is mostly avoided due to energy dissipation through the plastic deformation of specific zones at the end of the member. The hinge zones are purposefully weakened and regions outside the hinge zones are detailed stronger than the fuse zone keeping the remaining part of the structure elastic during the earthquake occurrence. In conventional reinforced concrete columns, this plastic hinge action can lead to severe damage in the column and require the replacement of the entire column. The CARD design philosophy uses replaceable fuse bars in the plastic hinge zone which can be used in retrofit situations. It is concluded from this research that this type of retrofit will ensure faster and cost-effective repairs after a severe earthquake. Thus this system can be used for reinforced columns that provide replaceable or renewable sacrificial plastic hinge zone components.

Louman et al. (2008) conducted a bidirectional cyclic loading on a 3D beam-column joint designed for damage avoidance. This fill-scale three-dimensional jointed precast prestressed concrete beam-to-column connection designed and constructed in

accordance with the Damage Avoidance Design philosophy was tested under displacement-controlled quasistatic reverse cyclic loading. The specimen was shown to perform well up to a 4% column drift with only some minor flexural cracking in the precast beams, while the precast column remained uncracked and free of damage. They concluded from this research that this excellent performance is due to the steel armoring of the beam ends to mitigate the potential for concrete crushing. This research gave a three-phase- force-displacement relationship and details of the pre-rocking flexural deformation of the beam; the rigid body kinematics during the rocking phase; and the yielding of the external dissipaters and post-tensioning tendons.

CHAPTER III

CONTINUOUS PRECAST CONCRETE DECK

3.1 Chapter Summary

Bridge Superstructures, commonly consist of the deck slab and support girders integrally connected to form the deck span. The choice of the type of construction for the deck slab plays an important role in the determining the construction time and cost of the project. Cast-in-place (CIP) deck panels require time consuming on-site construction as well as a stay-in-place forms as well as a substantial curing time but not markedly because curing of the topping slab still needs to occur. Full-depth precast deck panels provide an advantage of increased speed and cost, greater quality assurance and lower maintenance costs. The main construction feature that may slow the progress is the placement of the grouted haunch. However, the curing time is rapid and it should be possible to deal with one-span per day for a long bridge.

3.2 Chapter Scope

In this project, full depth precast deck panels have been designed. The plan view of a typical precast deck panel with pockets for the shear connectors is shown in Figure 3. These fell depth precast deck panels are 13 ft. wide, 8 ft. long and 7 in. thick are used with post-installed center guide-way that requires a high level of precision for installation. Figure 4 shows a cross section of the deck slab and the girders.

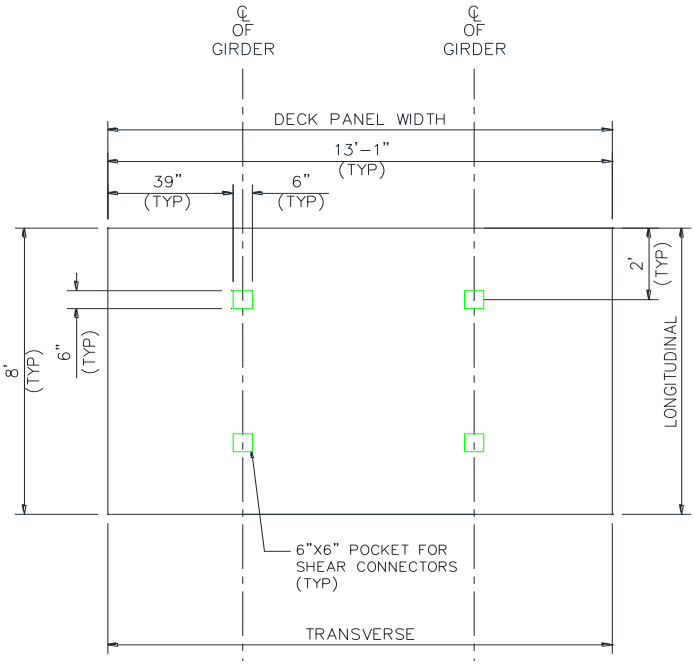

Figure 3 - Typical Precast Deck Panel with Pockets for Shear Connectors

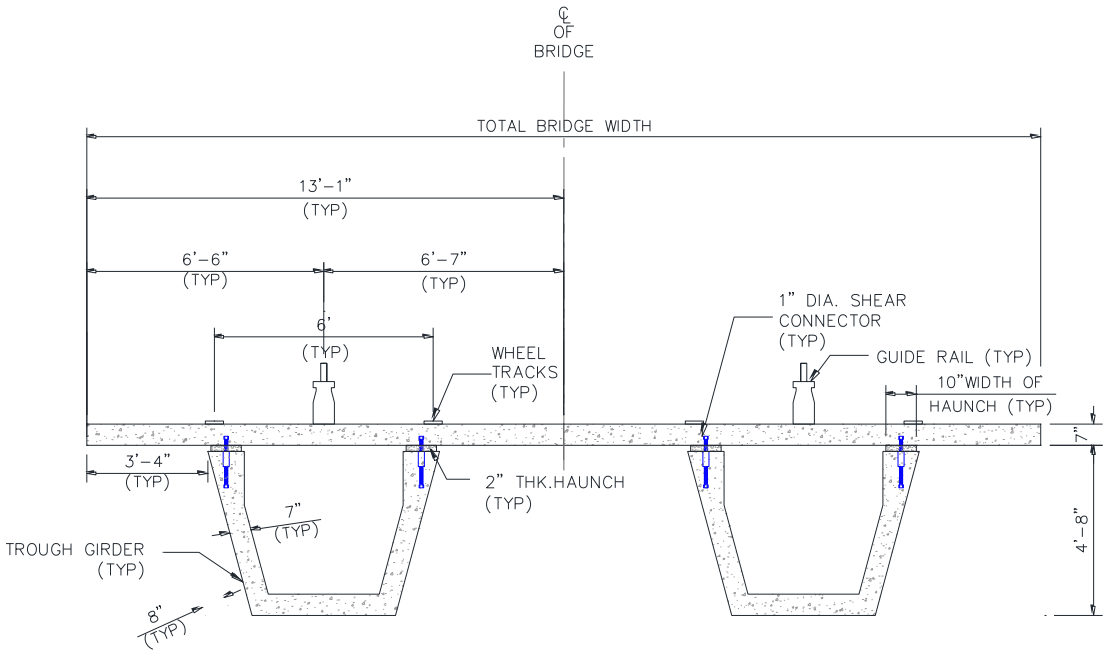

Figure 4 - Cross Section Showing Deck Slab and Girders

The deck consists of continuous spans of length 140 ft. each. Along the cross-section, there is a 3ft.-4 in. overhang on either side resulting in a total deck width of 26 ft.-2 in. The depth of the slab is considered to be a practical minimum from the point-of-view of strength and serviceability; however this depth has often been used in the past. The full-depth precast deck-panels are connected with the girder using shear connectors of 1-in. diameter. These shear connectors provide a composite action between the deck and the girder. Slab design has been based upon well-known yield line theory but modified due to recent work of Mander et al. (2011). To simplify construction, where possible a single-layer of isotropic reinforcement is proposed. However at turnout locations, the heavy wheel load passage across the panels necessitates a two-layer solution.

3.3 Deck Design Parameters

1. Structural Concrete:
   - Compressive strength at 28 days, $f'_c = 4$ ksi
2. Reinforcing Steel:
   - ASTM A615 Grade 604, fy = 60 ksi (ASTM A615, 2009)
   - Modulus of Elasticity, $E_s = 29{,}000$ ksi (AASHTO LRFD-10 Art. 5.4.3.2)
3. Concrete Cover:
   - 2.5 in. minimum clear cover to top reinforcement
   - 1.5-in. minimum clear cover to bottom reinforcement

3.4 Design Loading

Figure 5 shows the Freight Shuttle vehicle loading. The load factors, based on AASHTO LRFD Bridge Design Specifications (2010) values, are adopted as shown in Table 1. A live load factor of 1.75 is used based for the strength limit state, and a dynamic allowance factor (IM) is taken as 1.33 as per AASHTO LRFD (2010).

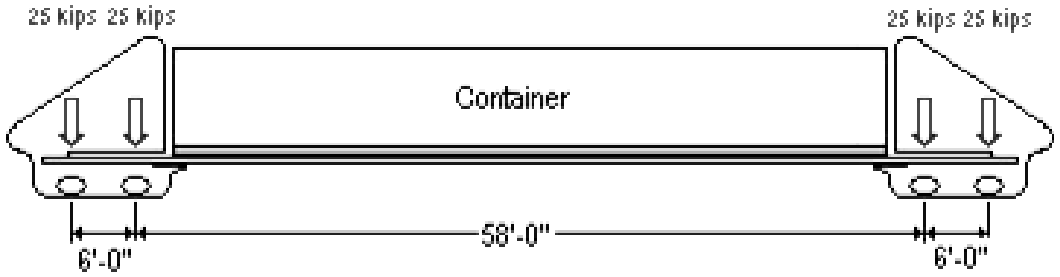

(a) Freight Shuttle Vehicle Loading

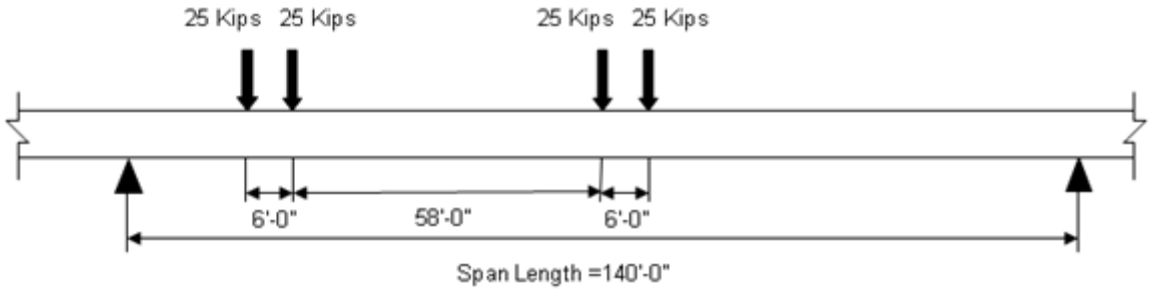

(b) Load of Freight Shuttle Vehicle on Deck Slab

Figure 5 - Freight Shuttle Vehicle Loading

Table 1 - AASHTO LRFD (2010) Load Factors and Maximum Factored Loads

	Wheel load (Kips)	**Multiple Presence Factor**	**Live load factor**	**Dynamic Allowance factor**	**Maximum Factored load (Kips)**
Freight Shuttle wheel Load	12.5	1.0	1.75	1.33	40
AASHTO LRFD Specification (2010)	-	3.6.1.1.2	3.4.1 (Strength I)	3.6.2.1	-

3.5 Analysis and Design of Deck Slab

The reinforcement for the deck slab is initially calculated based on the minimum reinforcement requirement as per the ACI Committee 318 (2008) Code of Practice. The capacity of the deck slab is calculated based on the yield line theory to check the adequacy of the provided reinforcement. Two layers of No. 4 bars at a spacing of 6 in. is provided in both longitudinal and transverse directions at curved locations of the bridge and a single layer of No. 4 bars at a spacing of 6 in. is provided at the straight alignment locations. Table 2 gives the moment capacity if the deck slab as per the yield line analysis. The provided negative and positive moment capacities and shear strengths along seams are given in Tables 3 and 4.

Table 2 - Moment Capacity of Deck Slab as per Yield Line Analysis

REINFORCEMENT	MOMENT CAPACITY, M AND M' (kip-in. /in.)
Single Layer	6.53
Double Layer	9.79

Table 3 - Capacity of Slab as per Yield Line Analysis for Single Layer Reinforcement

LOAD LOCATION	CAPACITY FOR SINGLE POINT LOAD (kips)	CAPACITY FOR DOUBLE POINT LOAD (kips)	LOAD DEMAND (kips)
Between Girders	73.84	55.54	40
Overhang	73.01 (Mechanism 1) 74.80 (Mechanism 2)	-	40

Table 4 - Capacity of Slab as per Yield Line Analysis for Double Layer Reinforcement

LOAD LOCATION	CAPACITY FOR SINGLE POINT LOAD (kips)	CAPACITY FOR DOUBLE POINT LOAD (kips)	LOAD DEMAND (kips)
Between Girders	110.76	83.31	40
Overhang	73.01 (Mechanism 1) 74.79 (Mechanism 2)	-	40

Yield line theory is based on the concept of determining the ultimate load capacity of the reinforced concrete slab by assuming a collapse mechanism defined by a pattern of yield lines which depicts the yielding of the reinforcement in the slab (MacGregor and White, 2004). The virtual work method is used for the deck slab design in which the ultimate moment is obtained by equating the internal energy dissipated on the yield lines during virtual rotation to the external virtual work done in deflecting the

slab. Standard yield line theory may be found in Park and Gamble (2000) and the necessary modifications for anchorage and half-depth panels in Mander et al. (2011).

The deck slab is analyzed for the yield line patterns as shown in Figure 6. The specific locations of the load considered are:-

1. Between girders - For single point load and double point load
2. At overhangs - For single point load

From the results of the yield line analysis presented in Tables 2, 3 and 4, it is found that the provided design reinforcement is adequate to carry the load of the Freight Shuttle vehicle safely.

The design of the deck slab is further checked by using the empirical design method as specified by AASHTO LRFD Bridge Design Specifications (2010) Section 9.7.2 based on certain geometric considerations of the deck slab. The limit states are automatically satisfied in this design and the primary structural action of the concrete decks is considered to be internal arching action.

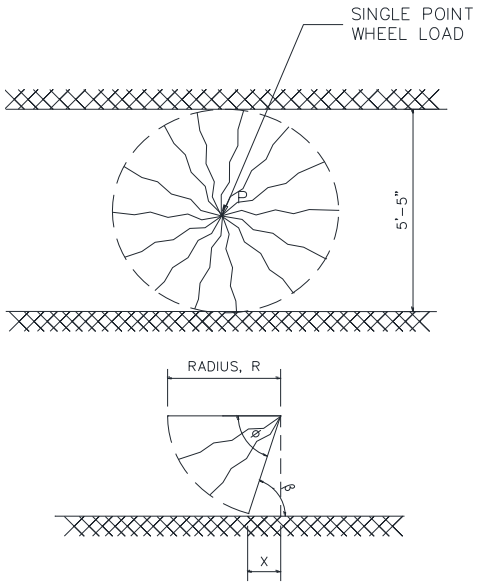

(a) Single Concentrated Wheel Load on Bridge Deck Interior Bay

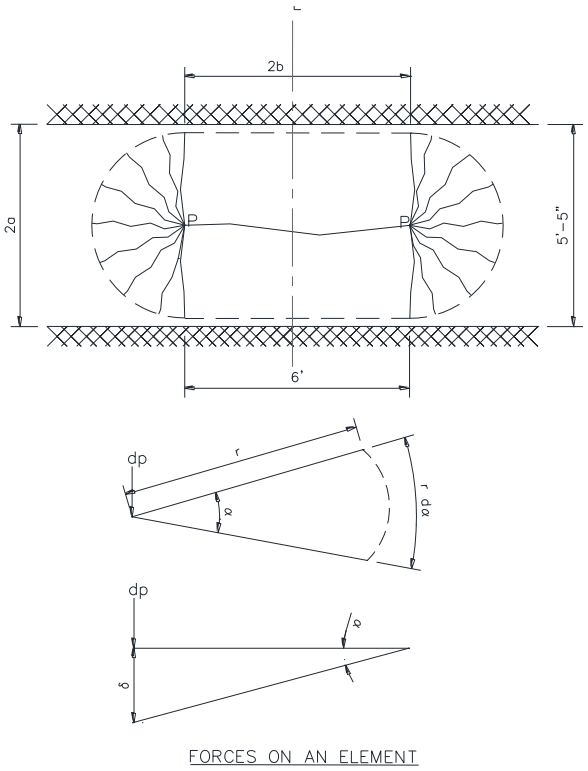

(b) Two Concentrated Wheel Loads on Bridge Deck Interior Bay

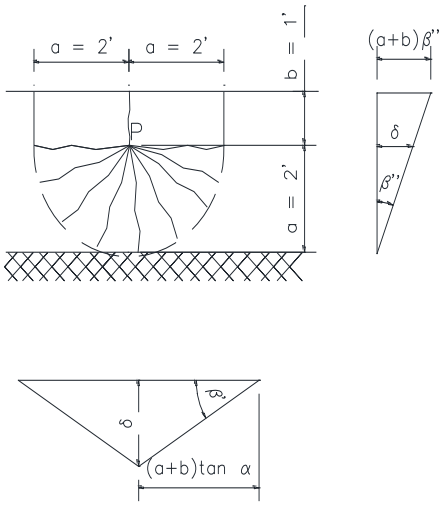

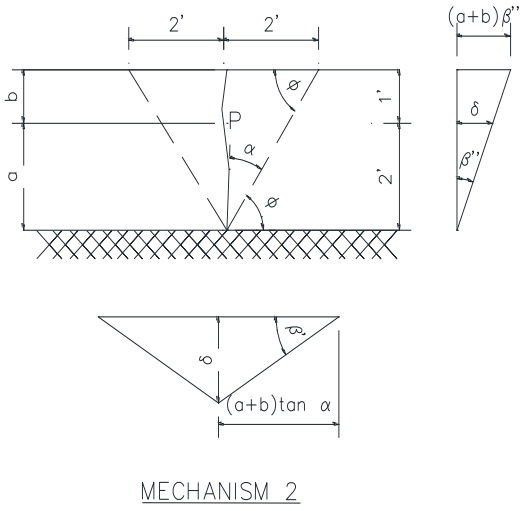

(c) Single Concentrated Wheel Load on Bridge Deck Overhang

Figure 6 - Yield Line Patterns for Deck Design

Figure 7 shows the final reinforcement detail at straight alignments and at curved alignments along turnouts.

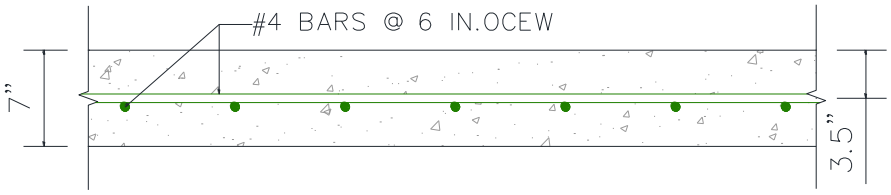

(a) Straight (tangent) alignment

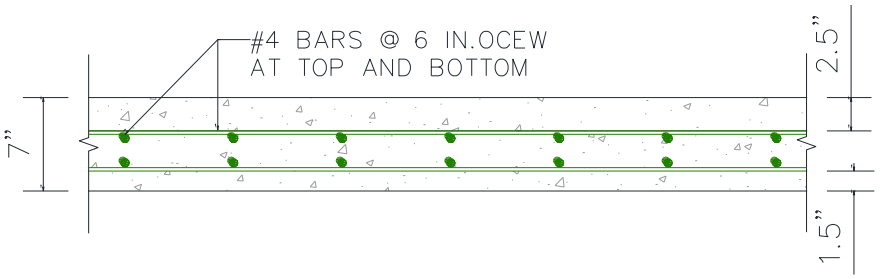

(b) Strengthened deck for curved sections where tracks may cross span

Figure 7 - Deck Slab Reinforcement Detail

3.6 Punching Shear Design

Punching shear in slabs occur due to the effect of a concentrated load on a relatively small area of the slab. In this case, freight shuttle vehicle wheel loads on the slab are checked for punching action on the slab. Figure 8 shows the critical perimeter for punching shear considered at a distance of d/2 from the edge of the loaded area. AASHTO LRFD Bridge Design Specifications (2010) Section 5.13.3.6 gives an empirical design equation for punching shear capacity in slabs and footings. The

punching shear capacity is also calculated as per ACI Committee 318 (2008), Equation 11-33, 11-34 and 11-35. Table 5 gives the values of the shear capacity of the deck slab calculated as per AASHTO (2010) and ACI Committee 318 (2008) Code of Practice.

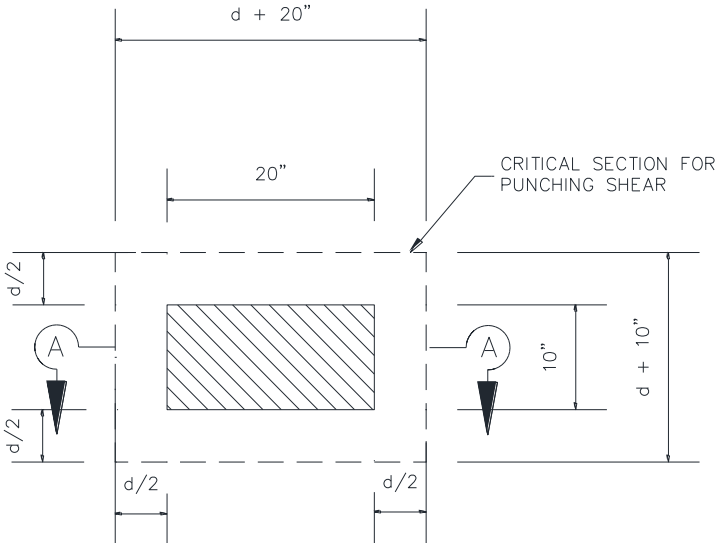

(a) Loaded area and critical section for punching shear

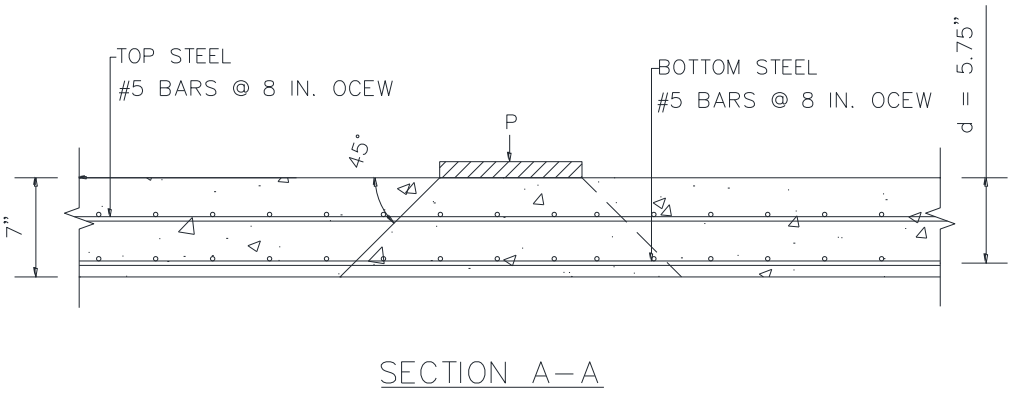

(b) Cross-section of slab showing the load distribution along the depth of the slab

Figure 8 - Punching Shear in Deck Slab

Table 5 - Punching Shear Check in Deck Slab

AASHTO SHEAR CAPACITY, Φ.V_{AASHTO} (Kips)	**ACI SHEAR CAPACITY, Φ.V_{ACI} (Kips)**	**SHEAR DEMAND, Vu (Kips)**	**RESULT**
58.74 (Single Layer)	49.14 (ACI -11-33)	40	SAFE
	47.81 (ACI - 11-34)	40	SAFE
Section 5.13.3.6	49.14 (ACI - 11-35)	40	SAFE

The optimized provided minimum depth is found to be safe in punching shear for both straight section where the vehicle wheel loads are transferred to the girders directly and the curved section where the wheel load directly comes on the slab. Hence there is no requirement for increasing the depth of the deck slab or provision of additional shear reinforcements to resist punching shear.

CHAPTER IV

CONTINUOUS SPLICED PRECAST PRESTRESSED CONCRETE GIRDERS

4.1 Chapter Summary

The use of precast prestressed concrete girders has facilitated long span girder segments which can be easily hauled and constructed by splicing together on the site. These continuous girders present a cost-effective solution with good serviceability and minimal maintenance. These precast girder sections are available in different standard forms of which the trough-girders become very attractive because of their shape, ease of construction and erection, effectiveness in terms of their high torsional rigidity and acceptable aesthetic appearance. The preferred superstructure solution comprises of precast prestressed concrete girders with precast concrete deck panels connected using shear connectors. These girders share the benefits of a long design life, good bearing strength with slender sections and easy maintenance with good visual appearance. The low dead weight of the superstructure proves advantageous with regards to the foundation and the settlement of the supports. There is considerable reduction in the cost due to the elimination of large false work support system since the girders themselves act as formwork once they are launched or lifted into place.

The use of twin trough girders with optimized span layout has minimum impact on the traffic and environment. A span length of 140 ft. has been chosen as this length is considered to be a practical maximum for transportable units. This leads to less number of transportation units of the girders and thereby the number of joints. There are also

improvements in the use of trough-girders due to the provision of the shallowest structural depth with maximum torsional stiffness. The girder has been designed for a combination of pre- and post-tensioned prestressing operations. Pretensioning of the trough girders and I-girders are carried out to balance the additional self-weight of the girder during transportation and erection and construction loads. Post-tensioning of the girders is carried out to balance the self-weight of the deck slab after it has been erected.

4.2 Optimized Prestressed Concrete Trough Girder Specification

Twin trough girders 4'-6" deep are used in this design each supporting an individual guide-way as shown in Figure 9. The span/depth ratio is approximately 30 – a practical span limit for a constant depth girder. The top width of the trough girder is 6'-4 ¼" and the bottom width is 3'-11 ¼". The span of the girders considered is 140 ft. which facilitates easy transportation of the precast sections to the site.

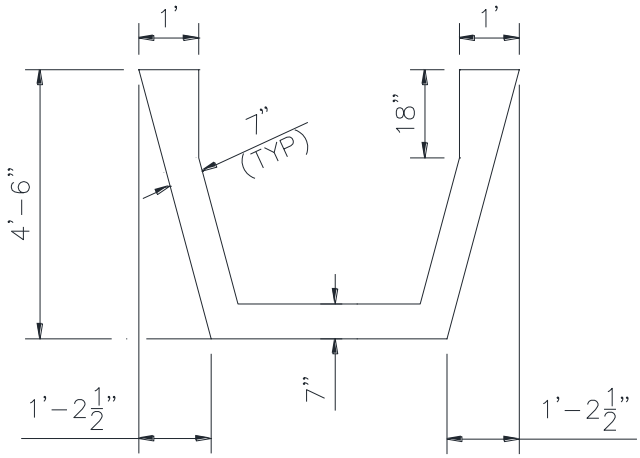

Figure 9 - Trough Girder Specification

The dimensions of the trough girders provide a slender and economic section which carries the loads of the freight shuttle vehicle safely. The trough girders are chosen since they provide the maximum torsional stiffness and allow for shallower structural depth to be used. These trough girders are found to provide a more structurally effective cross section as compared to AASHTO Type IV I-girders with a total weight in lb. /ft. about 40 percent less than the total weight of the I-girders required for the same bridge. Another important advantage of the trough shape of each girder is that it provides an inner void space of about 1025 sq. in. which can be used for multiple purpose like place for installation of the electrical conduits, fiber optical cables etc. in a protected non-exposed environment. Thus the shape and the void space of the trough girders prove highly beneficial.

4.3 AASHTO Type IV Prestressed Concrete I-Girder Specification

A comparative study is performed between the proposed Trough-girder design and the equivalent I-girder design for the same bridge system. For this study, the AASHTO Type IV girder section is used with specification details as shown in Figure 10.

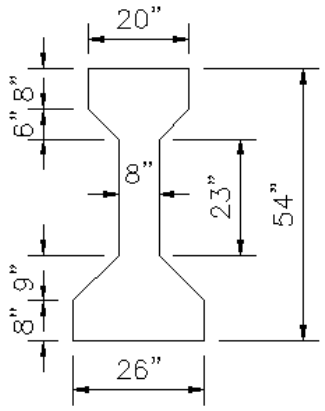

Figure 10- AASHTO Type IV I-Girder Specification
(AASHTO, 2010)

The equivalent design consists of four AASHTO Type IV girders with two girders supporting an individual guideway. The AASHTO Type IV girder is used widely in Texas and in other states since introduction in 1968. This girder section can be used for bridges spanning up to 130-ft. with normal concrete strengths. The fillets are provided between the web and the flanges to ensure a uniform transition of the cross section. The girder can hold a maximum of 102 strands.

Figures 11 and 12 show the cross-sectional elevation of the bridge with trough girders with single and twin pier respectively. Figure 13 shows the cross-sectional elevation of bridge with AASHTO Type IV I-girders.

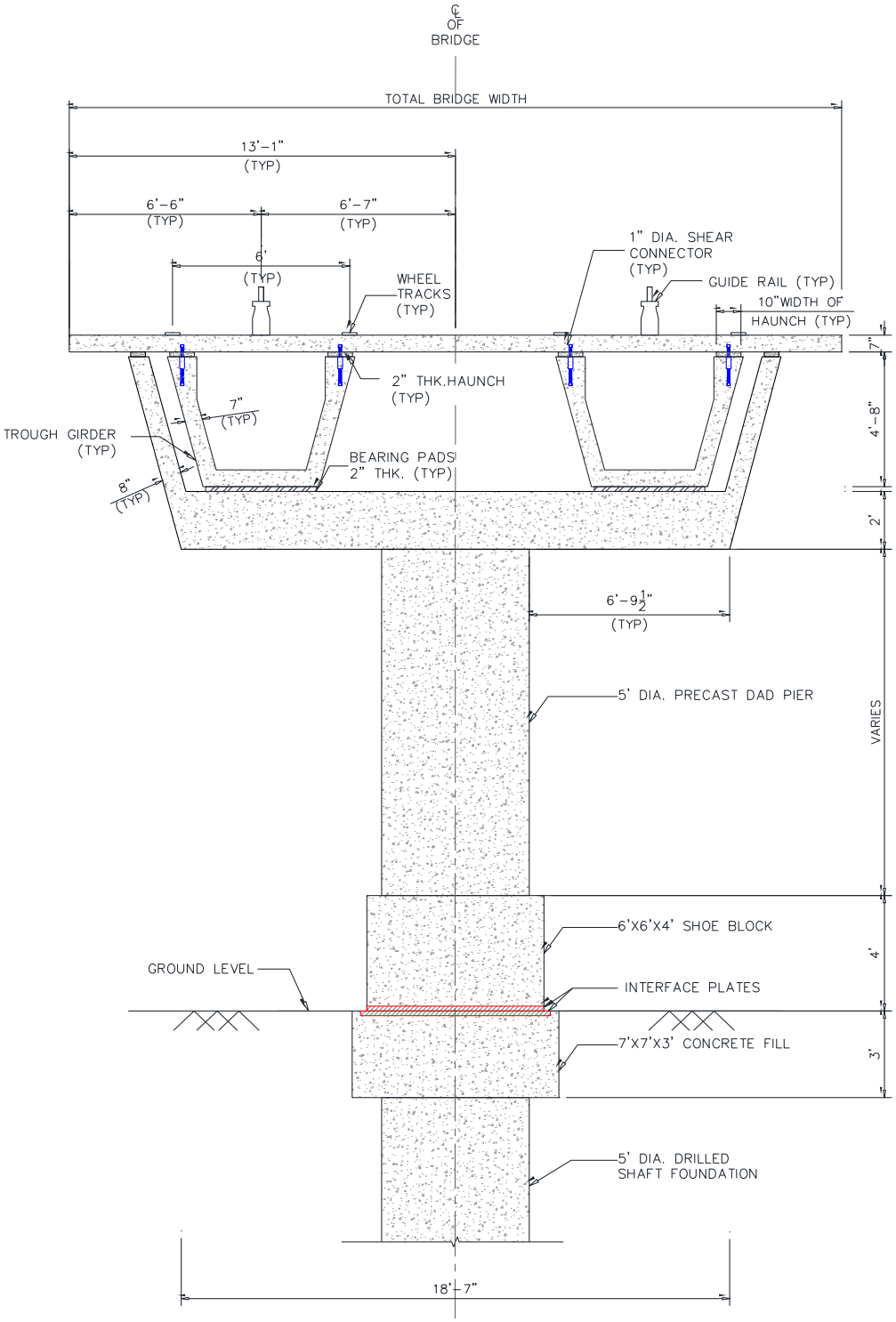

Figure 11 - Cross- Sectional Elevation of the Bridge with Trough-girders and Single Pier

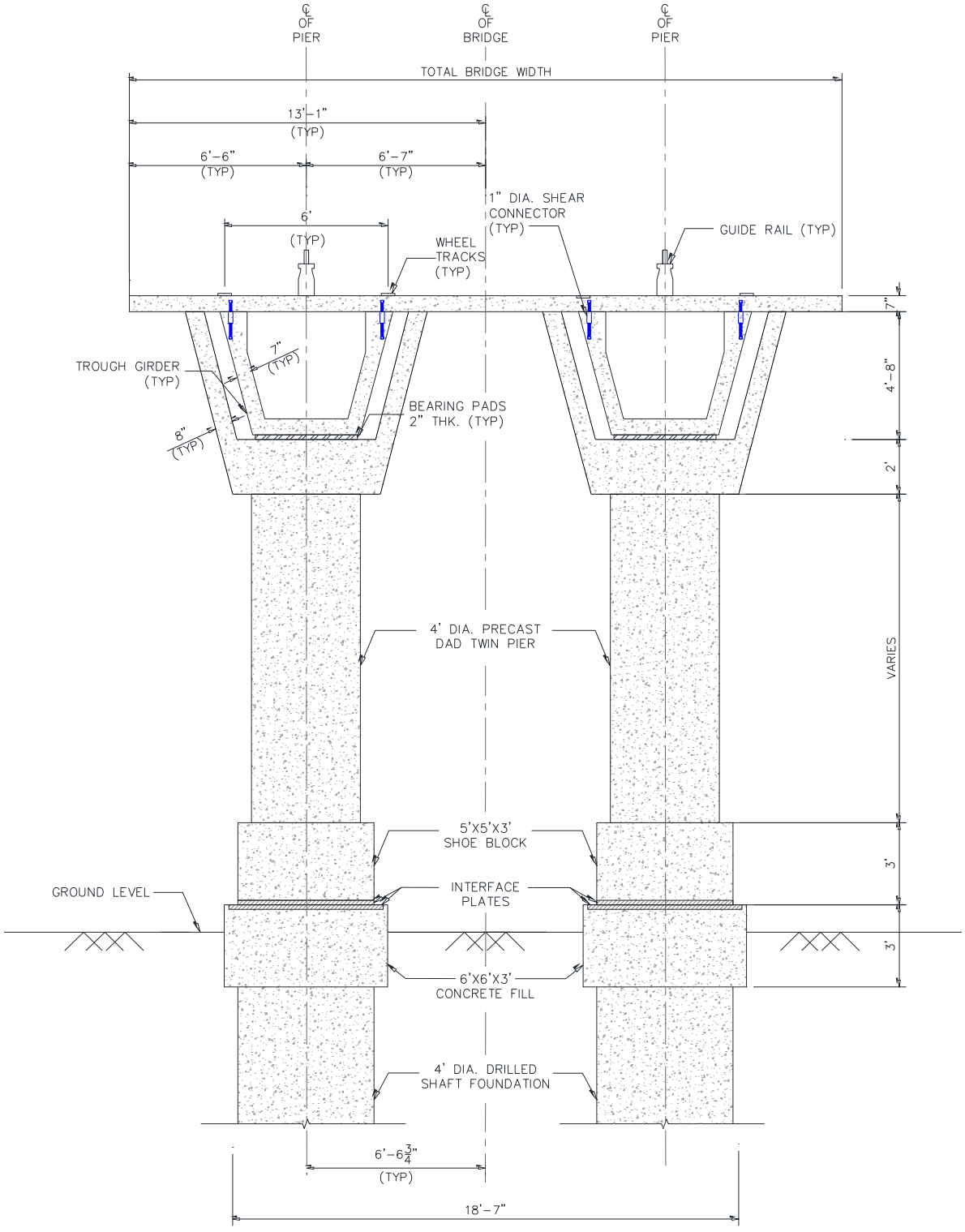

Figure 12 - Cross- Sectional Elevation of the Bridge with Trough-girders and Twin Pier

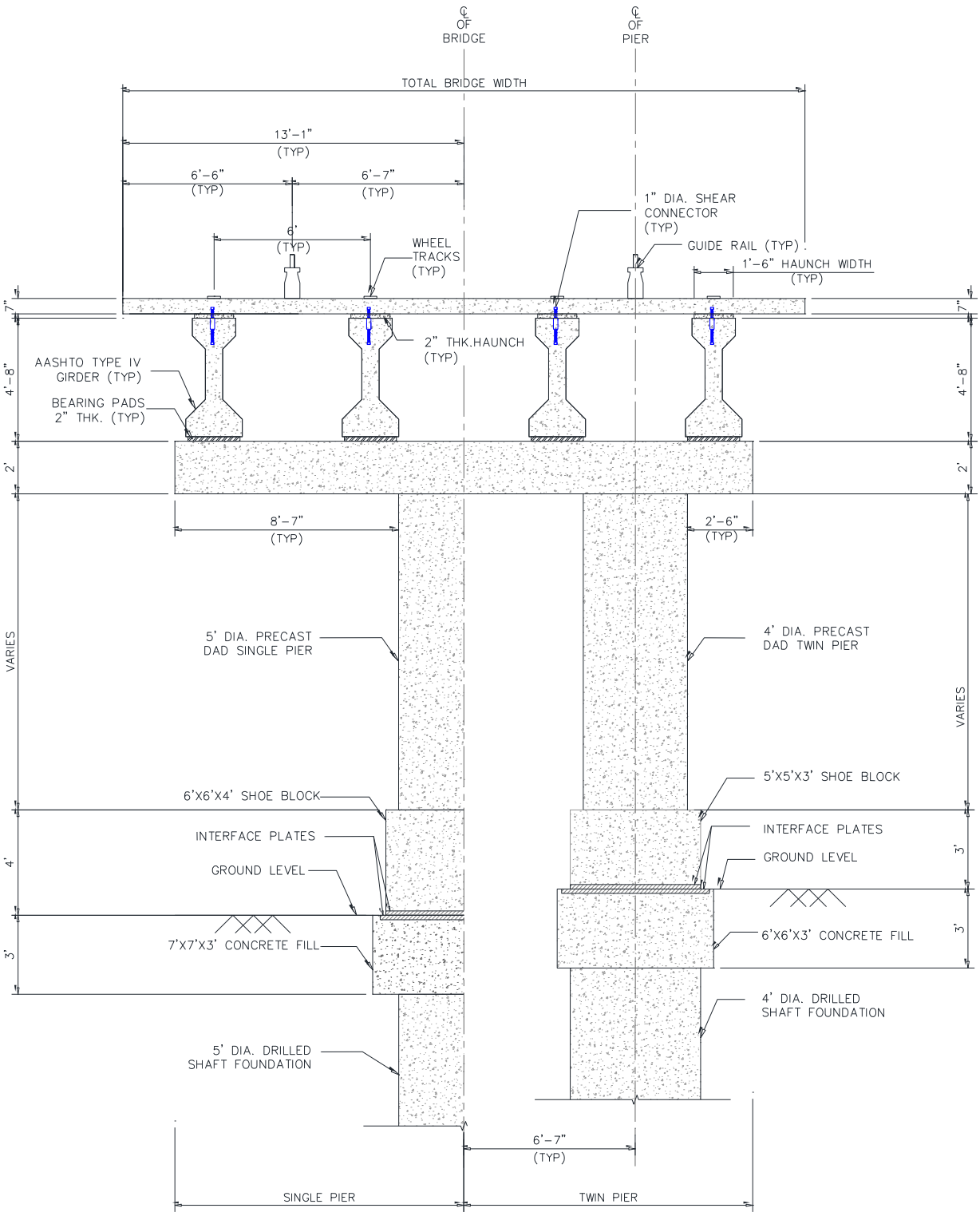

Figure 13 - Cross- Sectional Elevation of the Bridge with AASHTO Type IV I-girders

4.4 Analysis of Girders

Dead load analysis of the girder is performed by considering the self-weight of the girder, self-weight of the deck slab and the self-weight of the upstand and the rails. The moment and shear envelopes considering all these loads are developed for the simple spans.

Live load analysis of the girder is performed for the vehicular load of the freight shuttle. The freight shuttle consists of electrically powered vehicles propelled by linear induction motors that run on a specialized, derailment-proof guideway from ports to terminals at highway speeds with the use of an automated control system. The tandem wheel spacing of the vehicle is 6-ft. The total weight of a single vehicle is around 100 kips with the load being distributed on four axles of 25 kips each as shown in Figure 5.

The Live load analysis for the continuous girders is carried out using spreadsheets as well as using software, SAP2000 (v14.0.0). AASHTO LRFD (2010) Table 3.6.2.1-1 specifies the dynamic allowance to be taken as 33 percent of the static load effects for all limit states, except the fatigue limit state, and 15 percent for the fatigue limit state.

Thermal load analysis is performed for computing the primary and secondary thermal stresses in the girders. The primary thermal stresses are computed using the AASHTO LRFD (2010) temperature distribution parameters as shown in Figure 14. Secondary temperature stress analysis is done by applying unit moments at the interior supports. Settlement stresses are computed by subjecting one of the interior supports of the continuous girders to a settlement of ± 1-in. The girders are then checked for

allowable deflection under live load and impact as specified in AASHTO LRFD (2010) Art. 2.5.2.6.2.

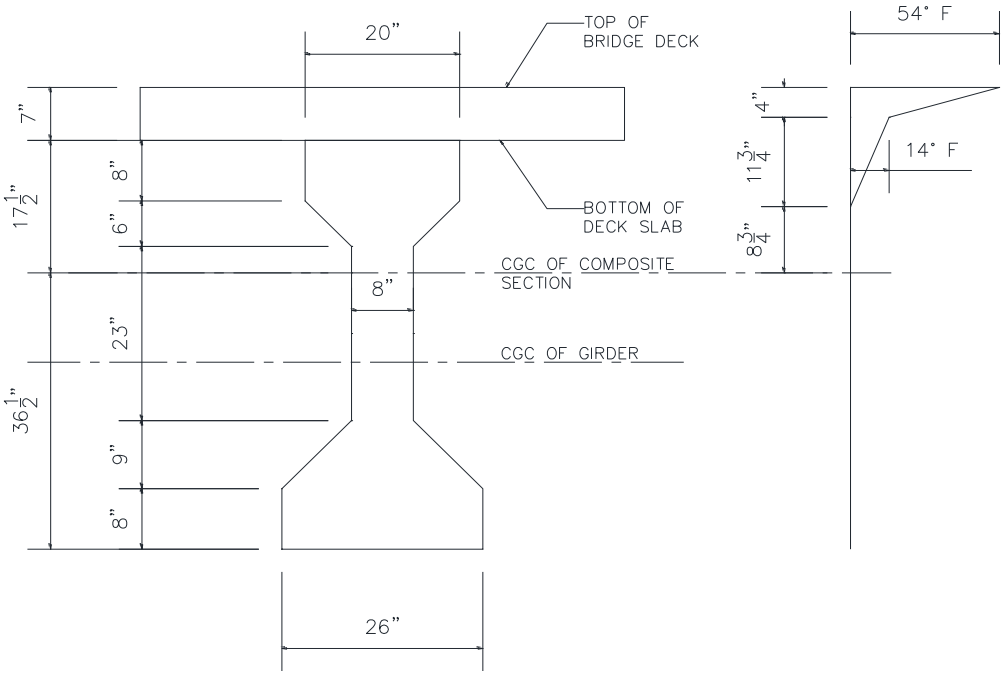

Figure 14 - AASHTO LRFD Thermal Stress Distribution (AASHTO, 2010)

4.5 Girder Design Parameters

1. Structural Concrete
   - Compressive strength at 28 days, f'c = 6 ksi
   - Coefficient of thermal expansion for concrete is taken as 6x10-6/^{o}F
2. Reinforcing Steel
   - ASTM A615 Grade 604, fy = 60 ksi (ASTM A615, 2009)
   - Modulus of Elasticity, E_s = 29,000 ksi (AASHTO LRFD Art. 5.4.3.2)

3. Prestressing Steel
    - Strands of 0.6-in diameter with ultimate stress f_{pu} = 270-ksi (AASHTO LRFD 2010) bundled using either 7 or 12 strands in a tendon
    - Modulus of Elasticity, E_p = 28,500 ksi (AASHTO LRFD Art. 5.4.4.2)
    - Friction coefficient of 0.25 and a wobble loss coefficient of 0.0015/ft.
4. Cover to Concrete
    - 1.0-in. minimum clear cover to reinforcement

4.6 Modified Design Approach

The dimensions of the trough girders provide a slender and economic section which carries the loads of the freight shuttle vehicle safely. The trough girders are chosen since they provide the maximum torsional stiffness and allow for shallower structural depth to be used. The section properties of the non-composite and composite girder section are computed. The composite section properties constitute the effective flange width of the girder. The modular ratio between the slab and the girder concrete is determined to compute the properties of the transformed composite section. The bending moments and shear forces due to live load are distributed to individual girders using simplified approximate distribution factors specified by the AASHTO LRFD (2010) Specifications. The distribution factors for moments due to live load are computed using AASHTO LRFD (2010) Table 4.6.2.2.2b-1 and Table 4.6.2.2.2d-1 for interior and exterior girders respectively. The distribution factors for shear due to live load are

computed using LRFD (2010) Table 4.6.2.2.3a-1 and LRFD (2010) Table 4.6.2.2.3b-1 for interior and exterior girders respectively.

A modified design approach involving the load balancing technique has been used for the girders in this project. The girders are designed for service loads and then checked for their ultimate capacity and stresses under live load and impact and temperature stresses. The pretension prestress layout for the trough girder and the I-girder are as shown in Figure 15 and Figure 16 respectively. The girders are pre-tensioned as simply-supported members for a total load of 1.2 times the unfactored self-weight of the girder to provide a factor of safety for the additional flexural stresses due to transportation and erection and to provide allowance for construction loads. For pretensioning of the girder, 0.6-in. dia. pretensioning strand with f_{pu} as 270-ksi ultimate strength of steel is considered. The initial stress in pretensioning strands at transfer f_{pi} is considered to be 0.7 f_{pu} (AASHTO LRFD Table 5.9.3-1) which is equal to 189-ksi.

A set of stress equations at transfer and at final are developed at the ends, maximum positive moment location and maximum negative moment location so as to develop a graph providing a feasible solution domain satisfying the allowable stress limits.

The equations are presented as follows: -

At girder ends - top fiber - final:

$$\frac{-F}{A} + \frac{F\,e}{S_{xt}} < f_t \tag{4.1}$$

At girder ends - top fiber - at transfer:

$$\frac{-F_i}{A} + \frac{F_i e}{S_{xt}} < f_{ti} \tag{4.2}$$

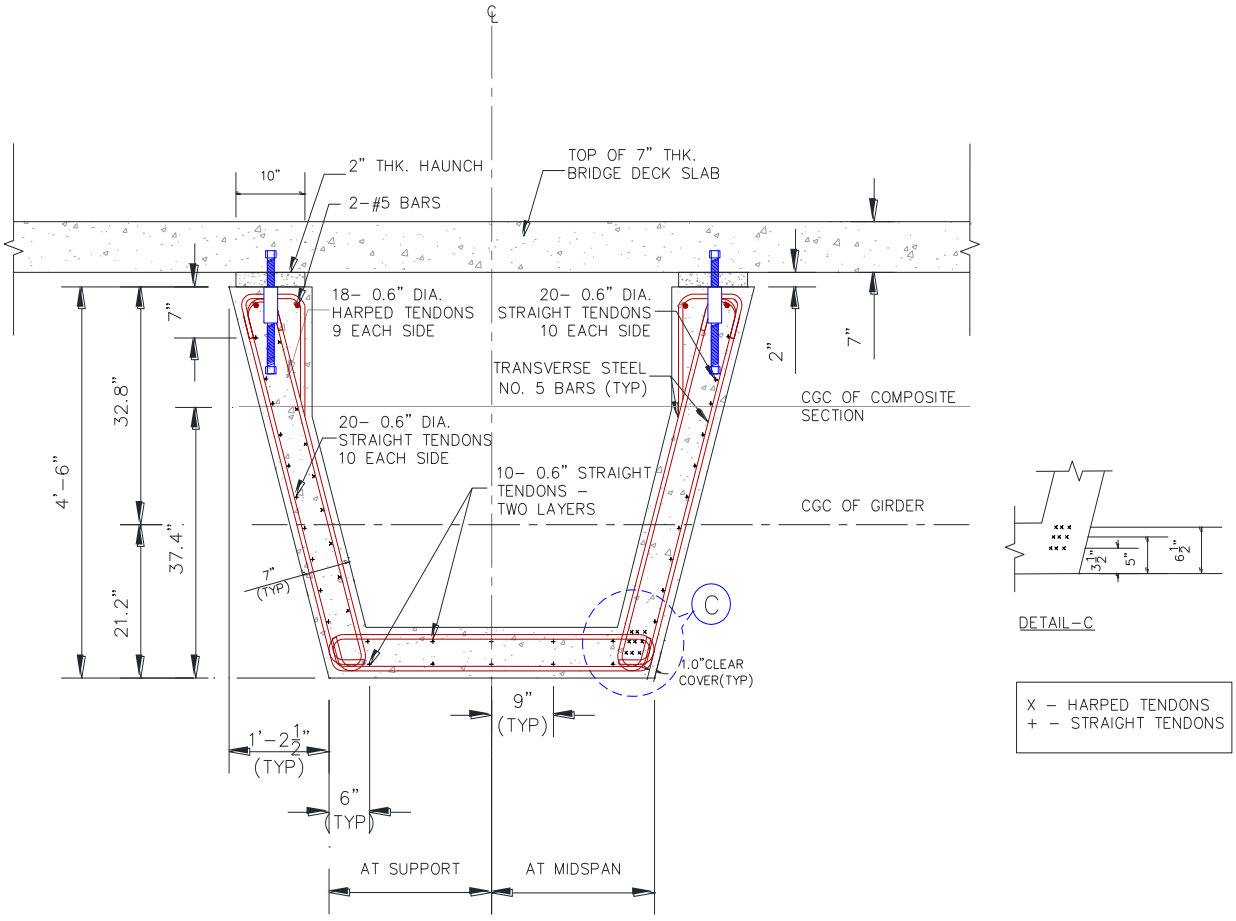

Figure 15 - Trough girder Pretension Prestress Layout

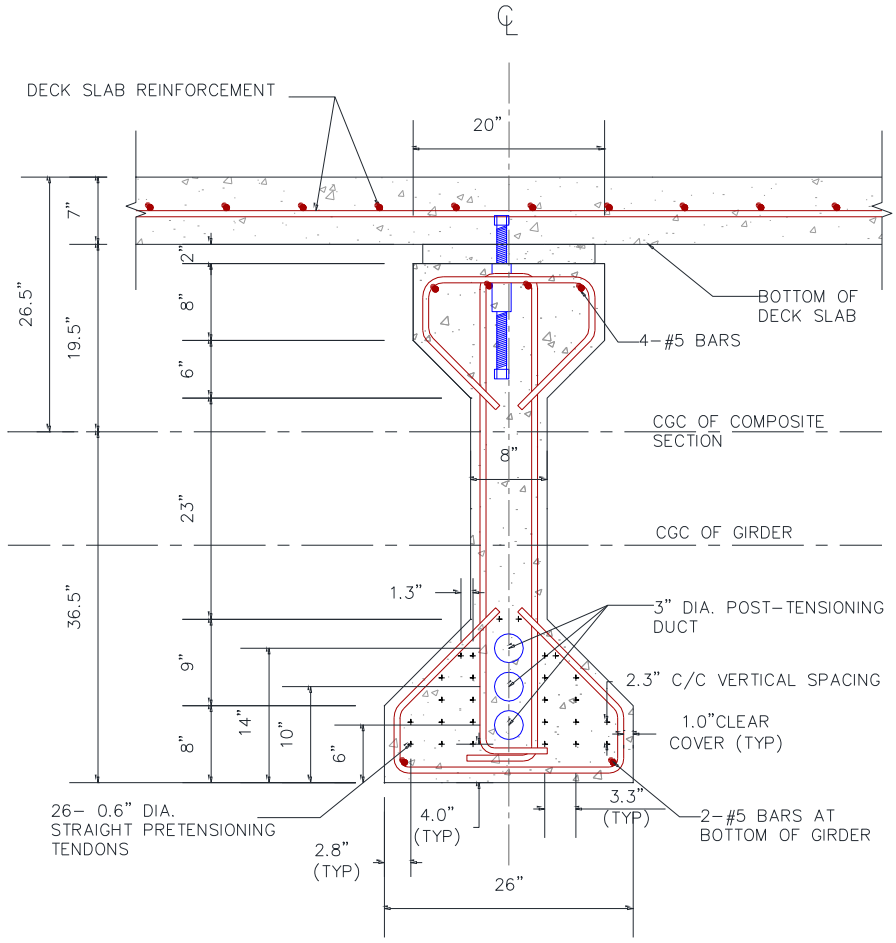

Figure 16 - I-girder Prestress Layout at Midspan

At girder ends - bottom fiber - final:

$$\frac{-F}{A} - \frac{F\,e}{S_{xb}} > f_c \tag{4.3}$$

At girder ends - bottom fiber - at transfer:

$$\frac{-F_i}{A} - \frac{F_i e}{S_{xb}} > f_{ci} \tag{4.4}$$

At midspan - top fiber - final:

$$\frac{-F}{A} + \frac{F\,e}{S_{xt}} - \frac{M_{D.C}}{S_{xt}} > f_c \tag{4.5}$$

At midspan - top fiber - at transfer:

$$\frac{-F_i}{A} + \frac{F_i\,e}{S_{xt}} - \frac{M_{D.C}}{S_{xt}} > f_{ci} \tag{4.6}$$

At midspan - bottom fiber - final:

$$\frac{-F}{A} - \frac{F\,e}{S_{xb}} + \frac{M_{D.C}}{S_{xb}} < f_t \tag{4.7}$$

At midspan - bottom fiber - at transfer:

$$\frac{-F_i}{A} - \frac{F_i\,e}{S_{xb}} + \frac{M_{D.C}}{S_{xb}} < f_{ti} \tag{4.8}$$

Boundary Constraints:

$$e > -y_t + \text{top cover} \tag{4.9}$$

$$e < y_b - \text{bottom cover} \tag{4.10}$$

Where,

F = Final force in the pretensioning strands after losses

F_i = Force at transfer in the pretensioning strands

e = Maximum eccentricity of the pretensioning strands from the C.G. of the girder

$M_{D.C}$ = Maximum moment in the simple span girder

A = Area of the girder section

S_x = Section Modulus

y = Depth of the neutral axis

f_t and f_{ti} = Allowable tensile service stress limit as specified in LRFD Art. 5.9.4.2

f_c and f_{ci} = Allowable compressive service stress limit as specified in LRFD Art. 5.9.4.2

The governing equations are identified from this graph forming the feasible domain and are solved so as to obtain the optimum maximum eccentricity and the final force in the tendons. The eccentricity of the strands is calculated from the centroid of the girder. Time dependent losses of 20 percent are considered at the final stages of pretensioning. The force at transfer is calculated after taking the losses into account to determine the optimum number of tendons required for pre-tensioning. A combination of straight and harped pretensioning is used for the trough girders while only straight pretensioning is considered for the I-girder. Straight pretensioning in I-girders is considered to reduce congestion of the pretensioning and the post-tensioning tendons in the 8-in. thick web of the AASHTO Type IV girder. The stresses in the girder section are checked after provision of pretensioning steel so that there is no moment due to eccentricity developed at the ends of the girder.

The losses in the prestressing force occur over time due to various reasons resulting in a reduced prestressing force. The prestress losses can be categorized as immediate losses and time dependent losses. The prestress loss due to initial steel relaxation and elastic shortening are grouped into immediate losses. The prestress loss due to concrete creep, concrete shrinkage and steel relaxation after transfer are grouped

into time dependent losses. The AASHTO LRFD (2010) Specifications specifies empirical formulas to determine the instantaneous losses. In this study, the approximate method of time-dependent losses given by AASHTO LRFD (2010) Article 5.9.5.3 is used for calculation of the percentage of time-dependent losses.

Once the girders reach the construction site, post-tensioning operations are carried out in two stages. Internal bonded post-tensioning is used for the I-girders and external unbonded post-tensioning is used for the trough girders. According to Crigler (2007), post-tensioning method of continuity between girders increases the span to depth ratio thus reducing the amount of construction materials and thus economizes the cost of the structure. This method helps to control other important parameters such as deflection, crack and long term durability.

Post-tensioning for I-girders is designed using internally bonded tendons. In case of a failure of the anchorage of the tendon, the loss of tendon force would be localized (Crigler, 2007). Post-tensioning of the girder in stages helps in increase in the amount of prestress that can be applied to the girder cross section and thus helps in maintaining longer spans. In the two stage post-tensioning approach, the girder is initially post-tensioned to balance the girder self-weight and the construction loads and then post-tensioned to carry the dead weight of the additional deck after the placement of the deck. Time dependent losses of 15 percent and friction losses of 15 percent have been considered for calculation of the final forces at transfer to determine the optimum number of tendons required for post-tensioning.

Post-tensioning for the trough girders is designed for externally unbonded tendons as shown in Figure 17.

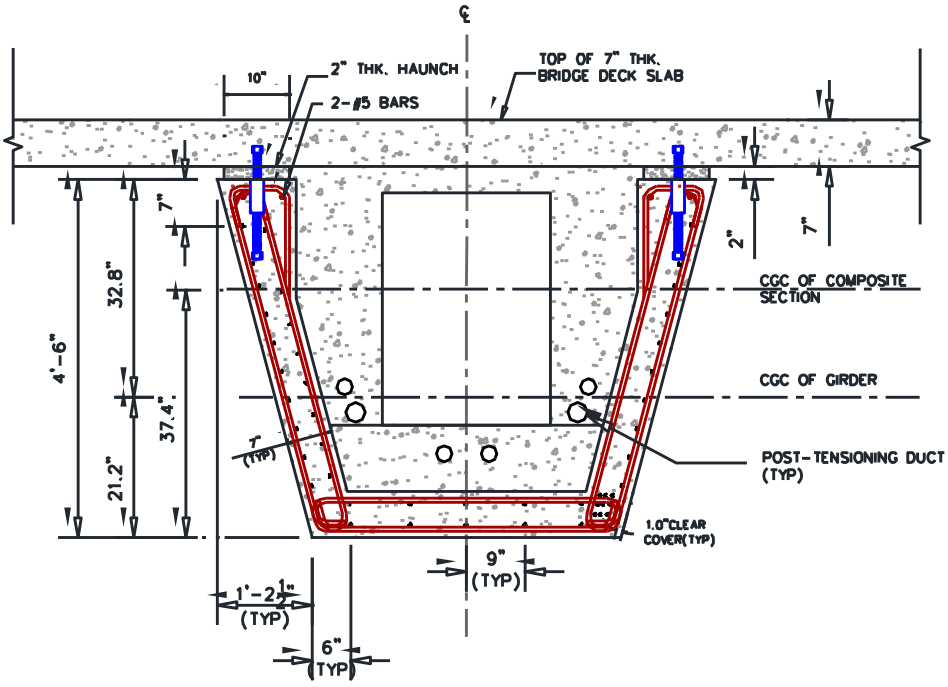

Figure 17 – Trough-girder Post-tension Layout at a Sample Section

According to Daly and Witarnawan (1997), the external unbonded post-tensioning system allows for greater control and adjustment of tendon forces, eases in inspection of loss of stress and damage in tendons due to impact or corrosion and also allows for replacement of tendons if required due to creep, relaxation or corrosion. The tendons can also be restressed in future for additional strengthening if necessary. Moreover the friction losses with external tendons will be lesser than internal bonded

tendons. Thus these external tendons can be provided in greater lengths and greater deviation angles. Anchorages and deviators can be installed easily in external post-tensioning.

The ultimate strength or capacity of the girder is checked using the plastic analysis mechanism. A graphic approach is adopted to relate the moment capacity with the bending moment diagram. The moment capacity of the girder is calculated based on the number, location and stress in the tendons. The design capacity of the girders is calculated at three locations: one-third span length of end span for maximum positive moment, face of diaphragm at support and at midspan of interior span. The design moment capacity of the girders is calculated considering a rectangular section behavior if the depth of the neutral axis of the composite section lies within the depth of the deck slab or a flanged section behavior for depth of neutral axis greater than the depth of the deck slab. The expressions for the depth of neutral axis and the moment capacity are computed as specified in AASHTO LRFD (2010) Art. 5.7.3. A rectangular section behavior is assumed initially to determine the depth of neutral axis.

The stress in the tendons is calculated as per the ACI Committee 318 (2008) Section 18.7. The equivalent uniformly distributed load is calculated from the live load moment as obtained from the live load analysis of the girder. The ultimate capacity of the girders is determined for Strength I Limit state. Load Factors and Load combinations are considered as specified in AASHTO LRFD Art. 3.4.1.

The total factored load effect is specified to be taken as

$$Q = \sum \eta_i \gamma_i Q_i \tag{4.11}$$

Where,

Q = Factored force effects

γ_i = Load factor, a statistically based multiplier applied to force effects specified by LRFD Table 3.4.1-1

Q_i = Unfactored force effects

η_i = Load modifier, a factor relating to ductility, redundancy and operational importance

$\eta_i = \eta_D \eta_R \eta_I$ = 1.00 in present case (LRFD Art. 1.3.2)

The following load combination for Strength I limit state is used in this case: -

$$Q = 1.25(DC) + 1.75(LL + IM) \quad \text{(LRFD Table 3.4.1-1)} \tag{4.12}$$

Thus a total factored load, Q = 1.25 (DC) + 1.75 (LL+ IM) is calculated. The plastic analysis is performed to find 'λ' using the following equation to cause a collapse mechanism under load 'Q': -

$$\lambda. (LL+IM) = Wu - 1.25 (DC) \tag{4. 13}$$

Where,

Wu = Equivalent uniformly distributed load computed from the Moment Capacity of the girders.

If this value of $\lambda \geq 1.75$, then the design is safe else the capacity of the section needs to be strengthened by providing additional mild steel. The final step is to ensure that the capacity is greater than the demand.

The primary thermal stresses are computed using the AASHTO LRFD (2010) temperature distribution parameters shown in Figure 14. Secondary temperature stress analysis is done by applying unit moments at the supports. These primary and secondary thermal stresses are combined to obtain the total thermal stress in the girder. The service stress analysis of the girder is performed after all the stresses are obtained. Final stresses at the midspan and the support are calculated by superposing the calculated stresses at the top and bottom of the girder under the various prestressing operations. The stresses are checked against the permissible values for the service limit state after losses as specified in AASHTO LRFD Art. 5.9.4.2. The allowable value for compressive stress is $0.45f_c'$ and for tensile stress is $0.19\sqrt{f_c'}$. Any stress exceedance is accounted for by providing additional mild steel reinforcement.

4.7 Girder Shear Design

A new approach has been used for shear design that integrates both the transverse shear (stirrup requirements) and the longitudinal interface shear between precast deck slab and girders (shear connectors). This is based on an advanced truss modeling approach first proposed by Kim and Mander (2007) and extended for non-contact splice deck-girder connectors by Brey (2010). The shear reinforcement and shear connector detail for the trough girder and I-girder are as shown in Figure 18.

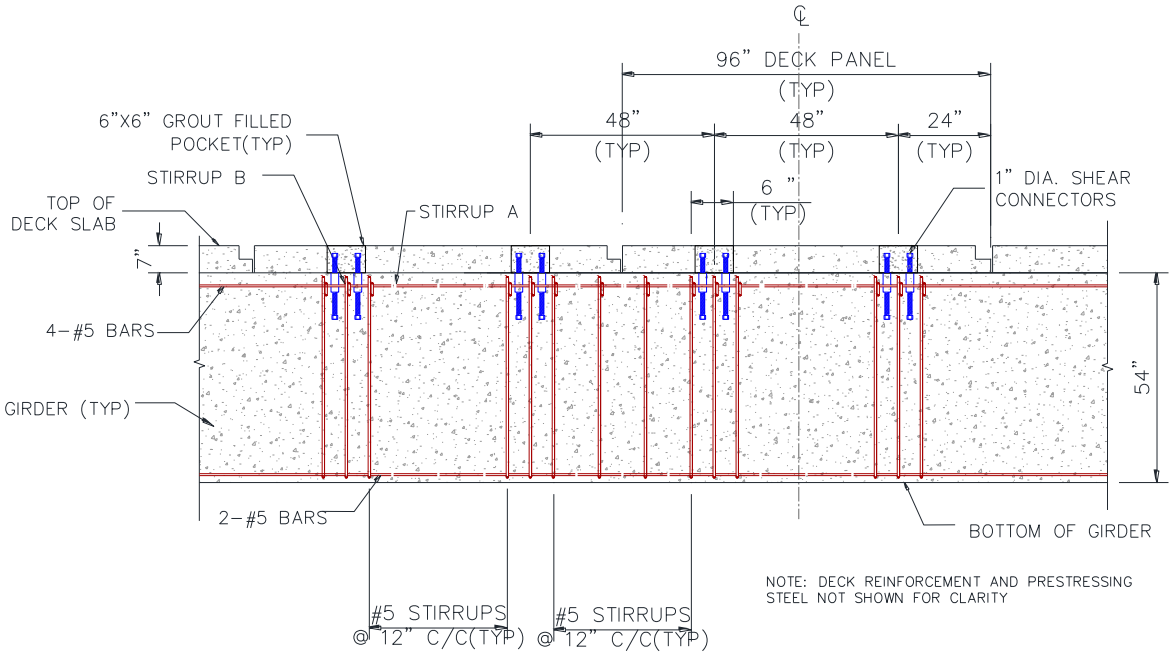

(a) Side Elevation of I- girder

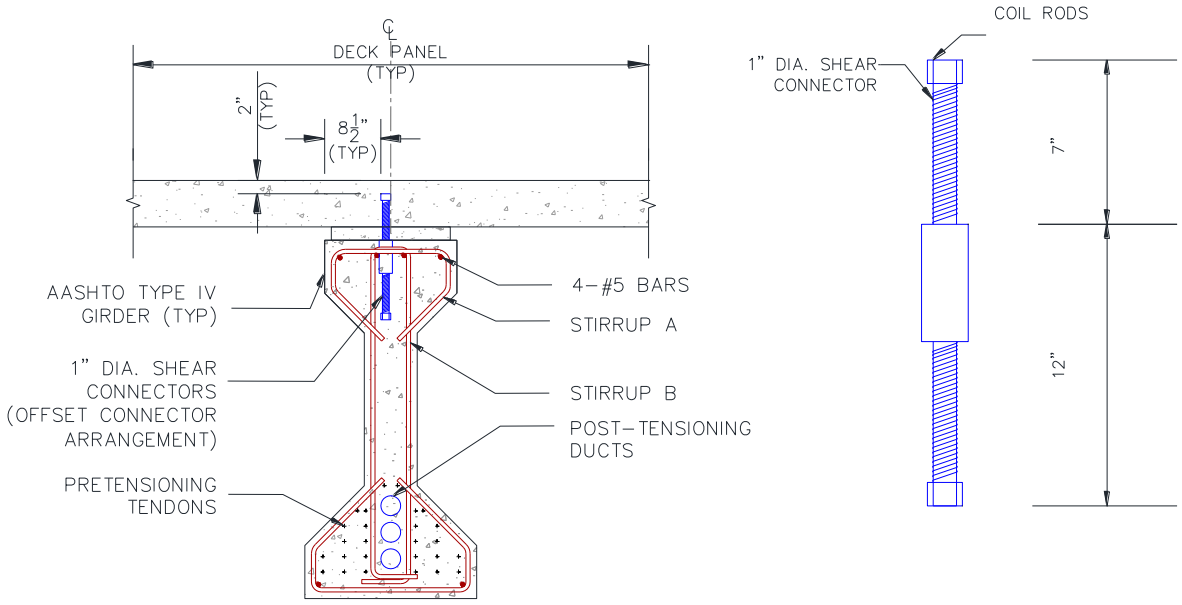

(b) Cross Section of I-girder Showing Shear Connectors

Figure 18 - Shear Connector Details for Girder

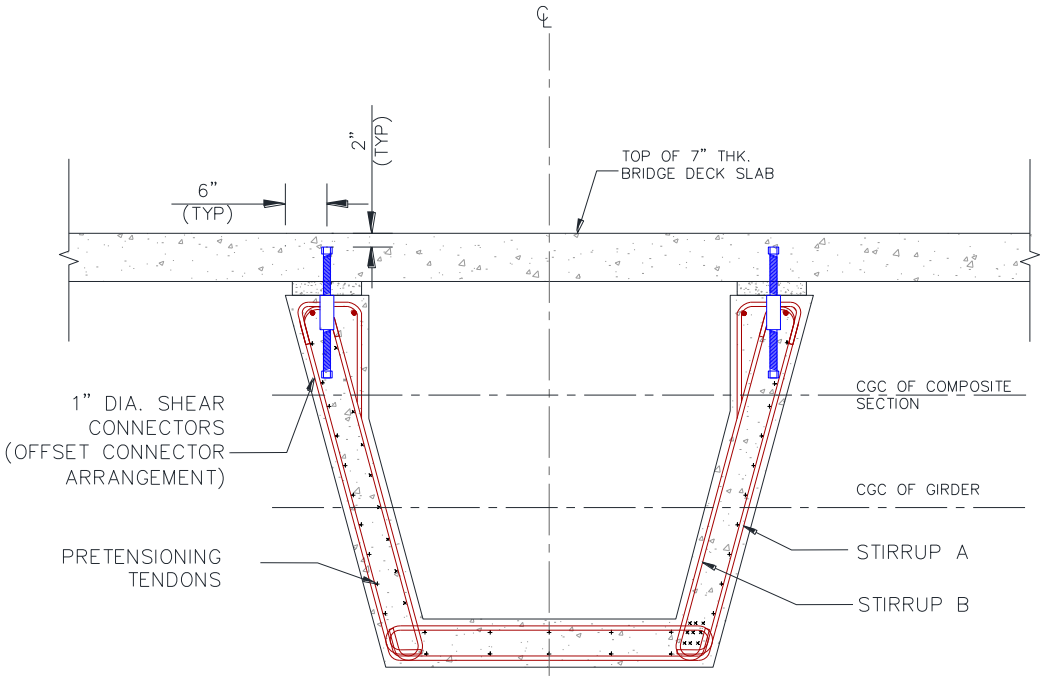

Figure 18 - Continued

The deck slab consists of panels 8’ long, 13’-1” wide and 7” thick and pockets of size 6” x 6”. These pockets are to be later filled with grout after placing the connectors. The shear connectors consists of two 1” dia. coil rods and having threads which are later coupled together to form the connector. The coil rods used in this design are chosen because they are economic (they are less expensive as compared to fine threaded rods and high-strength bolts). The bottom portion of the connector with the coupler is to be cast in the beam embedded up to a depth of 12 times the diameter of the connector. The top portion of the connector is to be placed 2 in. below the top of slab. The anchorage of the connectors is enhanced by placing nuts at the top of the connectors. An offset connector arrangement is provided for this design. Closely spaced hoops of No.5 bars at

6 in. are provided near the location of the connectors to resist the high pull-out force and hence prevent damage of the girder.

Shear connectors are used to transfer the horizontal shear between the deck and the girder. These connectors incorporate a composite action between the top flange of the girder and the deck which prevents the movement of the deck slab over the girder. This composite section has a higher capability to resist loads due to its increased section modulus. At ultimate limit state, for a cast-in-situ slab over precast, prestressed concrete girders, the cracks pass through the flange-web interface and a stress field analogous to a truss develops. This cracking proposes serious issues in case of precast deck panels with distinct deck-to-girder connectors which are widely spaced than the normal transverse shear reinforcement. The traditional beam theory disregards the decreased ability of shear stresses to transfer across open cracks. A truss model serves as one of the design methods that consider this cracking in a full-depth precast deck-on-girder system.

Several experiments were carried out by Mander et al. (2010), Henley (2009) and Brey (2010) examining connector capacity as well as deck-connector-girder interaction under interface shear. Brey (2010) then went on to use a truss modeling approach as shown in Figure 19, to evaluate the performance and interaction of deck-haunch-girder system using coil rod shear connectors and threaded rod shear connectors to design for shear forces created during service loading condition. He examined that the two main mechanisms causing failure in a bridge constructed with precast deck panels-on-precast prestressed concrete girders are: (i) Sliding shear between the deck panels and girder, and (ii) Web shear in the precast prestressed girders.

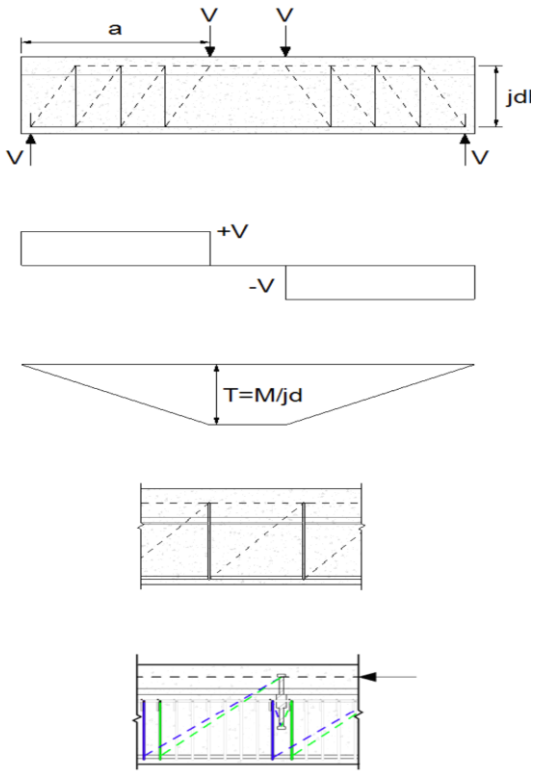

Figure 19 - Truss Model Representation of Cracked Deck-Girder System (Brey, 2009)

The shear connectors extend from the precast, prestressed girders into the pockets provided in the precast deck panel forming a non-contact splice. The friction caused by the connectors offers horizontal resistance to the sliding shear. The compressive force acts along the top chord of the truss model and as a result of equilibrium, an equal and opposite tensile force acts along the bottom chord. These two forces create a force couple which is equal to a resisting moment. The sliding shear capacity for a single panel is then determined by dividing the resisting moment by the length of the panel. The number of pockets can be determined such that the single deck panel shear capacity is greater than the shear demand. The spacing of the pockets is

dependent on the number of pockets present in a single line along the length of the deck panel. The non-contact splice that accommodates the shear connectors consists of a group of transverse hoops in the girder having a capacity exceeding the full tensile capacity of the shear connectors in a pocket. The number of transverse hoops in the group required to resist the tensile load of the shear connector are determined. The overall procedure follows the design of the transverse shear reinforcement to resist the net shear force within the girder and design of the connectors to resist a sliding shear mechanism at the interface between the deck panels and the girder. The shear capacity of the transverse shear reinforcement is determined from Kim and Mander (2005) for an expected crack angle in a girder under elastic conditions taking account of service loading with the given design of longitudinal and transverse reinforcement.

A minimum amount of the shear reinforcement in the girders is provided using AASHTO LRFD (2010) Art. 5.8.2.5. Shear reinforcement is designed and provided for the girders if the maximum shear in the section exceeds the nominal shear resistance provided by the concrete and the prestressing steel as specified in AASHTO LRFD (2010) Art 5.8.2.4. The girders are reinforced for shear and diagonal tension stresses considering a variable angle truss analogy with modified compression strength of concrete popularly known as “Modified Compression Field Theory”. This theory takes into account different factors such as strain condition of the section, and shear stress in the concrete to predict the shear strength of the section. This theory is believed to yield a more realistic estimate of the shear strength of the concrete. The shear strength of concrete is approximated based on a parameter β. The critical section for shear is

calculated based on the angle of inclination of the diagonal compressive stress, θ. The critical section for shear near the supports is taken as the larger value of $0.5d_v\cot\theta$ or d_v, measured from the face of the support. The effective shear depth, d_v is calculated as minimum of the distance of the resultants of tensile and compressive forces, 0.9 times the effective depth and 0.72 times the depth of the composite section.

4.8 Design Alternatives of Equivalent I-girder Sections

Different alternatives of design using equivalent I-girder sections are considered for a comparative study to arrive at an optimal solution for the proposed bridge system. For this project, the AASHTO Type IV girder section is used with specification details as shown in Figure 10. The different alternative designs using I-girders are as follows:-

a. Simply supported I-girders pre-tensioned to carry all the dead loads and live loads.
b. I-girders pre-tensioned to carry all the dead loads and made continuous to carry live loads and impact loads provided by additional mild steel in the deck.
c. I-girders pre-tensioned for self-weight and construction loads and post-tensioned for continuity (Two Stage Post-tensioning).
d. I-girders pre-tensioned for self-weight and construction loads and post-tensioned for continuity (Single Stage Post-tensioning).

From the results, it is found that the alternative (a) of using simply-supported I-girders failed primarily due to deflection under the live and impact load of the freight shuttle vehicle. The amount of prestressing steel is found to be uneconomical compared to other solutions. Replacing the two numbers of AASHTO Type IV I-girders with three

numbers supporting individual guideway provided satisfactory results for this case. Alternative (b) is found satisfactory for deflection but failed under tensile stress exceedance at top at midspan which may lead to development of cracks causing corrosion of deck reinforcement. This alternative is desirable because of the relatively simple construction but the amount of mild steel reinforcement required for continuity is uneconomical leading to congestion of reinforcement in the deck slab. Alternatives (c) and (d) present the post-tensioning solutions for the girders. Some of the advantages of this type of continuity system are elimination of end anchorage zone and congestion of reinforcement at ends in the girder section and better serviceability and durability of the deck by elimination of cracking. Alternative (c) provided satisfactory results and is found to be safe for all the allowable service stresses considered in the design. This alternative used a two-stage post-tensioning approach where the first stage post-tensioning balances the self-weight of the girder and second stage post-tensioning balances the weight of the deck to behave as a composite section for continuity. This design is further modified as alternative (d) to reduce the number of post-tensioning tendons by carrying out single stage post-tensioning balancing the whole weight of the composite section. The deflection for both the alternatives under the live load and impact load is found to be safe for allowable deflection as specified in AASHTO LRFD (2010) Art. 2.5.2.6.2.

Post-tensioning operation is expensive but this can be balanced with appropriate and efficient design of the girders with less number of substructure units and wider spacing between girders. Alternatives (c) and (d) provided constructible solutions for the

bridge and are compared with the proposed trough girders. The results of comparison are as shown in Table 6.

4.9 Comparison of Proposed Trough-girder Design with AASHTO Type IV I-girder Design

The proposed trough girder section used in the design of this research study provides a slender and economic section with web and flange thickness equal to 7" which is effective to carry the loads of the freight shuttle vehicle safely. A practical span/depth ratio of 30 is achieved by using this lighter and shallow depth section. The span of the girders considered is 140-ft. which facilitates easy transportation and erection of the precast sections to the site.

The trough girders provide the maximum torsional stiffness and allow for a smooth ride of the freight shuttle vehicle. They provide a structurally effective cross section as compared to the commonly used AASHTO Type IV I-girders particularly in Texas with a total weight in lb. /ft. about 40 percent less than the total weight of the I-girders required for the same bridge. Another important advantage of the trough shape of each girder is that it provides an inner void space of about 1025 sq. in. which can be used for multiple purpose like place for installation of the electrical conduits, fiber optical cables etc. in a protected non-exposed environment. Thus the shape and the void space of the trough girders prove to be highly beneficial.

External post-tensioning is used in the trough girders which facilitate easy installation of the tendons and reduced or no interruptions to the regular function of the structure. This is a deviation from the commonly used practices particularly in Texas where post tensioning is done using internally bonded tendons for the I-girders. According to Daly and Witarnawan (1997), external post-tensioning, allows for ease in inspection of loss of stress and damage in tendons due to impact or corrosion and also allows for replacement of tendons if required due to creep, relaxation or corrosion. The tendons can also be replaced in future for additional strengthening if necessary. Moreover the friction losses with external tendons will be lesser than internal bonded tendons thus these external tendons can be provided in greater lengths and greater deviation angles. Anchorages and deviators can be installed easily.

Table 6 – Comparison of Design Results for the Girders

PARAMETERS FOR COMPARISON	**PROPOSED TROUGH GIRDERS**	**AASHTO TYPE IV I GIRDERS**	
		Alternative (c)[Section 4.8]	**Alternative (d)**[Section 4.8]
Total Number of girders required	2 Nos.	4 Nos.	4 Nos.
Depth	54 in.	54 in.	54 in.
Total Area	2181 sq.in.	3156 sq.in.	3156 sq.in.
Total Weight	2272 lb./ft.	3288 lb./ft.	3288 lb./ft.
Total number of tendons for Pre-tensioning *(for Single Span)*	96 Nos.	104 Nos.	104 Nos.
Total number of tendons for Post-tensioning *(for Single Span)*	168 Nos.	208 Nos.	160 Nos.
Deflection under Live and Impact Load *(Allowable deflection as specified in AASHTO LRFD (2010) Art. 2.5.2.6.2. is equal to 2.10 in.)*	1.32 in.	1.49 in.	1.49 in.

CHAPTER V

MODULAR DAMAGE AVOIDANCE PRECAST CONCRETE BRIDGE PIERS

5.1 Chapter Summary

Construction of the superstructure and substructure at a reduced time without traffic disruption is a major concern in bridge construction. Precast concrete construction has brought about a highly efficient technique of modular construction. Precast concrete bridge piers are economical, durable, easily fabricated and constructed. This study compares two types of bridge pier system. One system comprises of the conventional method of pier design using cast-in-place reinforced concrete using mild steel reinforcing bars. The second system is the Damage Avoidance Design (DAD) which uses precast concrete pier reinforced with both mild steel and unbonded post-tensioning tendons and consisting of steel interface plates at the ends and the pier is made to rock on these interface plates. The results of both the designs is studied and compared to each other. The joints have been specially detailed preventing the formation of plastic hinges. The post tensioning contributes to the moment capacity of the column and thus reduces the requirement for longitudinal mild steel reinforcement than if it was designed using the conventional method of design practice. Moreover the Dywidag bars provide stiffness and as a means of anchoring the structure to the ground and thus increasing its lateral capacity in earthquakes.

5.2 Pier Design Parameters

1. Structural Concrete
   - Compressive strength at 28 days, f'c = 6 ksi
2. Reinforcing Steel
   - Reinforcing steel bars per ASTM A615 Grade 604, f_y = 60 ksi (ASTM A615, 2009)
3. Prestressing Steel
   - High-alloy high-strength Dywidag thread bar of 1.5 in diameter with f_{pu} = 160 ksi.
   - Friction coefficient of 0.25 and a wobble loss coefficient of 0.0015/ft.
4. Cover Concrete
   - 2 in. minimum clear cover to reinforcement.

5.3 Design Loads

The superstructure contributory area load on each column is calculated. Table 7 gives the loading considered on a single pier bridge structure.

Table 7 – Design Load on Pier

TYPE OF LOADING	LOAD ON SINGLE PIER
Dead Load of superstructure	1342 kips
Live Load of superstructure	223 kips

5.4 Design of Conventional Piers

Reinforced concrete columns have been the most common type of conventional pier design. Spiral circular columns and tied columns are the two frequently used types of reinforcement arrangement in columns. Tied columns are mostly used in non-seismic regions and spiral columns are used in regions of high seismic activity. Spiral circular piers have been considered for this project since ductility is an essential issue in the high earthquake prone regions. Moreover, this arrangement makes it economical to utilize the extra strength resulting from the higher φ factor.

The ACI Committee 318 (2008) column interaction diagrams have been used to calculate the percentage of reinforcement required for the pier design. This percentage of reinforcement obtained from the interaction charts is multiplied with the gross cross sectional area of the column to obtain the reinforcing area of steel required. The amount of spiral reinforcement ratio is calculated from the spiral reinforcement ratio which is the ratio of the volume of spiral reinforcement to the volume of the core measured out-to-out of the spirals. The center to center spacing of spirals is calculated as per the ACI Committee 318 (2008) Eq. 10-6.

Figure 20 shows the reinforcement detail of the single and twin pier designed as per the conventional method of ductile design and detailed as per ACI Committee 315 (2004). This design of conventional piers designed as per ductile design results in damage at the plastic hinge zone which is irreparable thus affecting the serviceability of the bridge pier after an earthquake (Mander et al., 1997). Thus the Damage Avoidance Design is established to reduce post-earthquake damage.

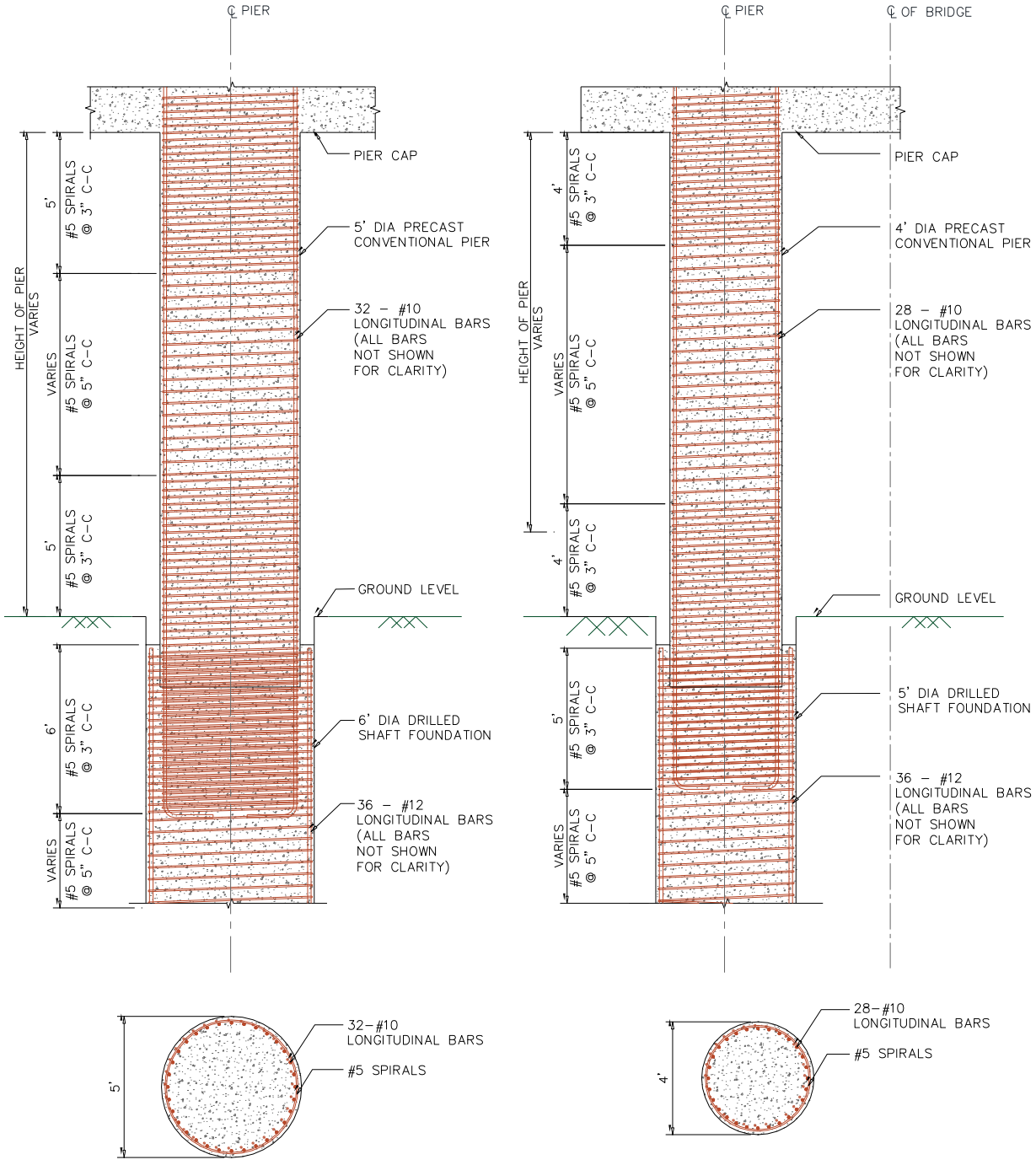

Figure 20 - Reinforcement Detail of Single and Twin Conventional Pier

5.5 Design Procedure of DAD Piers

Precast concrete construction has brought about a highly efficient technique of modular construction. Use of precast piers have resulted in the quality control of the products, reduction in the construction time and a more environment friendly surrounding with maximum work zone safety.

Damage Avoidance Design has been found to be highly beneficial in high earthquake prone areas. This concept of rocking structures in bridge piers have been proved highly efficient by Mander and Cheng (1997) and Hewes and Priestley (2001). A displacement-based design method was adopted by Mander and Cheng (1997) to evaluate the force-deformation capacity of the structure through rigid body kinematics. This concept was investigated and adopted for bridge piers subjected to both unidirectional and bidirectional earthquakes. This concept of Damage Avoidance Design has been incorporated in the bridge pier design system for this project due to its modularity, serviceability and reduced life cycle costs in seismic zones.

The bridge pier considered is 16-ft. high and having longitudinal spans of 140-ft. length on each side with a span width of 2-ft. – 2-in. Two alternatives of single pier and twin pier are considered for the bridge pier system. The seismic weight of the superstructure on an end pier is calculated to be 1350 kips. The pier is assumed to be located in a highly seismic zone in United States with the Design Basis Earthquake (DBE) as 0.4g. The moment demand is calculated for pier based on its base shear capacity, height of seismic center of mass and weight of superstructure on the pier. The

moment capacity of the DAD pier is contributed by a combination of gravitational load, longitudinal unbonded tendons, and additional energy dissipater devices. Rigid body kinematics is considered to be the mechanism for the behavior of the pier to earthquake effects (Solberg et al., 2009). The moment necessary for uplift is calculated by,

$$M_y = (P + F).\frac{B}{2} + A_s.\sigma_y.\frac{2e + B}{2} \tag{5.1}$$

In the above equation, P is the axial load on the pier due to gravity, F is the effective prestress, B is the width of the rocking base of the column, A_s is the cross sectional area of the energy dissipaters, σ_y is the yield stress of the energy dissipaters and e is the eccentricity of the energy dissipaters from the center line. The required moment capacity of the pier is achieved by modifying the geometry of the interface plates or by adding additional prestress or energy dissipaters (Solberg et al., 2009).

The displacement of the pier at uplift is calculated to investigate the elastic behavior of the pier. The displacement of the pier is a function of I_{eff}, the effective moment of inertia of the cross section of the pier. I_{eff} is taken as 0.25 I_{gross}. Formation of plastic hinge is prevented in a Damage Avoidance Design pier since the post-yield response of the DAD pier is limited to the rocking region (Solberg et al., 2009). Thus it is detailed as per the nominal longitudinal and transverse steel requirements. The shear reinforcement requirements are calculated based on the ACI Committee 318 (2008) Code Provisions.

Figure 21 shows the reinforcement detail of the single and twin pier as per the Damage Avoidance Design.

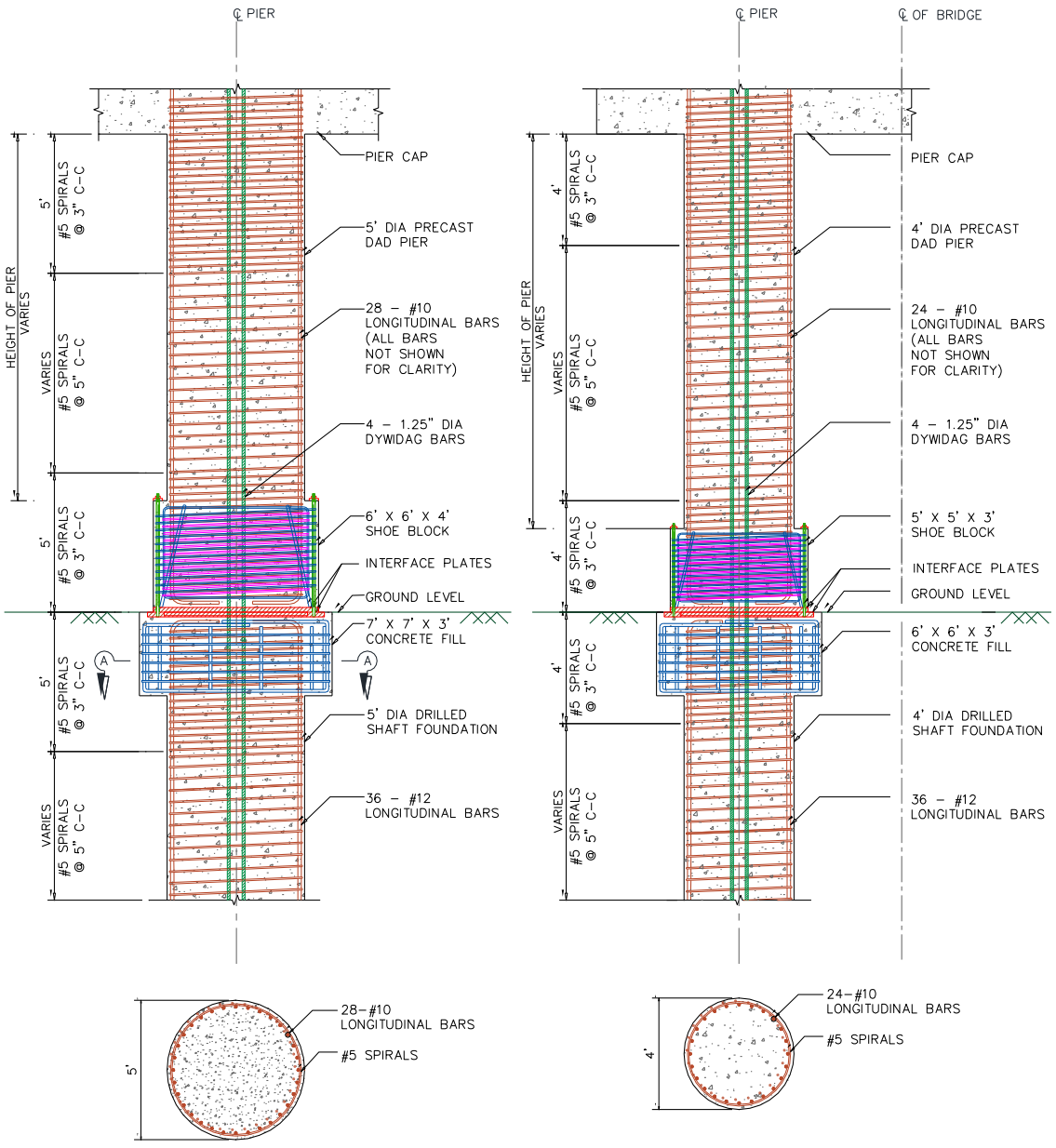

Figure 21 - Reinforcement Detail of Single and Twin DAD Pier

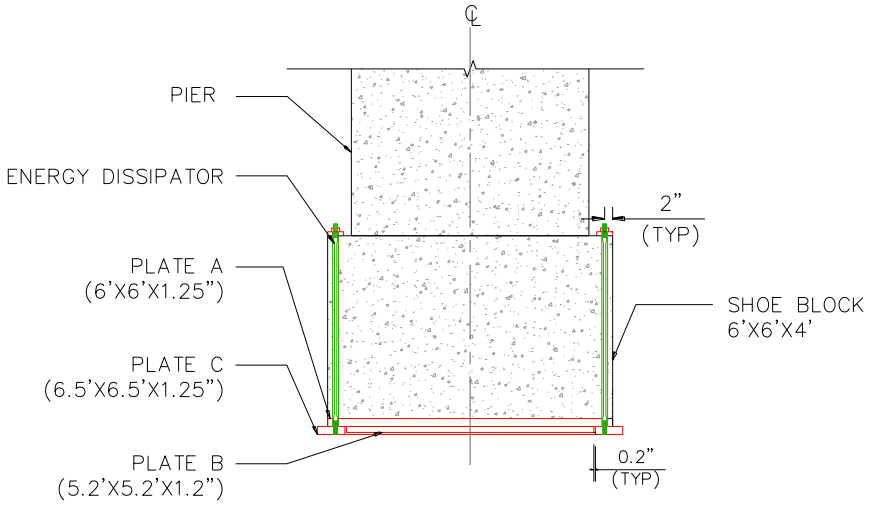

(a) Geometry of Shoe Block and Interface Plates

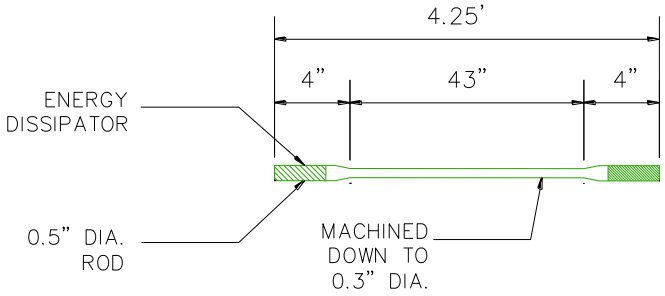

(b) Energy Dissipater Details

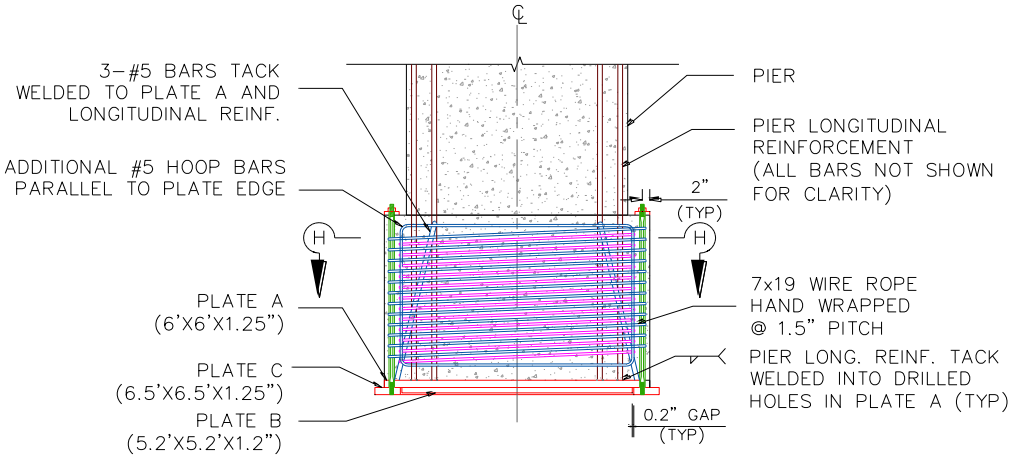

(c) Reinforcement Details of Shoe Block

Figure 22- Shoe Block Details

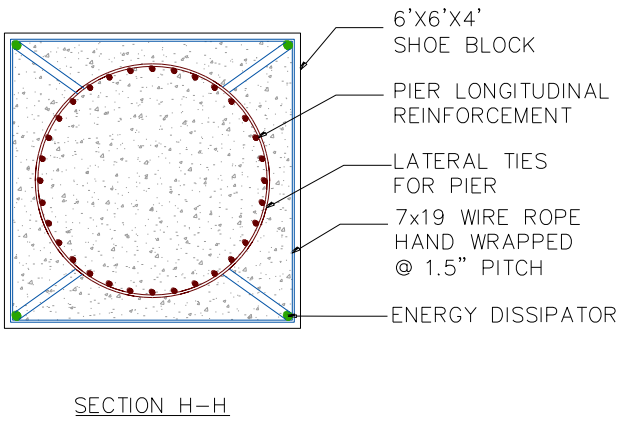

(d) Plan view showing Reinforcement Arrangement in Shoe Block and Pier

Figure 22- Continued

The single pier system requires a 5-ft. dia. column and a twin pier system requires 4-ft. dia. twin piers to carry the superstructure load. Four number of 1.25in. diameter Dywidag bars have been used for the unbonded post-tensioning of the piers. Figure 22 shows the shoe block details for the DAD pier. Interface plates A, B and C is used at the bottom of the pier to act as the armoring rocking surface. The interface at the base of the column is to be constructed by bolting plate B with plate A to form a shear key which will help in resting the plate in the square hole of plate C. A small gap is placed on both sides of the steel plates to prevent rubbing against the surface during the rocking phenomenon. Longitudinal reinforcement is to be tack welded into the holes drilled in plate A. No. 5 spirals are to be wrapped around these longitudinal bars. Three No. 5 bars should be tack welded to plate A at each corner and to the pier's longitudinal reinforcement to create a diagonal mechanism to resist the expected strut forces (Solberg, 2007). Additional hoop bars are to be placed parallel to the edge of the plate.

Two layers of high strength wire rope of the type of wire rope 7x19 are wrapped around the inner diagonal reinforcement and the outer cage to improve the confinement of concrete and prevent excessive cracking. The energy dissipaters used are No. 4 threaded bars with central 43 in. segment machined down to 0.3 in. diameter. The energy dissipaters are designed for tension only and are screwed vertically into plate C through ducts at the corner of each plate and should be stressed to 0.5 f_y by a torque wrench. They can be replaced after an earthquake occurrence. Thus the concentrated axial loads are well resisted by the connection at the pier-foundation interface. The energy dissipater devices help in providing additional lateral resistance and can be removed after an earthquake occurrence (Solberg, 2007).

5.6 Comparison of Conventional and DAD Pier Design

The study compared two types of bridge pier system. One system comprises of the conventional method of pier design using cast-in-place reinforced concrete using mild steel reinforcing bars. The second system is the Damage Avoidance Design (DAD) which uses precast concrete pier reinforced with both mild steel and unbonded post-tensioning tendons and consisting of steel interface plates at the ends and the pier is made to rock on these interface plates. The results of both the designs is studied and compared to each other as shown in Table 8.

Table 8 - Reinforcement Details of Single and Twin Pier

DESIGN TYPE	SINGLE PIER	TWIN PIER
Conventional Design	32- # 10	28- # 10
Damage Avoidance Design	28- # 10 + 4- 1.25-in. Dywidag bars	24- # 10 + 4- 1.25-in. Dywidag bars

Two design options have been provided for appropriate use in seismic and non-seismically active zones. It was found by investigations and research carried out by Mander et al. (2007) that the Damage Avoidance Design is more effective in seismically active zones with minimal damage. The lack of severe damage in this bridge pier system was found to potentially reduce the life-cycle costs of the bridge and negligible displacements ensured higher serviceability after an earthquake. The post tensioning contributes to the moment capacity of the column and thus reduces the requirement for longitudinal mild steel reinforcement than if it was designed using the conventional method of design practice. Moreover the Dywidag bars provide stiffness and as a means of anchoring the structure to the ground and thus increasing its lateral capacity in earthquakes.

CHAPTER VI

CONSTRUCTION OF PROPOSED BRIDGE SYSTEM

6.1 How to Construct the Bridge before Designing?

Large infrastructure projects are characterized by mass construction, extensive project duration. The choice of the method of construction plays a very important role in the overall cost of the bridge structure. The technological aspects of construction combined with the design concepts determine economic viability of any project. Inappropriate methods of bridge construction causes further traffic delays and congestion in addition to the daily traffic volume. Hence the development of faster methods of construction of the bridge is very essential. One of the most efficient method of bridge construction is the use of precast, prefabricated systems which are manufactured at the precasting plant and then brought to the job site and assembled together to connect the components. A precast concrete system proves highly beneficial in places where the components are used repeatedly for mass construction since the same moulds and formwork can be used for repetitive production and the contractor gets familiarized with the type of construction after a short construction time. This standardization of elements will lead to reduction in fabrication cost by reusable formworks, will enable faster construction and thus reduces the overall economy of the project. A comprehensive evaluation of the current state of practices for bridge construction has been studied for this project and the most feasible solution for this project is suggested. An integration of the design philosophy with the construction

technique has been done to device a system which is flexible and adaptable to the different bridge configuration, location and different construction schedules.

The type of various bridge elements is chosen based on the constructability issues. The full depth precast concrete deck panels require very less formwork as compared to conventional cast-in-situ concrete deck slabs. These full depth precast panels allows for deck replacement and any repair maintenance required in future. This repair maintenance work can be done overnight. This contributes to a major advance to this project since the precision and perfect alignment of the bridge elements plays a major role for the smooth working of the Freight Shuttle. The use of precast substructure helps in reducing construction by eliminating the time for erection of formwork, placement of reinforcement cage, casting and curing of concrete. The precast concrete girders similarly reduced the construction time.

The drilled shaft foundations proposed for this project also contributes towards the accelerated and efficient bridge construction. This construction reduces noise pollution like in case of pile driving and also reduces damage to the adjacent structures. The equipment used for the construction of drilled shafts consists of drilling augers mounted on cranes which are very mobile and rapid means of drilling in any type of soil conditions. The drilled shaft foundations reduce the number of elements required in a foundation as compared to pile groups.

Thus this precast construction will contribute to the management of time, cost, quality and safety.

6.2 Steps involved in the Construction of the Bridge System

Figure 23 shows an overview of the procedure for the proposed bridge system. A step by step procedure of the construction activities are further explained in a sequential manner.

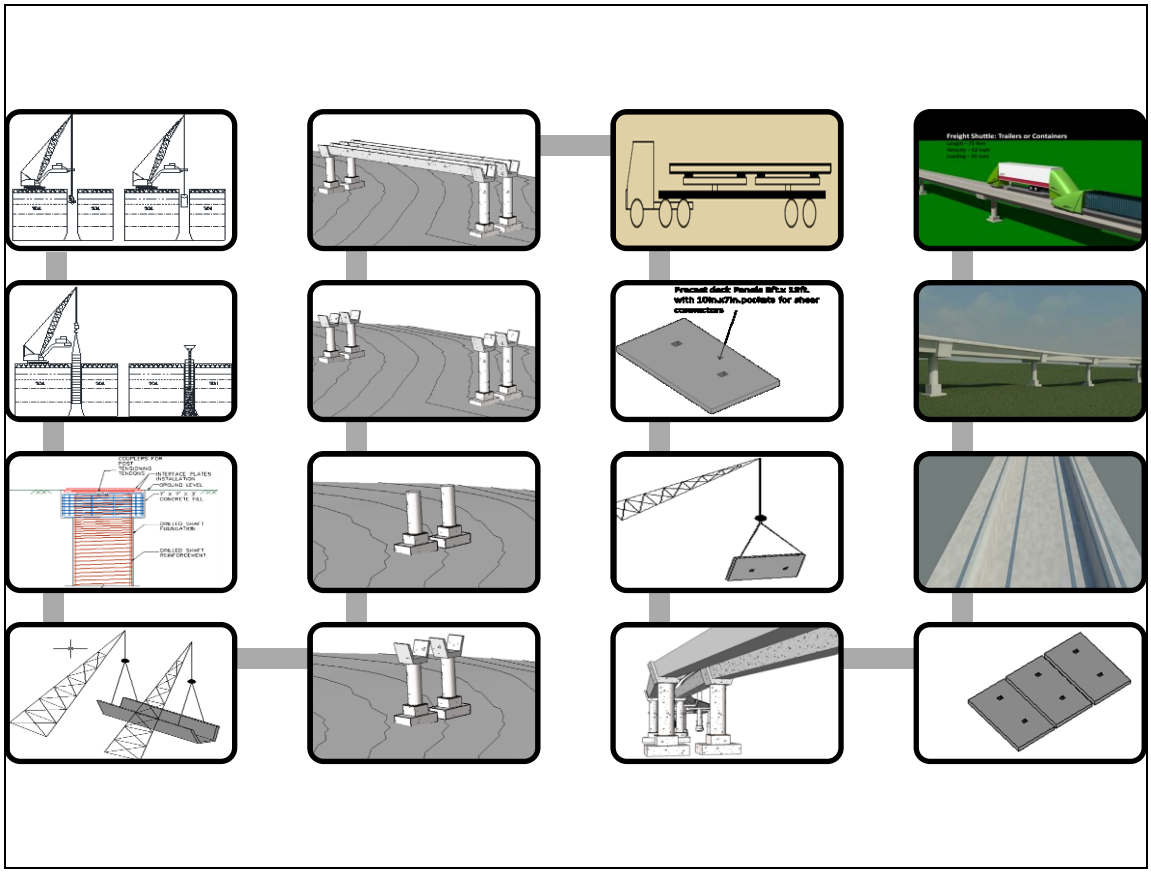

Figure 23 - An Overview of Construction Procedure for the Proposed Bridge System

Step 1 - Drill Shaft Boring and Dewatering (if required)

Figure 24 shows the procedure of drilled shaft boring to a desired depth and dewatering-if necessary by the drilling contractor. Three types of drill shaft construction can be done depending on the type of the soil. The types include dry shaft, wet shaft and cased shaft construction. In dry shaft construction, the drilled shaft is bored to the design depth and the dewatering is done to remove any accumulated loose material. In wet shaft construction, soil stabilization slurry is put into the drilled shaft to prevent the surrounding soil of the shaft from caving in. Cased shaft method of construction is to be used in soils with excess tendency to undergo collapse or deformation.

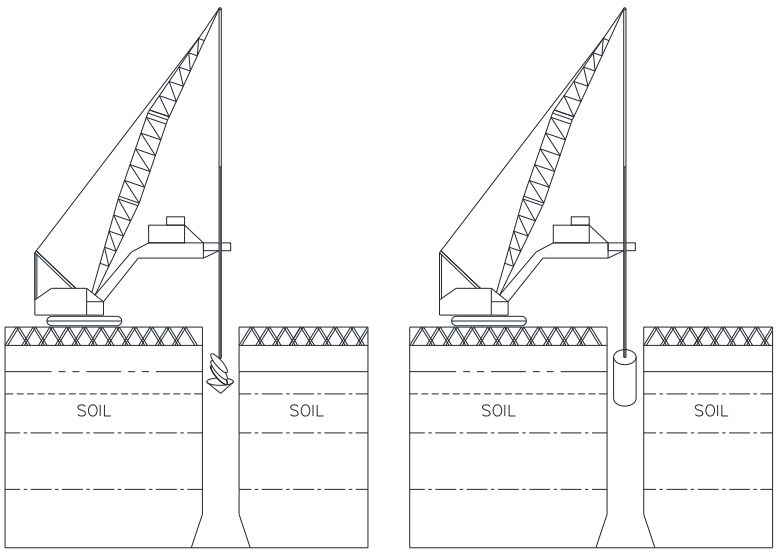

Figure 24 - Drill Shaft boring to designed depth and dewatering

Step 2 - Reinforcement Cage Placement and Concrete Casting

Figure 25 shows the placement of reinforcement cage and concrete casting by the foundation contractor.

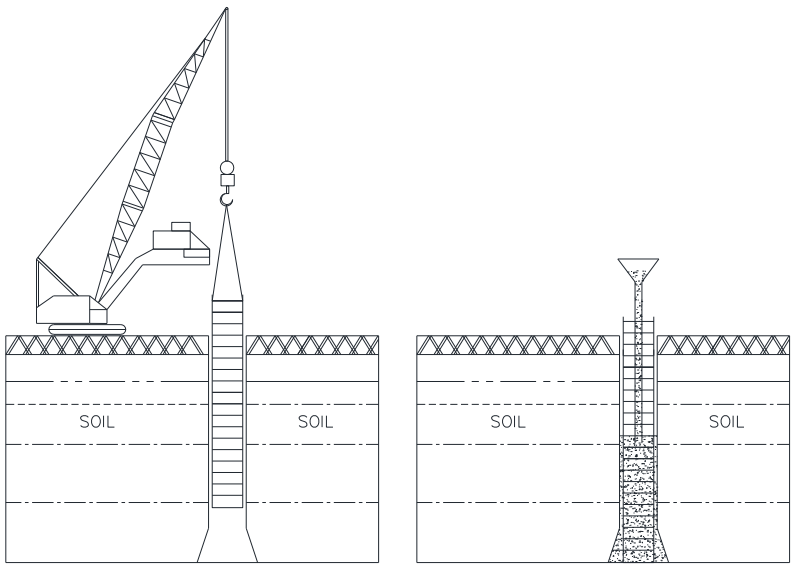

Figure 25 - Positioning of Reinforcement Cage and Concrete Casting

Step 3 – Construction of Concrete Fill, Installation of Steel Armoring Plates

Figure 26 a and b shows the excavation for concrete fill and placement of reinforcement cage for concrete fill respectively by the building contractor

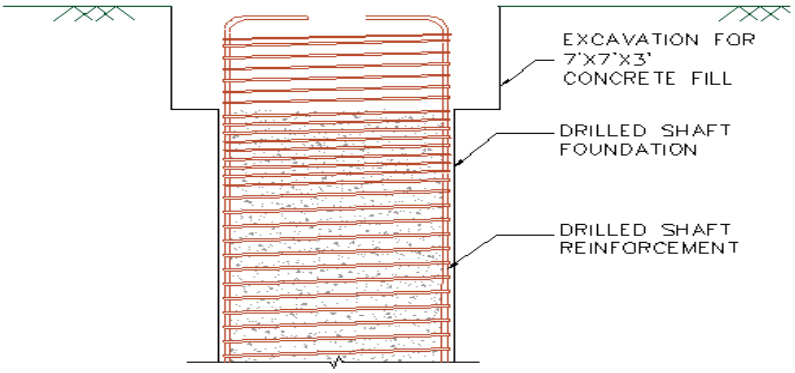

(a) Excavation for Concrete Fill

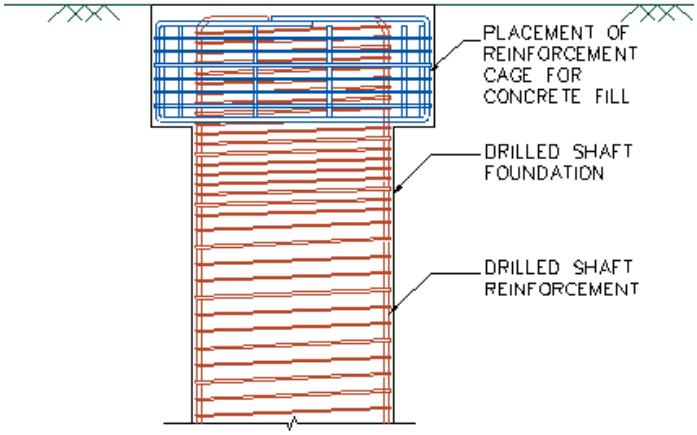

(b) Placement of Reinforcement cage for Concrete Fill

Figure 26 - Construction of the Concrete Fill

Figure 27 shows the installation of steel armoring plates for the DAD pier and the coupler installation for the post-tensioning tendons.

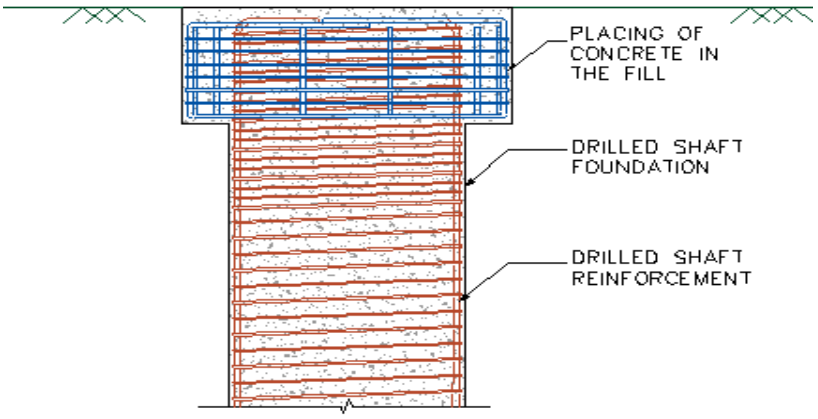

(a) Placing of Concrete in the fill

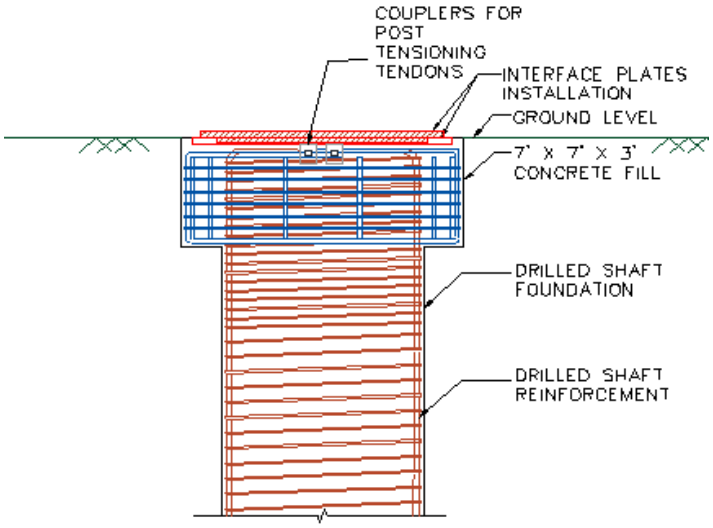

(b) Installation of interface armoring plates and couplers for Post-tensioning

Figure 27 - Installation of Steel Plates and Couplers

Step 4- Placement of DAD Pier and Concreting of Shoe Block

Figure 28 shows construction of the DAD Column and Shoe block. The concreting of the shoe block is done after the leveling of the column by the general contractor.

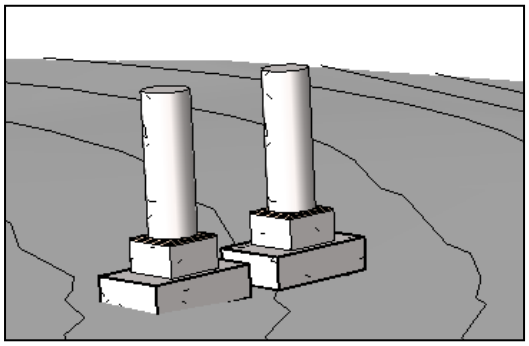

Figure 28 - Construction of the DAD Column and Shoe block

Step 5 – Placement of Pier Cap Beam

Figure 29 shows the placement of the precast pier cap beam after the piers are in place by the building contractor.

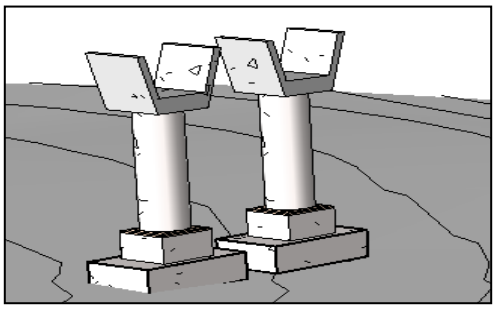

Figure 29 - Pier Cap Beam Placement

Step 6 – Lifting of girders and Seating of spans

Figure 30 gives the step by step procedure of lifting the girders and then placing them over the spans. The girders are to be transported to the site using high capacity trailer trucks and then lifted to place suing hydraulic or crawler cranes.

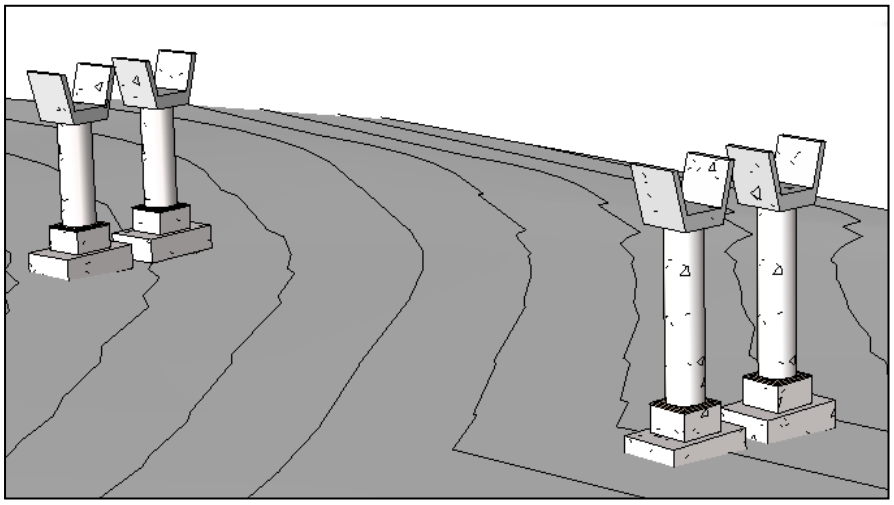

(a) Piers with Precast Pier Cap Beams ready for Girder Placement

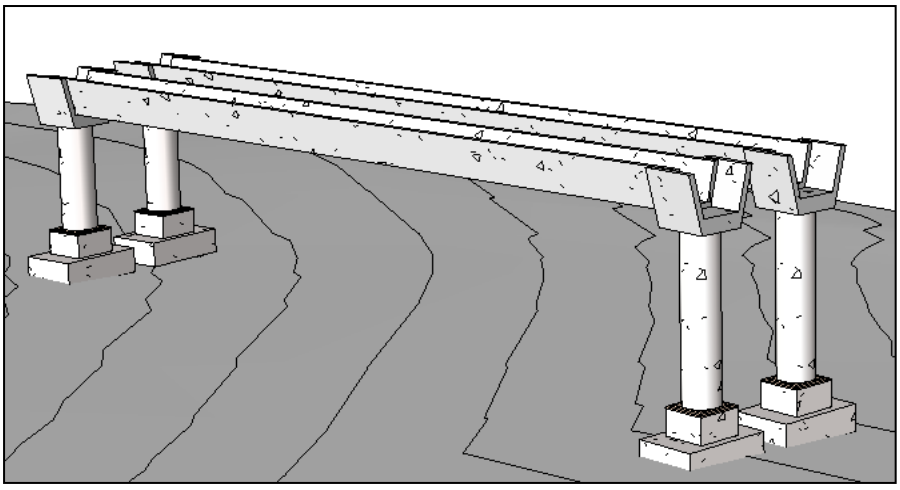

(b) Placement of Precast Concrete Pretensioned Girders

Figure 30 - Seating of Precast Concrete Girder Spans

Step 7 - Joining the Girder Segments

Figure 31 shows the precast concrete girders placed on the spans by the building contractor.

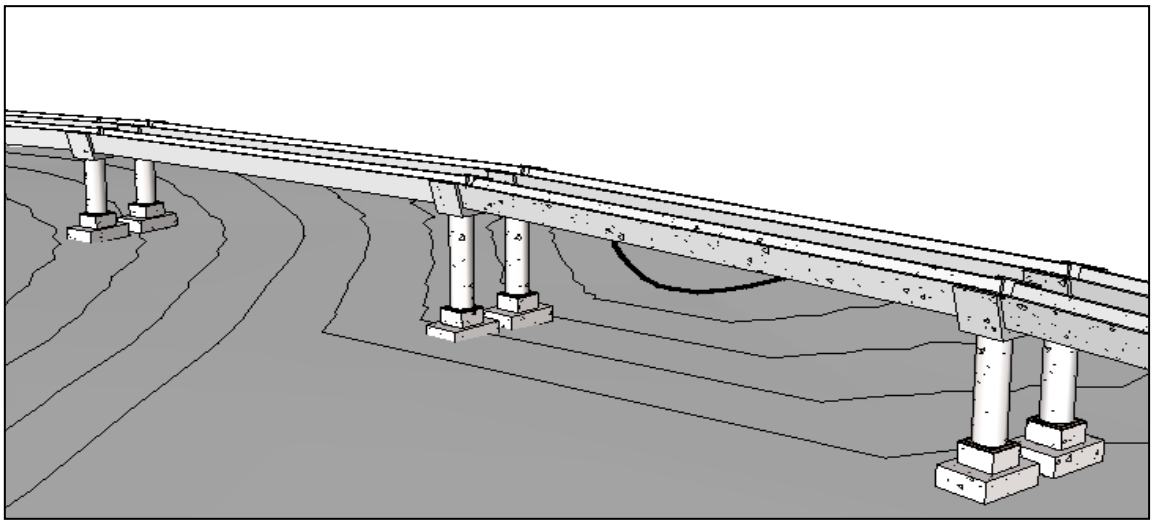

Figure 31 - Joining of Precast Girder Segments

Step 8 – Post-tensioning of Girders and Precast Columns

After placing the girder spans in place, the stage 1 post-tensioning is to be carried out making the girders continuous.

Step 9 – Transportation and Placement of Precast Deck Panels

Figure 32 explains how the precast concrete deck panels are transported to the site and lifted using cranes and then placed on the precast concrete girders. This operation is carried out by the building contractor. Full depth precast panels are used for

the deck. After transportation of the panels to the job site, the panels will be ready to be erected on the girders. The panels will need to be leveled using leveling screws or shims to provide a smooth ride of the freight shuttle vehicle.

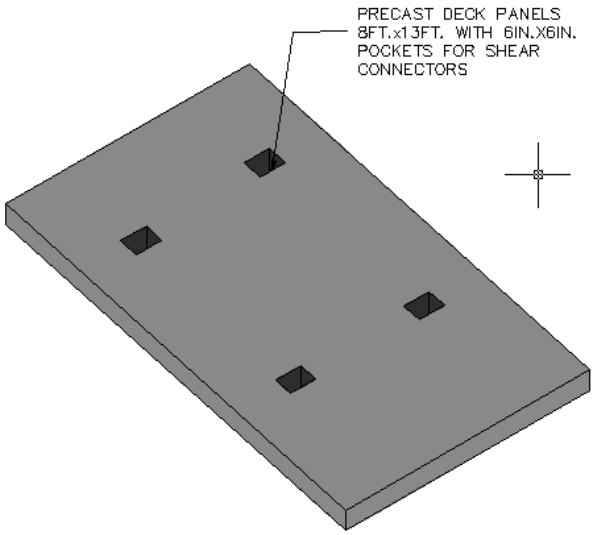

(a) Precast deck Panels 8-ft.x 13-ft.with 6-in.x6-in.pockets for Shear Connectors

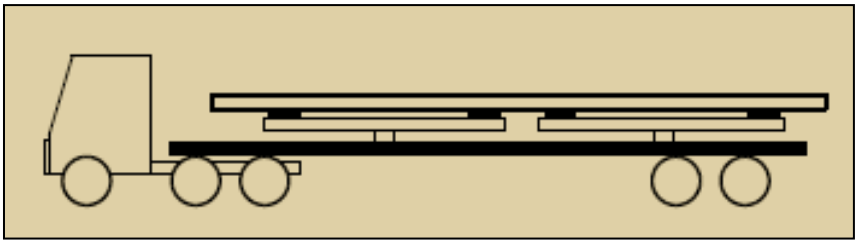

(b) Transportation of Precast Concrete Deck panels to the job site

Figure 32 - Construction of Bridge Deck Panels

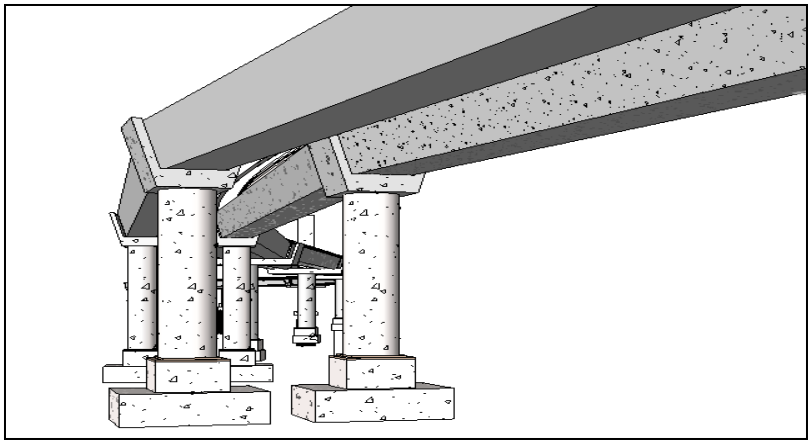

(c) View 1 of the bridge with the Precast Concrete Trough-girders in place

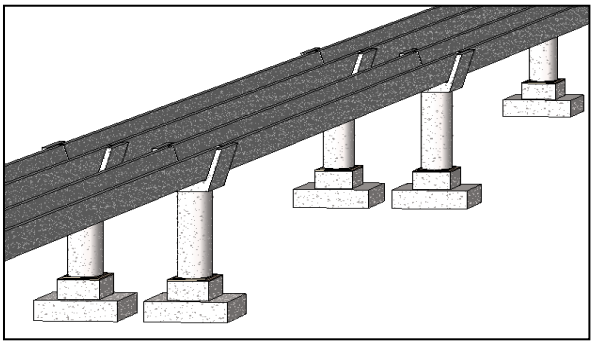

(d) View 2 of the bridge with the Precast Concrete Trough-girders in place

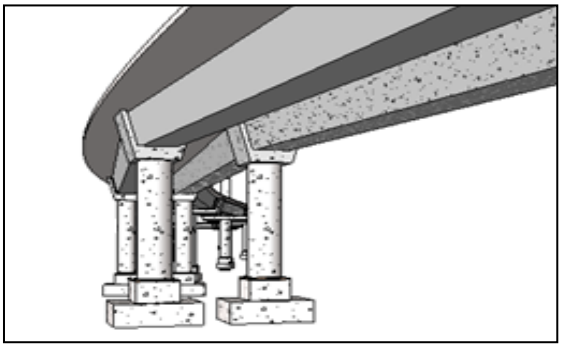

(e) View 3 of the Bridge with the Precast Deck panels installed

Figure 32 - Continued

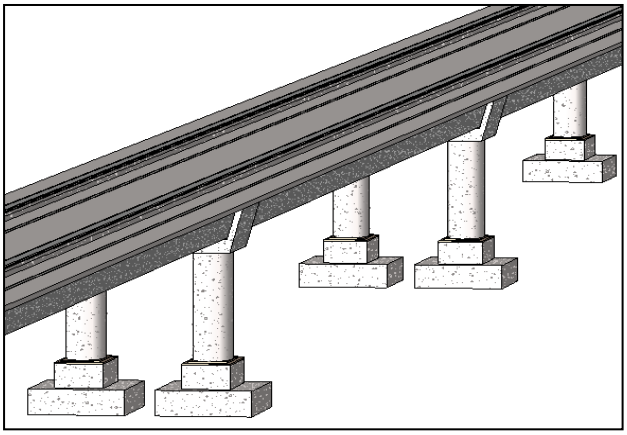

(f) View 4 of the Bridge with the Precast Deck panels installed

Figure 32 - Continued

Step 10 – Grouting of Precast Deck Panels and Installation of Shear Connectors

Grouting of deck panels will be carried out by the building contractor. After placing the panels in place, adjacent panels are grouted in the transverse direction using non-shrink grout. The panels will be connected to the girders using shear connectors which are placed in the shear pockets provided in the precast deck panels. These pockets are also to be grouted and this connection between the deck and girder will develop a composite action.

Step 11 – Post-tensioning of Girders – Stage 2

After the panels are put in place and are joined transversely using non-shrink grout, they are left for the drying of the grout. Once the deck slab is dry, the second stage of longitudinal post-tensioning is to be carried out for this composite section.

Step 12 – Installation of Running Rails and Upstand

Figure 33 shows the deck slab after installation of the rails and upstand for the freight shuttle movement.

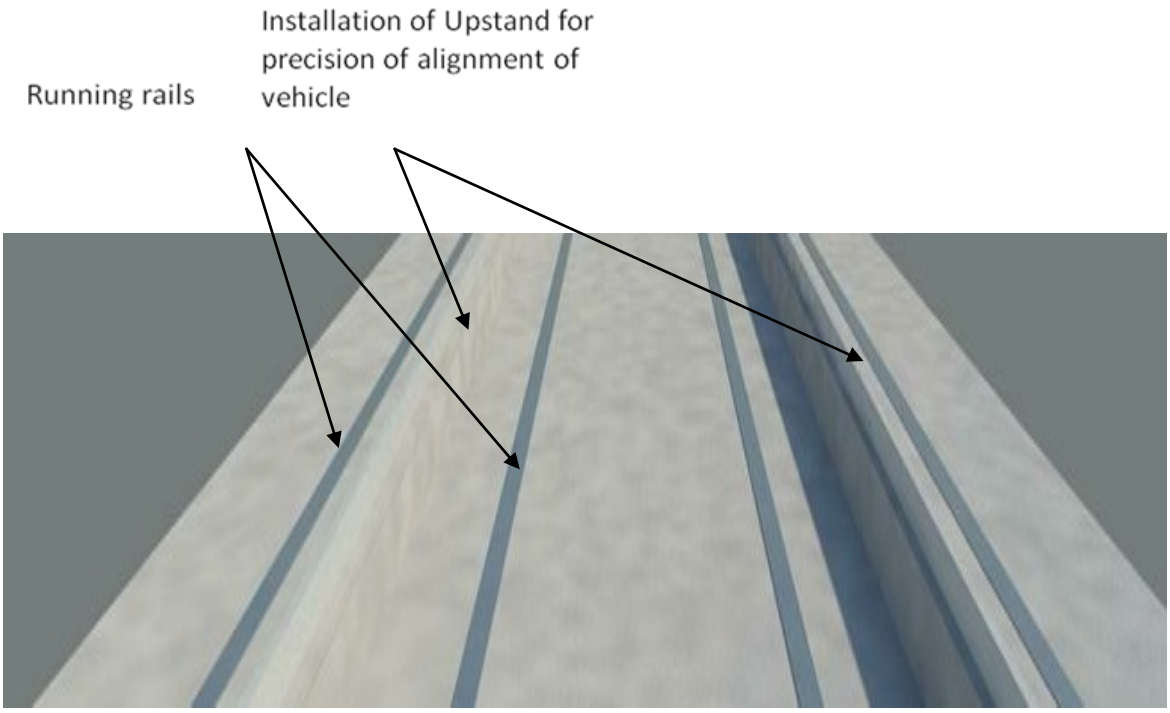

Figure 33- Installation of Running Rails and Upstands

Step 13 – Completion and Clean Up

Figure 34 shows different views of the finished guideway system for the Multimodal Freight Shuttle.

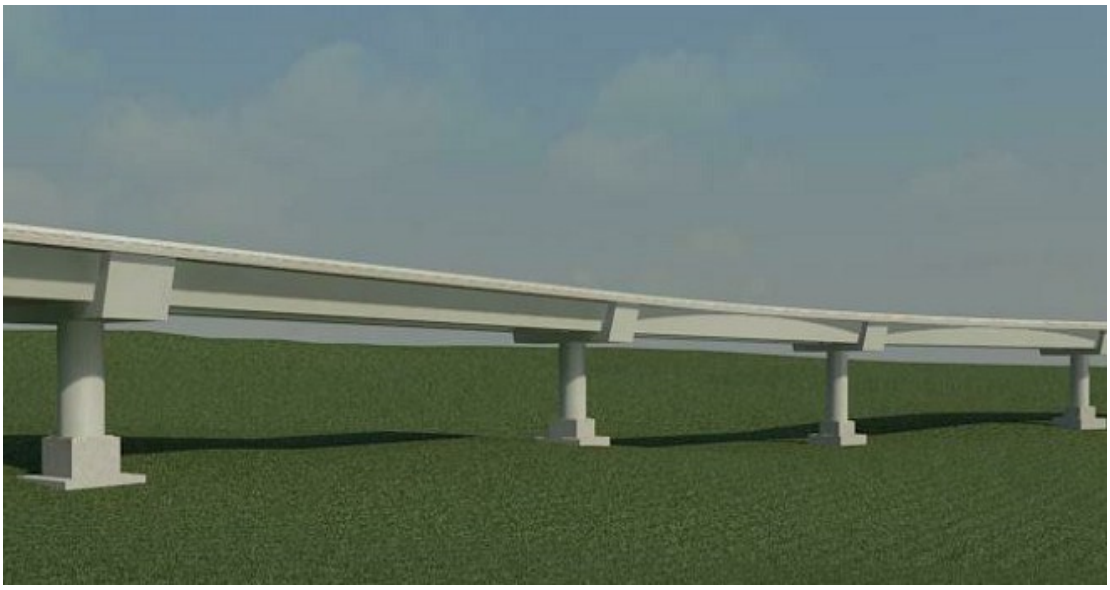

(a) View 1

(b) View 2

Figure 34 - Finished Guideway System for the Multimodal Freight Shuttle System

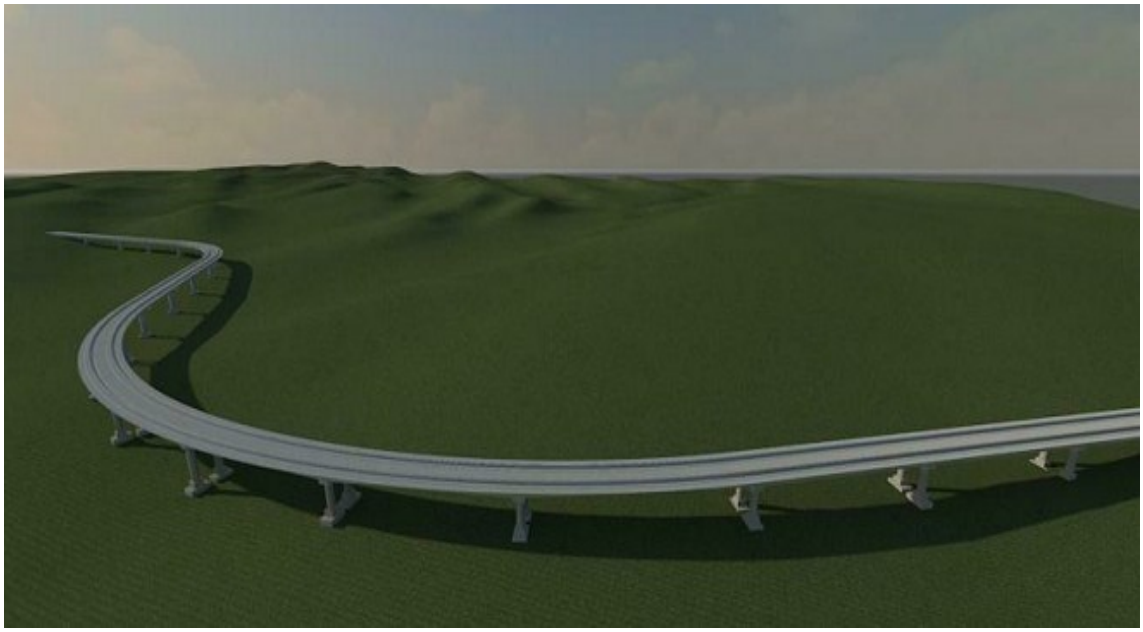

(c) View 3

(d) View 4

Figure 34 – Continued

(e) View 5 (Roop et al., 2011)

Figure 34 - Continued

CHAPTER VII

SUMMARY AND CONCLUSIONS

7.1 Summary and Conclusions

Precast, prestressed concrete girders are the predominant element used in Texas bridges. This is a reflection of the durability, low cost, and adaptability of prestressed concrete. A key factor in TxDOT's widespread use of precast, prestressed concrete components is cross-section standardization, facilitating economical mass production of these bridge elements. However, no one cross-section is optimal for all bridges, leading to variations of section type and size, each targeted to address specific bridge geometries and construction challenges. The design of the precast, prestressed elevated bridge system components developed for the Multimodal freight shuttle transportation project is compared with the conventional design. Based on the research presented herein, the key findings, advantages and significant features of the new design over the standard section are addressed as follows: -

1. Prefabricated precast, prestressed bridge system aids in rapid construction and deals with site constraints like time of closure of traffic. Precast concrete bridge components offer a potential alternative to conventional reinforced, cast-in-place concrete components. Precast concrete construction leads to speedy construction, causes minimum interruption to traffic, reduces impact on the surrounding environment and also improves the life-cycle cost of the structure.

2. A high performance and high precision solution is a major requirement for this bridge project since the vehicle alignment and a level ride is of major concern. Thus a perfect balance between design and construction technologies is of prime importance which can be achieved by proposed design solutions and construction methodologies.
3. An optimization has been done for the layout which includes best arrangement of the bridge component members such as the span length based on maximum transportable length of girder segments, full-depth precast deck panels, continuous post-tensioned prestressed spliced girders and precast prestressed modular bridge piers.
4. The depth of the deck slab (7 in.) has been optimized to the minimum taking into account the serviceability requirements such as cracking and deflection and also punching shear considerations under concentrated wheel loads.
5. The girders are so aligned so that the wheels of the vehicle operating over the deck panel exactly coincide over the webs of the girders. This helps in economizing the reinforcement in the slab by providing only one layer both-ways. Two layers of reinforcement both-ways are provided only in curved panels. This helps in a major cost saving of deck slab reinforcement for large scale construction.
6. The commonly used TxDOT U beams are of the depth 40-in. and 54-in. having maximum span lengths of 105 and 120-ft. respectively. Whereas the proposed trough girders in this case have been designed for span lengths of 140-ft. taking into account all serviceability criteria. The girder section properties have been optimized to the maximum and this will lead to economy in material and overall cost.

7. Proposed trough girders provide a slender and economic section with web and flange thickness equal to 7” which is effective to carry the loads of the freight shuttle vehicle safely. Maximum allowable span/depth ratio is used. These girders provide a torsionally effective cross section with a total lifting weight in lb/ft. about 40 percent less than the total weight of the AASHTO TYPE IV I-girders required for the same bridge. The inner void space is beneficial for passage of electrical and fiber optic cables.
8. Harped strands are used in combination with straight strands for the trough girders to control concrete stresses at the ends of pretensioned girders, decrease the number of pretention prestress strands and to contribute to the shear capacity of the section.
9. Post-tensioning for the trough girders is designed using externally unbonded tendons. This is a deviation from the commonly used practices in Texas where post tensioning is done using internally bonded tendons. The external unbonded post-tensioning systems allows for greater control and adjustment of tendon forces, ease in inspection of loss of stress and damage in tendons due to impact or corrosion and also allows for replacement of tendons if required due to creep, relaxation or corrosion. The tendons can also be restressed in future for additional strengthening if necessary.
10. The Damage Avoidance Design (DAD) concept given by Mander and Cheng (1997) based on the dissipation of seismic energy by rocking of the pier is found to be a more effective solution compared to the conventional pier design. The post-tensioning contributes to the moment capacity of the columns and thus reduces the

requirement of longitudinal mild steel reinforcement than if it is designed using the conventional method of design practice. Moreover the Dywidag bars provide stiffness and as a means of anchoring the structure to the ground and thus increasing its lateral capacity in earthquakes. The energy dissipation devices used provided additional lateral resistance.

11. A DAD pier is recommended to be used for the particular bridge structure since it reduces a major financial loss due to repair and replacement of the damaged pier and closure time of traffic during the repair. Thus the damage caused to the plastic hinge zone during a severe earthquake which cannot be repaired in a conventional pier is overcome in a Damage Avoidance Design.

7.2 Recommendations for Future Work

1. Additional research is required to validate the performance of the proposed guideway design under the dynamic loading of the Freight Shuttle using a structural analysis and design software.
2. Splicing technology, constructed and proven successful by different state DOTs should be considered as a potential option to construct new effective long span continuous bridge structures in Texas. The current state of art and practice and the NCHRP study reports 517 by Castrodale et al. (2004) and 519 by Miller et al. (2004) illustrate additional concepts and advantages of spliced girder bridges where multiple continuous spans are required. Modifications in the construction techniques can be done to further refine the proposed design solution for greater span lengths.

3. One of the major probable cause of the failures in bridge is due to vehicle collision (Wardhana and Hadipriono, 2003) and it has been on a rise with the increase in the traffic density and high speed of vehicles. It is important to be able to understand the behavior of structural members, especially bridge piers subjected to collision impact loading in order to prevent these structures from collapse and ensure the safety of road users. It would be beneficial to do some analytical research on these proposed pier solutions for the impact loading and analyze them to check if any additional retrofitting is required to make the piers safe against vehicle impact loading.
4. Detailed cost analysis of the proposed continuous bridge system needs to be done depending on the location of fabrication of bridge components and the construction site and the available local cost data.

REFERENCES

AASHTO. (2010). AASHTO LRFD *bridge design specifications and commentary*, *AASHTO LRFD-10,* 5th ed., Washington, DC.

ACI Committee 318. (2008). *Building code requirements for structural concrete (ACI 318-08) and commentary (ACI 318R-08)*, Farmington Hills, MI.

ACI Committee 315. (2004). *Details and detailing of concrete reinforcement (ACI 315R-04),* Farmington Hills, MI.

Aktan, A.E., Culmo, M.P., Frangopol, D.M., French, C.W., Rabbat, B.G., Ralls, M.L., Russell, H.G., Sanders, D.H., Showers, J., Tadros, M.K., and Woods, S.W. (2000). "Concrete bridges." *Transportation in the new millennium: state of the art and future directions, perspectives from transportation research board standing committee,* Transportation Research Board, Washington, DC.

Aslam, M., Goddon, W.G., and Scalise, D.T. (1980). "Earthquake rocking response of rigid blocks." *Journal of Structural Engineering*, *ASCE*, 106(2), 377-392.

ASTM Standard A615 / A615M. (2009). *Standard specification for deformed and plain carbon-steel bars for concrete reinforcement, ASTM International,* West Conshohocken, PA.

Badie, S.S., Tadros, M.K., and Girgis, A.F. (2008). "Full-depth precast concrete bridge deck panel systems." *National Cooperative Highway Research Board Report 584,* Transportation Research Board, Washington, DC.

Beacham, D., and Derrick, D. (1999). "Longer bridge spans with Nebraska's NU I-girders." *Transportation News 202*, Transportation Research Board, Washington, DC.

Billington, S.L., Barnes, R.W., and Breen, J.E. (1999). "A precast segmental substructure system for standard bridges." *PCI Journal*, 44 (4), 56-73.

Biswas, M. (1986). "Precast bridge deck design systems." *PCI Journal,* 31(2), 40-94.

Blakeley, R.W.G., and Park, R. (1971). "Seismic resistance of prestressed concrete beam-column assemblies." *ACI Journal*, 68 (9), 677-692.

Brey, R., (2010). "A systematic investigation of shear connectors between full-depth precast panels and precast prestressed bridge girders." M.S. Thesis, Texas A&M University, College Station, TX.

Castrodale R.W., White C.D. (2004). "Extending span ranges of precast prestressed concrete girders." *National Cooperative Highway Research Program Report 517,* Transportation Research Board, Washington, DC.

Cheng, T.C., Mander, J.B. (1997). "Seismic design of bridge columns based on control and repairability of damage." *Technical Report NCEER-97-0013,* Multidisciplinary Center for Earthquake Engineering Research, Buffalo, NY.

Corven, J.A. and Moreton, A.J. (2002). "New directions for Florida post-tensioned bridges: post-tensioning in Florida bridges." *Florida Department of Transportation Report Vol. 1,* Corven Engineering, Inc., Tallahassee, FL.

Crigler, J. (2007). "Post-tensioning revisited." *Structure Magazine, July 2007 – Concrete, D - Product Watch*, 64-67.

Daly, A., F., and Witarnawan, W. (1997). "Strengthening of bridges using external post-tensioning." *Published Paper PA11,* Road Research Development Project, Transport Research Laboratory, Berkshire, UK.

Dhakal, R., P., Mander, J., B., Mashiko, N. (2007). "Bidirectional pseudodynamic Tests of bridge piers designed to different standards." *Journal of Bridge Engineering*, *ASCE*, 12 (3), 284-295.

Eberhard, M., Stanton, J., Heiber, D., Wacker, J. (2005). "Precast concrete pier systems for rapid construction of bridges in seismic regions." *Research Report Contract T2695-Task 53,* Washington State Transportation Center (TRAC). Olympia, WA.

El-Sheikh, M.T., Sause, R., Pessiki, S. and Lu, L. (1999). "Seismic behavior and design of unbonded post-tensioned precast concrete frames." *PCI Journal*, 44 (3), 54-71.

Fallaha, S., Sun, C., Lafferty, M., and Tadros, M. (2004). "High performance precast concrete NUDECK panel system for Nebraska's skyline bridge." *PCI Journal*, 49(5), 40-50.

Ficenec J.A., Kneip S.D., Tadros M.K. and Fischer L.G. (1993). "Prestressed spliced I-girders: Tenth street viaduct project, Lincoln, Nebraska." *PCI Journal*, 38(5), 38-48.

French, C.W., Amu, O. and Tarzikhan, C. (1989a). "Connection between precast elements – failure outside connection region." *ASCE Journal of Structural Engineering*, 115 (2), 316-340.

French, C.W., Hafner, M., and Jayshankar, V. (1989b). "Connections between precast elements – failure within connection region." *ASCE Journal of Structural Engineering*, 115 (12), 3171-3192.

Goldberg, D. (1987). "Precast prestressed concrete bridge deck panels." *PCI Journal,* 32(2), 26-45.

Henley, M.D. (2009). "Shear connections for the development of a full-depth precast concrete deck system." M.S. Thesis, Texas A&M University, College Station, TX.

Hewes, J.T., Priestley, M.J.N. (2002). "Seismic design and performance of precast concrete segmental bridge columns." *Structural Systems Research Project*, Report No. SSRP– 2001/25, University of California, San Diego, CA.

Hieber, D.G., Wacker J.M., Eberhard M.O., and Stanton J.F. (2004). "State-of-the-art report on precast concrete systems for rapid construction of bridges." *Report WA-RD 594.1*, Washington State Transportation Center, University of Washington, WA

Hueste, M.B., Adil, M.S., Adnan, M., and Keating, P.B. (2006). "Impact of LRFD specifications on Texas bridges." *Report 0-4751-1,* Texas Transportation System, Texas A&M University, College Station, TX.

Issa, M., Idriss, A., Kaspar, I., and Khayyat, S. (1995). "Full-depth precast/ prestressed concrete bridge deck panels." *PCI Journal,* 40(1), 74-85.

Kaar, P.H., Kriz, L.B., and Hognestad, E. (1960). "Precast-prestressed concrete bridges, 1.Pilot tests of continuous girders." *Journal of PCA Research and Development Laboratories*, 2(2), 21-37.

Kim, J.H., and Mander, J. (2005). "Theoretical shear strength of concrete columns due to transverse steel." *Journal of Structural Engineering*, ASCE, 131(1), 197-199.

Kim, J.H., and Mander, J. (2007). "Influence of transverse reinforcement on elastic shear stiffness of cracked concrete columns." *Engineering Structures*, 29(8), 1798-1807.

LoBuono, Armstrong, & Associates (1996). "*Development of precast bridge substructures*." Florida Department of Transportation, Tallahassee, FL.

Louman, L., Mander, J.B. and Dhakal, R.P. (2008). "Bi-directional cyclic loading experiment on a 3D beam-column joint designed for damage avoidance." *Journal of Structural Engineering,* 134 (11), 1733-1742.

MacGregor, J.G., and Wight, J.K. (2004). *Reinforced concrete mechanics and design*, 4th ed., John Wiley & Sons, Inc., New York.

Mander, J.B., and Cheng, C.T. (1997). "Seismic resistance of bridge piers based on damage avoidance design." *Technical Report NCEER-97-0014,* National Center for Earthquake Engineering Research, State Univ. of New York, Buffalo, NY.

Mander, J.B. (2000). "Damage avoidance seismic design of bridge piers." *NZCS Technical Report TR 23*, New Zealand Concrete Society Conf., Wairakei, NZ, 42–49.

Mander, T. J. (2009). "Structural performance of a full-depth precast concrete bridge deck system." M.S. Thesis, Texas A&M University, College Station, TX.

Mander, T.J., Henley, M.D., Scott, R.M., Head, M.H., Mander, J.B., and Trejo, D., (2009). "Experimental investigation of full-depth precast overhang panels for concrete bridge decks." *ASCE Structures Congress*, Austin, TX.

Mander, T.J., Henley, M.D., Scott, R.M., Head, M.H, Mander, J.B., and Trejo, D. (2010). "Experimental performance of full-depth precast, prestressed concrete overhang, bridge deck panels." *Journal of Bridge Engineering,* 15 (5), 503- 510.

Mander, T.J. Mander, J.B., and Head, M.H. (2011). "Modified yield line theory for full-depth precast concrete bridge deck overhang panels." *Journal of Bridge Engineering,* 15 (5), 503- 510.

Matsumoto, E.E., Kreger, M.E., Waggoner, M.C., and Sumen, G. (2002). "Grouted connection tests in development of precast bent cap systems." *Transportation Research Record 1814*, Transportation Research Board, Washington DC.

Mattock, A.H., and Kaar, P.H. (1960). "Precast-prestressed concrete bridges III: further tests of continuous girders." *Journal of PCA Research and Development Laboratories*, 2(3), 51–78.

Meek, J.W. (1978). "Dynamic response of tipping core buildings." *Earthquake Engineering & Structural Dynamics*, 6(5), 437-454.

Merrill, B.D. (2002). "Texas' use of precast concrete stay-in-place forms for bridge decks." *TxDOT Concrete Bridge Conference*, Fort Worth, TX.

Miller R.A., Castrodale R.W., Mirmiran A. (2004), "Connection of simple span precast concrete girders for continuity." *National Cooperative Highway Research Program Report 519*, Transportation Research Board, Washington, DC.

Newhouse, C.D., Roberts-Wollmann, C.L., and Cousins, T.E. (2005). "Development of an optimized continuity diaphragm for new PCBT girders." *Report PB2006-100962 VRTC 06-CR3*, Virginia Transportation Research Council, Charlottesville, VA.

Park, R., and Gamble, W.L. (2000). *Reinforced concrete slabs*, 2nd ed., John Wiley & Sons, Inc., New York.

Pekcan, G., Mander, J. B., and Chen, S. S. (2000). "Experiments on steel MRF building with supplemental tendon system." *Journal of Structural Engineering*, 126(4), 437-444.

Priestley, M.J.N. and Tao, J.R. (1993). "Seismic response of precast prestressed concrete frames with partially debonded tendons." *PCI Journal*, 38 (1), 64-81.

Priestley, M.J.N. and MacRae, G.A. (1996). "Seismic tests of precast beam-to-column joint subassemblages with unbonded Tendons." *PCI Journal*, 41 (1), 64-81.

Ronald, H.D. (2001). "Design and construction considerations for continuous post-tensioned Bulb Tee girder bridges." *PCI Journal,* 46 (3), 44-66.

Roop, S.S., Pearson, D.F., Warner, J.E., Farnsworth, S.P., Vadali, S.R., and Lee, S. (2005). "A comprehensive commodity/freight movement model for Texas." *Technical Report 0-4430-S*, Texas Transportation Institute (TTI), Texas A&M University System, College Station, TX.

Roop, S.S., Ragab, A.H., Yager, M.A., Mander, J.B., Olson, L.E., Morgan, C., Parkar, A.S., Protopapa, A.A., Warner, J.E. and Roy, S.S. (2011). "The SAFE freight shuttle: a proposal to design, build, and test an alternative container transport system." *Technical Report 9-1528-S,* Texas Transportation Institute (TTI), Texas A&M University System, College Station, TX.

Roy, S. (2011). "Design and construction integration of a continuous precast prestressed concrete bridge system." M.S. Thesis, Texas A&M University, College Station, TX.

Shahawy, M.A. (2003). "NCHRP synthesis 324: prefabricated bridge elements and systems to limit traffic disruption during construction." *National Cooperative Highway Research Program*, Transportation Research Board, Washington, DC.

Solberg, K.M. (2007). "Experimental and financial investigations into the further development of damage avoidance design." M.E. Thesis*,* University of Canterbury, Christchurch, NZ.

Solberg, K., Mashiko, N., Mander, J.B. and Dhakal, R.P. (2009). "Performance of a damage-protected highway bridge pier subjected to bidirectional earthquake attack." *ASCE Journal of Structural Engineering,* 135(5), 469-478.

Stanton, J.F., Anderson, R.G., Dolan, C.W. and McCleary, D.E. (1987). "Moment resistant connections and simple connections," *PCI Journal*, 32 (2), 62-74.

Sun C. (2004). "High performance concrete bridge stringer system." Ph.D. Dissertation, The University of Nebraska- Lincoln.

Tadros, M.K., Ficenec, J.A., Einea, A., and Holdsworth, S. (1993). "A new technique to create continuity in prestressed concrete members." *PCI Journal,* 38(5), 30–37.

Tadros, M.K. and Baishya, M.C. (1998). "Rapid replacement of bridge decks." *NCHRP Report 407*, National Cooperative Highway Research Program, Washington DC.

Tadros, M.K. (2007). "Design aids for threaded rod precast prestressed girder continuity system." *Nebraska Department of Roads Research Report*, STPD-92-7 (103), University of Nebraska, Lincoln, NE.

Trejo, D., Hite, M., Mander, J.B., Mander, T., Henley, M., Scott, R., Ley, T., and Patil, S. (2008). "Development of a precast bridge deck overhang system for the Rock Creek bridge." *Technical Report* 0-6100-2, Texas Transportation Institute, Texas A&M University, College Station, TX.

Texas Department of Transportation (TxDOT). (2004). *Standard specifications for construction and maintenance of highways, streets and bridges*, State Publications Clearinghouse, Item 421, 516-535, (Available online).

Wardhana, K., and Hadipriono, F.C. (2003). "Analysis of recent bridge failures in the United States." *Journal of Performance of Construction Facilities,* 17(3), 144-150.

Yamane, T., Tadros, M.K., Badie, S.S., and Baishya, M.C. (1998). "Full-depth precast prestressed concrete bridge deck system." *PCI Journal*, 43 (3), 50-66.

APPENDIX

DESIGN CALCULATIONS

1) ANALYSIS OF GIRDERS

a. DEAD LOAD

DATA			
Span of the bridge	=	**140**	ft
Dead weight of the girder	=	1.136	kip/ft
Dead weight of the slab	=	0.925	kip/ft
Dead weight of the rail upstand	=	**0.5**	kip/ft

DEAD LOAD MOMENT ENVELOPE					
Location	**Distance from Left support**	**Girder Weight**	**Slab Weight**	**Superimposed Rail Upstand Weight**	**Moment Envelope**
i	**xi**	**Mg**	**Ms**	**Mr**	**Mi (kip-ft)**
1	0	0.00	0.00	0.00	0.00
	3.68	284.85	232.12	125.41	642.39
2	7	528.66	430.80	232.75	1192.20
3	14	1001.67	816.25	441.00	2258.91
4	21	1419.03	1156.35	624.75	3200.13
5	28	1780.74	1451.11	784.00	4015.85
6	35	2086.81	1700.51	918.75	4706.07
7	42	2337.22	1904.58	1029.00	5270.80
8	49	2531.99	2063.29	1114.75	5710.03
9	56	2671.11	2176.66	1176.00	6023.77
10	63	2754.58	2244.68	1212.75	6212.01
11	70	2782.41	2267.35	1225.00	6274.76
12	77	2754.58	2244.68	1212.75	6212.01
13	84	2671.11	2176.66	1176.00	6023.77
14	91	2531.99	2063.29	1114.75	5710.03
15	98	2337.22	1904.58	1029.00	5270.80
16	105	2086.81	1700.51	918.75	4706.07
17	112	1780.74	1451.11	784.00	4015.85

DEAD LOAD MOMENT ENVELOPE					
Location	**Distance from Left support**	**Girder Weight**	**Slab Weight**	**Superimposed Rail Upstand Weight**	**Moment Envelope**
i	**xi**	**Mg**	**Ms**	**Mr**	**Mi (kip-ft)**
18	119	1419.03	1156.35	624.75	3200.13
19	126	1001.67	816.25	441.00	2258.91
20	133	528.66	430.80	232.75	1192.20
21	140	0.00	0.00	0.00	0.00

DEAD LOAD SHEAR ENVELOPE					
Location	**Distance from Left support**	**Girder Weight**	**Slab Weight**	**Superimposed Rail Upstand Weight**	**Shear Envelope**
i	**xi**	**Vg**	**Vs**	**Vr**	**Vi (kips)**
1	0	79.50	64.78	35.00	179.28
	3.68	75.32	61.38	33.16	169.85
2	7	71.55	58.30	31.50	161.35
3	14	63.60	51.83	28.00	143.42
4	21	55.65	45.35	24.50	125.50
5	28	47.70	38.87	21.00	107.57
6	35	39.75	32.39	17.50	89.64
7	42	31.80	25.91	14.00	71.71
8	49	23.85	19.43	10.50	53.78
9	56	15.90	12.96	7.00	35.86
10	63	7.95	6.48	3.50	17.93
11	70	0.00	0.00	0.00	0.00
12	77	-7.95	-6.48	-3.50	-17.93
13	84	-15.90	-12.96	-7.00	-35.86
14	91	-23.85	-19.43	-10.50	-53.78
15	98	-31.80	-25.91	-14.00	-71.71
16	105	-39.75	-32.39	-17.50	-89.64
17	112	-47.70	-38.87	-21.00	-107.57
18	119	-55.65	-45.35	-24.50	-125.50
19	126	-63.60	-51.83	-28.00	-143.42
20	133	-71.55	-58.30	-31.50	-161.35
21	140	-79.50	-64.78	-35.00	-179.28

b. LIVE LOAD

i) Two Freight Shuttle vehicles spaced at 12-ft clear distance over Simply-Supported Span

DATA											
Span of the bridge	=	**140**	ft								
Loading of the **Vehicle 1**	=	**25**	kips	**25**	kips	**25**	kips	**25**	kips		
C/C spacing between the axles	=		**6**	ft	**58**	ft	**6**	ft			
Loading of the **Vehicle 2**	=	**25**	kips	**25**	kips	**25**	kips	**25**	kips		
C/C spacing between the axles	=		**6**	ft	**58**	ft	**6**	ft			
Distance between front axle of Vehicle 1 and rear axle of Vehicle 2	=	**12**	ft								

Location	**Distance from Left support**	**Position1**			**Position2**			**Position3**			**Position4**		
i	**xi**	**Va**	**Vb**	**Mi1**	**Va**	**Vb**	**Mi2**	**Va**	**Vb**	**Mi3**	**Va**	**Vb**	**Mi4**
1	0.0	91.4	33.6	0.0	115.3	34.6	0.0	109.2	40.7	0.0	119.6	30.3	0.0
2	7.0	110.0	40.0	620.0	107.8	42.1	755.0	116.4	33.5	665.0	112.1	37.8	785.0
3	14.0	102.5	47.5	1285.0	100.3	49.6	1405.0	108.9	41.0	1375.0	104.6	45.3	1465.0
4	21.0	95.0	55.0	1845.0	92.9	57.1	1950.0	101.4	48.5	1980.0	97.1	52.8	2040.0
5	28.0	87.5	62.5	2300.0	85.4	64.6	2390.0	93.9	56.0	2480.0	89.6	60.3	2510.0
6	35.0	80.0	70.0	2650.0	77.9	72.1	2725.0	86.4	63.5	2875.0	82.1	67.8	2875.0
7	42.0	72.5	77.5	2895.0	70.4	79.6	2955.0	78.9	71.0	3165.0	74.6	75.3	3135.0
8	49.0	65.0	85.0	3035.0	62.9	87.1	3080.0	71.4	78.6	3350.0	67.1	82.9	3290.0
9	56.0	57.5	92.5	3070.0	55.0	70.0	3080.0	63.9	86.1	3430.0	47.9	77.1	2680.0

10	63.0	76.1	73.9	3042.5	72.7	52.3	3128.8	45.9	79.1	2741.3	30.0	70.0	1890.0
11	70.0	94.6	55.4	3125.0	90.4	59.6	3275.0	29.3	70.7	1900.0	25.0	75.0	1750.0
12	77.0	87.1	62.9	3210.0	82.9	67.1	3330.0	24.3	75.7	1720.0	21.3	78.8	1636.3
13	84.0	79.6	70.4	3190.0	75.4	74.6	3280.0	20.7	54.3	1590.0	18.9	56.1	1590.0
14	91.0	72.1	77.9	3065.0	67.9	82.1	3125.0	18.6	31.4	1540.0	16.4	33.6	1495.0
15	98.0	64.6	85.4	2835.0	60.4	89.6	2865.0	16.1	33.9	1425.0	13.9	36.1	1365.0
16	105.0	57.1	92.9	2500.0	52.9	97.1	2500.0	13.6	36.4	1275.0	11.4	38.6	1200.0
17	112.0	49.6	100.4	2060.0	45.4	104.6	2030.0	11.1	38.9	1090.0	8.9	41.1	1000.0
18	119.0	42.1	107.9	1515.0	37.3	87.7	1391.3	8.6	41.4	870.0	6.4	43.6	765.0
19	126.0	35.4	89.6	955.0	30.7	69.3	820.0	6.1	43.9	615.0	3.9	46.1	495.0
20	133.0	30.0	70.0	490.0	25.7	74.3	370.0	3.6	46.4	325.0	1.4	48.6	190.0
21	140.0	25.0	75.0	0.0	21.8	53.2	0.0	1.1	48.9	0.0	0.0	25.0	0.0

Location	Distance from Left support	Moment Envelope	Shear Envelope
i	xi	Mi (kip-ft)	Vi (kips)
1	0	0.00	119.64
2	7	785.00	116.43
3	14	1465.00	108.93
4	21	2040.00	104.64
5	28	2510.00	101.43
6	35	2875.00	93.93
7	42	3165.00	89.64
8	49	3350.00	87.14
9	56	3430.00	82.14
10	63	3330.00	79.64
11	70	3275.00	74.29
12	77	3330.00	-79.64
13	84	3430.00	-82.14
14	91	3350.00	-87.14
15	98	3165.00	-89.64
16	105	2875.00	-93.93
17	112	2510.00	-101.43
18	119	2040.00	-104.64
19	126	1465.00	-108.93
20	133	785.00	-116.43
21	140	0.00	-119.64

ii) Two Freight Shuttle vehicles spaced at 12-ft clear distance over Continuous Span

DATA									
Span of the bridge	=		**140**	ft					
Loading of the **Vehicle 1**	=	**25**	kips	**25**	kips	**25**	kips	**25**	Kips
C/C spacing between the axles	=		**6**	ft	**58**	ft	**6**	ft	
Loading of the **Vehicle 2**	=	**25**	kips	**25**	kips	**25**	kips	**25**	kips
C/C spacing between the axles	=		**6**	ft	**58**	ft	**6**	ft	
Distance between front axle of Vehicle 1 and rear axle of Vehicle 2	=	**12**	ft						

FOR MAXIMUM POSITIVE MOMENT AT 0.4L OF END SPAN								
Fixed End Moments in First Span due to Vehicle 1 and 2 Moving From LEFT to RIGHT (kip-ft)								
Axle Load (kips) ---->	**25**		**25**		**25**		**25**	
Span (ft)	**MF LEFT**	**MF RIGHT**	**MF LEFT**	**MF RIGHT**	**MF LEFT**	**MF RIGHT**	**MF LEFT**	**MF RIGHT**
0	-1341.4	1042.9	-1546.4	1152.9	-1717.8	1717.9	-1701.8	1851.8
7	-1598.4	1172.0	-1857.5	1294.3	-1719.3	1872.5	-1787.0	1989.1
14	-1892.4	1315.4	-2056.1	1443.2	-1792.4	2006.9	-1794.2	2099.4
21	-2076.2	1464.1	-2158.0	1583.8	-1789.8	2112.0	-1739.2	2166.9
28	-2165.6	1602.3	-2178.9	1700.4	-1727.1	2172.1	-1637.6	2175.9
35	-2176.1	1714.2	-2134.5	1777.3	-1620.2	2171.5	-1505.4	2110.7
42	-2123.7	1784.2	-2040.6	1798.7	-1484.9	2094.4	-1358.1	1955.5
49	-2024.0	1796.3	-1912.9	1748.9	-1336.7	1925.1	-1211.5	1694.5
56	-1892.9	1735.0	-1764.3	1717.8	-1191.5	1647.7	-1078.6	1417.9
63	-1715.9	1718.7	-1707.7	1830.7	-1060.5	1380.7	-955.8	1246.4
70	-1701.8	1851.8	-1780.0	1970.7	-938.6	1222.8	-840.7	1046.4
77	-1787.0	1989.1	-1797.4	2085.9	-825.4	1011.0	-734.0	951.9
84	-1794.2	2099.4	-1750.3	2160.5	-719.1	933.7	-623.0	1020.6
91	-1739.2	2166.9	-1654.4	2178.8	-606.6	1024.4	-507.5	1033.6
98	-1637.6	2175.9	-1525.5	2125.2	-490.8	1032.7	-392.4	1011.2
105	-1505.4	2110.7	-1379.4	1983.8	-376.3	1004.7	-283.1	947.9
112	-1358.1	1955.5	-1231.8	1738.9	-268.3	935.3	-184.9	838.7
119	-1211.5	1694.5	-1096.8	1453.0	-172.0	819.1	-102.8	678.3

FOR MAXIMUM POSITIVE MOMENT AT 0.4L OF END SPAN								
Fixed End Moments in First Span due to Vehicle 1 and 2 Moving From LEFT to RIGHT *(kip-ft)*								
Axle Load (kips) ---->	**25**		**25**		**25**		**25**	
Span (ft)	**MF LEFT**	**MF RIGHT**	**MF LEFT**	**MF RIGHT**	**MF LEFT**	**MF RIGHT**	**MF LEFT**	**MF RIGHT**
126	-1078.6	1417.9	-973.0	1268.4	-92.7	650.9	-42.3	461.3
133	-955.8	1246.4	-856.3	1080.1	-35.7	425.4	-8.5	182.6
140	-840.7	1046.4	-748.9	969.0	-6.2	137.4	0.0	0.0

FOR MAXIMUM POSITIVE MOMENT AT 0.4L OF END SPAN								
Fixed End Moments in First Span due to Vehicle 1 and 2 Moving From RIGHT to LEFT *(kip-ft)*								
Axle Load (kips) ---->	**25**		**25**		**25**		**25**	
Span (ft)	**MF LEFT**	**MF RIGHT**	**MF LEFT**	**MF RIGHT**	**MF LEFT**	**MF RIGHT**	**MF LEFT**	**MF RIGHT**
0	-1042.88	1341.41	-1152.87	1546.42	-1717.86	1717.86	-1851.79	1701.79
7	-1172.01	1598.35	-1294.26	1857.53	-1872.45	1719.33	-1989.07	1787.00
14	-1315.44	1892.42	-1443.15	2056.13	-2006.85	1792.44	-2099.36	1794.21
21	-1464.12	2076.24	-1583.80	2157.99	-2111.99	1789.80	-2166.89	1739.18
28	-1602.30	2165.56	-1700.44	2178.85	-2172.13	1727.15	-2175.93	1637.64
35	-1714.22	2176.13	-1777.33	2134.45	-2171.53	1620.26	-2110.71	1505.36
42	-1784.15	2123.70	-1798.72	2040.56	-2094.42	1484.87	-1955.50	1358.07
49	-1796.33	2024.03	-1748.87	1912.92	-1925.06	1336.72	-1694.54	1211.54

FOR MAXIMUM POSITIVE MOMENT AT 0.4L OF END SPAN								
Fixed End Moments in First Span due to Vehicle 1 and 2 Moving From RIGHT to LEFT *(kip-ft)*								
Axle Load (kips) ---->	**25**		**25**		**25**		**25**	
Span (ft)	**MF LEFT**	**MF RIGHT**	**MF LEFT**	**MF RIGHT**	**MF LEFT**	**MF RIGHT**	**MF LEFT**	**MF RIGHT**
56	-1735.01	1892.85	-1717.81	1764.34	-1647.70	1191.58	-1417.87	1078.56
63	-1718.71	1715.94	-1830.71	1707.68	-1380.68	1060.57	-1246.36	955.79
70	-1851.79	1701.79	-1970.74	1779.97	-1222.76	938.67	-1046.43	840.71
77	-1989.07	1787.00	-2085.85	1797.36	-1010.97	825.46	-951.94	733.96
84	-2099.36	1794.21	-2160.46	1750.26	-933.69	719.16	-1020.58	622.99
91	-2166.89	1739.18	-2178.82	1654.40	-1024.42	606.65	-1033.62	507.45
98	-2175.93	1637.64	-2125.17	1525.54	-1032.70	490.87	-1011.15	392.42
105	-2110.71	1505.36	-1983.78	1379.43	-1004.74	376.33	-947.94	283.13
112	-1955.50	1358.07	-1738.89	1231.83	-935.28	268.30	-838.72	184.85
119	-1694.54	1211.54	-1452.99	1096.83	-819.06	172.01	-678.26	102.81
126	-1417.87	1078.56	-1268.39	973.04	-650.85	92.72	-461.30	42.28
133	-1246.36	955.79	-1080.10	856.33	-425.38	35.69	-182.58	8.49
140	-1046.43	840.71	-968.95	748.91	-137.42	6.15	0.00	0.00

Positive Moment Envelope for End Span due to Vehicles 1 and 2 Moving From LEFT to RIGHT *(kip-ft)*						
Location	**Distance from Left support**	**Position1**	**Position2**	**Position3**	**Position4**	**Moment Envelope**
i	**xi**	**Mi1**	**Mi2**	**Mi3**	**Mi4**	**Mi**

Positive Moment Envelope for End Span due to Vehicles 1 and 2 Moving From LEFT to RIGHT (kip-ft)						
Location	**Distance from Left support**	**Position1**	**Position2**	**Position3**	**Position4**	**Moment Envelope**
i	**xi**	**Mi1**	**Mi2**	**Mi3**	**Mi4**	**Mi**
1	0	0.00	0.00	0.00	0.00	0.00
2	7	567.57	695.87	582.13	693.21	695.87
3	14	1164.68	1273.53	1188.86	1266.10	1273.53
4	21	1645.32	1737.51	1679.11	1727.91	1737.51
5	28	2014.30	2093.16	2062.30	2088.38	2093.16
6	35	2277.29	2346.67	2348.34	2357.73	2357.73
7	42	2440.77	2505.08	2547.61	2546.64	2547.61
8	49	2512.08	2576.26	2671.00	2666.32	2671.00
9	56	2499.38	2508.91	2729.85	2028.43	2729.85
10	63	2400.90	2410.96	2016.00	1169.71	2610.00
11	70	2313.27	2370.47	1101.21	976.43	2400.00
12	77	2200.29	2246.03	876.63	800.61	2246.03
13	84	1996.59	2037.18	683.68	661.11	2037.18
14	91	1712.62	1754.69	534.58	506.61	1754.69
15	98	1359.34	1409.82	365.70	348.43	1409.82
16	105	948.18	1014.31	195.55	191.11	1014.31
17	112	491.04	580.39	28.51	38.74	580.39
18	119	0.35	-6.72	-131.47	-104.99	-131.47
19	126	-511.04	-621.94	-280.85	-236.81	-621.94
20	133	-1030.61	-1111.39	-416.52	-190.00	-1111.39
21	140	-1547.14	-1526.97	-535.79	0.00	-1547.14

Positive Moment Envelope for End Span due to Vehicles 1 and 2 Moving From RIGHT to LEFT (kip-ft)						
Location	**Distance from Left support**	**Position1**	**Position2**	**Position3**	**Position4**	**Moment Envelope**
i	**xi**	**Mi1**	**Mi2**	**Mi3**	**Mi4**	**Mi**
1	0	0.00	0.00	0.00	0.00	0.00
2	7	534.14	660.34	594.36	711.01	711.01
3	14	1093.26	1201.86	1226.26	1313.70	1313.70
4	21	1538.19	1635.05	1752.90	1814.75	1814.75
5	28	1879.23	1969.93	2180.67	2219.99	2219.99
6	35	2126.23	2216.01	2515.09	2534.42	2534.42
7	42	2288.53	2382.34	2760.88	2762.20	2762.20
8	49	2374.99	2477.55	2921.87	2906.65	2921.87
9	56	2393.98	2478.78	3001.11	2299.62	3001.11
10	63	2387.01	2495.59	2322.08	1511.99	2900.00
11	70	2426.03	2539.41	1487.68	1387.19	2750.00
12	77	2396.11	2498.92	1330.56	1282.82	2550.00
13	84	2282.22	2376.50	1211.42	1228.25	2376.50
14	91	2088.93	2176.18	1153.09	1140.81	2176.18
15	98	1819.97	1901.17	1049.91	1030.58	1901.17
16	105	1478.16	1553.83	924.39	897.91	1553.83
17	112	1065.86	1135.69	537.21	742.85	1135.69
18	119	584.00	566.73	607.02	565.15	565.15
19	126	99.14	50.45	414.79	363.32	50.45
20	133	-308.02	-335.74	199.47	190.00	-335.74
21	140	-725.62	-656.71	-40.00	0.00	-725.62

FOR MAXIMUM NEGATIVE MOMENT AT INTERIOR SUPPORT			
Location	**Distance between the vehicles placed at equal distance from Interior Support**	**Maximum Negative Moment**	**Reaction at Support**
i	**xi (ft)**	**Mi (Kip-ft)**	**Vi (Kips)**
1	14	-1519.11	80.85
2	28	-1725.89	77.33
3	42	-1861.25	73.29
4	56	-1931.51	68.80
5	70	-1942.97	63.88
6	84	-1901.95	58.59
7	98	-1814.73	52.96
8	112	-1687.65	47.05
9	126	-1526.99	40.91
10	140	-1339.08	34.56

ANALYSIS OF DECK SLAB

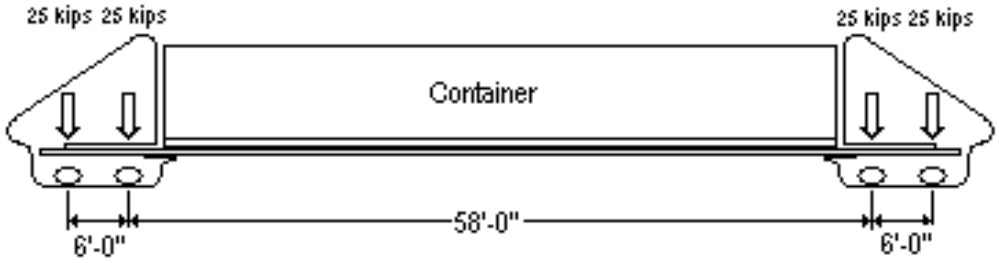

(a) Freight Shuttle vehicle loading

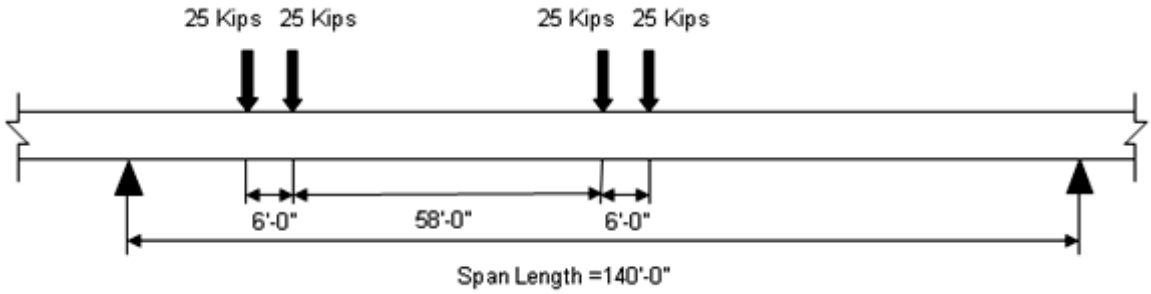

(b) Load of Freight Shuttle vehicle on deck slab

Freight Shuttle Vehicle Loading

Reinforcement requirement as per ACI-318

Minimum reinforcement requirement as per ACI code = 0.002

Hence minimum reinforcement required = 0.002 x 7 = 0.014 in^2/in.

Using No. 4 bars, Area of one bar = 0.196 in^2

Required Spacing of No.4 bars = $\frac{0.196}{0.014}$ = 14 in.

Minimum spacing provided is not less than twice the depth of the slab = 14 in.

Hence **provide No. 4 bars at 6" spacing in one layer at straight locations.**

CHECK FOR CAPACITY OF DECK SLAB USING YIELD LINE THEORY FOR SINGLE LAYER OF REINFORCEMENT:

Thickness of slab = 7 in.

Effective depth of slab = 3.5 in.

jd = 0.95 x 3.5 = 3.325 in.

For the provided reinforcement of No.4 bars @ 6" spacing in one layer,

Moment M= M' = As x fy x jd $= \frac{0.196}{6}$ x 60 x 3.325 $= 6.53$ kip $-$ in/in

CASE 1: BETWEEN GIRDERS – SINGLE POINT LOAD

For single point load on slab the following yield line pattern is considered:-

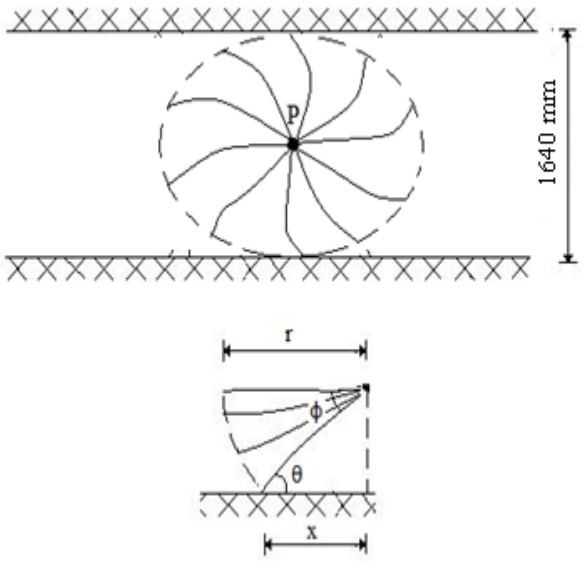

P = Intensity of the point load.

δ = Deflection of slab below point load.

r = Radius of the arc of the yield line pattern.

M, M' = Moment at top and bottom per unit length of slab respectively.

Equating the external work done to the internal work done,

dP. δ = (M+M'). r. dα . (δ/r)

For a complete circle, α = 2 π radians

$$\int_0^{\alpha} dP = \int_0^{\alpha} (M + M')d\alpha$$

$$P = 2\pi(M + M')$$

$$P = 0.9 \text{ x } (6.53 \text{ x } 2)\text{x } 2\,\pi = 73.84 \text{ kips}$$

Maximum point load considered on slab = 40 kips < 73.84 kips

Hence **SAFE.**

CASE 2: BRIDGE DECK OVERHANG – SINGLE POINT LOAD

Mechanism 1

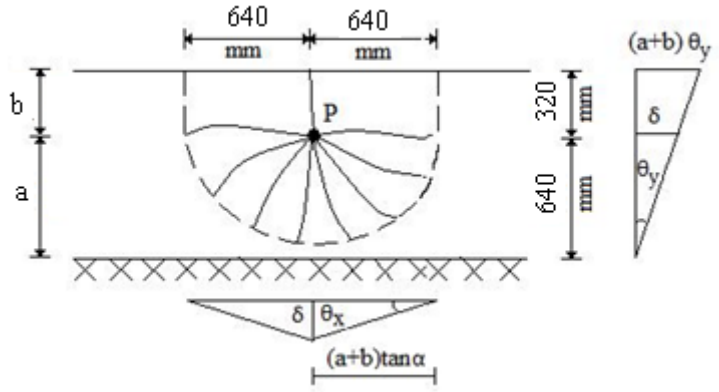

P = Intensity of the point load.

δ = Deflection of slab below point load.

r = Radius of the arc of the yield line pattern.

M, M' = Moment at top and bottom per unit length of slab respectively.

a = Distance of the point load from the fixed end of the overhang = 600 mm

b = Distance of the point load from the free end of the overhang = 300 mm

Equating the external work done to the internal work done,

$$P.\delta = (M + M')(a.\pi)\left(\frac{\delta}{a}\right) + 2.(M + M').(b).\left(\frac{\delta}{a}\right)$$

$$P = \Phi.(M + M')\left(\pi + \frac{2b}{a}\right)$$

Moment calculation on the cantilever portion of the slab,

Top and bottom reinforcement provided is No.4 bars at 6" spacing.

$$M = M' = \frac{0.196}{6}\ x\ 60\ x\ 0.95\ \ x\ (7 - 1.25) = 6.53\ k - in/in$$

$$P = 0.9\ x\ (6.53 + 6.53)\ (\pi + \frac{2x320}{640})$$

$$P = 73.01\ \text{kips} > 40\text{kips}$$

Hence **SAFE**.

Mechanism 2:-

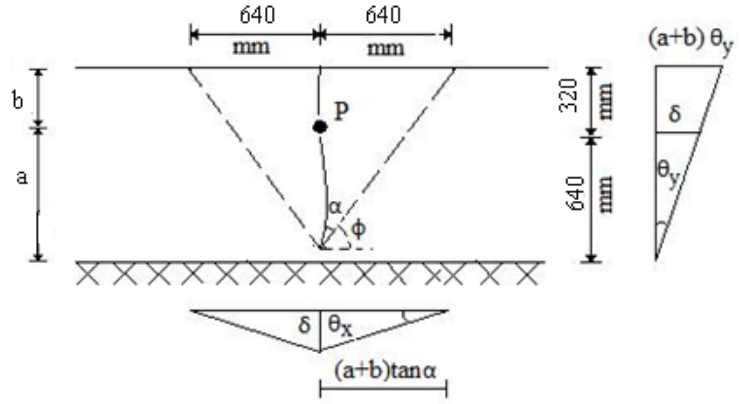

P = Intensity of the point load.

δ = Deflection of slab below point load.

r = Radius of the arc of the yield line pattern.

M, M' = Moment at top and bottom per unit length of slab respectively.

a = Distance of the point load from the fixed end of the overhang = 600 mm

b = Distance of the point load from the free end of the overhang = 300 mm

Equating the external work done to the internal work done,

$$P \cdot \delta = 2[(M + M')(a + b)\left(\frac{\theta_y}{\tan\alpha}\right) + M'.(a + b).(\tan\alpha.\theta_y)]$$

$$P = (2 + \frac{2b}{a})[(M + M').\cot\alpha + M'.(\tan\alpha)]$$

The minimum value of P occurs when $\frac{dp}{d\alpha} = 0$

$$\frac{dp}{d\alpha} = (M + M')\text{cosec}^2\alpha + M'(\sec^2\alpha) = 0$$

$$\tan\alpha = \sqrt{\frac{M + M'}{M'}}$$

$$P = \Phi.4\left(1+\frac{b}{a}\right)(M+M')\sqrt{\frac{M'}{(M+M')}}$$

$$P = 0.9 \text{ x } 4\left(1+\frac{1}{2}\right)(6.53+6.53)\sqrt{\frac{6.53}{(6.53+6.53)}}$$

$P = 74.8$ Kips > 40 kips

Hence **SAFE**.

CASE 3 :- BETWEEN GIRDERS – TWO POINT LOADS

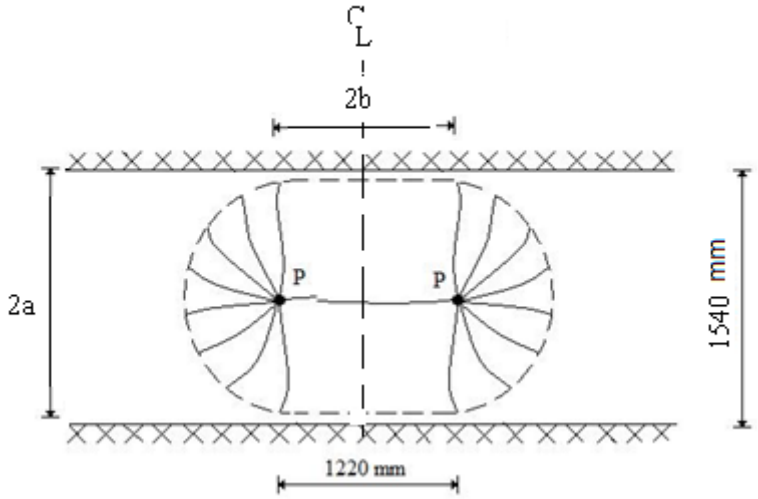

$$P = \Phi.(M+M').\left(\pi+\frac{2b}{a}\right)$$

$$= 0.9 \text{ x } (6.53+6.53)\text{x}\left(\pi+\frac{2x1220}{1540}\right) = 55.54 \text{ kips}$$

Maximum wheel point loads considered on the deck slab = 40 kips < 55.54 kips

Hence **SAFE**.

CHECK FOR CAPACITY OF DECK SLAB USING YIELD LINE THEORY FOR DOUBLE LAYER OF REINFORCEMENT:

Minimum reinforcement requirement as per ACI code = 0.002

Hence minimum reinforcement required = 0.002 x 7 = 0.014 in^2/in.

Using No. 4 bars, Area of one bar = 0.196 in^2

Required Spacing of No.4 bars = $\frac{0.196}{0.014}$ = 14 in.

Minimum spacing provided is not less than twice the depth of the slab = 14 in.

Hence **provide No. 4 bars at 6" spacing in two layers at curved locations.**

ANALYSIS OF DECK SLAB USING YIELD LINE THEORY

Check for the capacity of the deck slab:-

Thickness of slab = 7 in.

Effective depth of slab = 7 - 1.25 = 5.75 in.

jd = 0.95 x 5.75 = 5.46 in.

For the provided reinforcement of No.4 bars @ 6" spacing in two layers,

Moment capacity M= M' = As x fy x jd = $\frac{0.196}{6}$ x 60 x 5.46 = 9.79 kip − in/in

CASE 1: BETWEEN GIRDERS- SINGLE POINT LOAD:-

For single point load on slab the following yield line pattern is considered:-

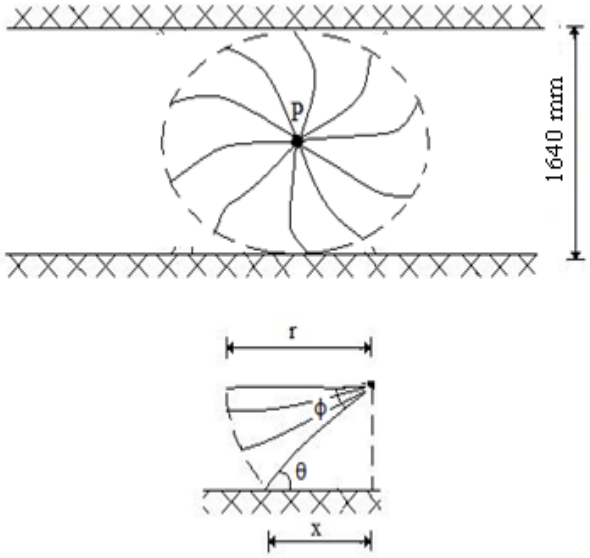

P = Intensity of the point load.

δ = Deflection of slab below point load.

r = Radius of the arc of the yield line pattern.

M, M' = Moment at top and bottom per unit length of slab respectively.

Equating the external work done to the internal work done,

dP. δ = (M+M') . r . dα . (δ/r)

For a complete circle, α = 2 π radians

$$\int_0^{\alpha} dP = \int_0^{\alpha} (M + M')d\alpha$$

$$P = 2\pi(M + M')$$

$$P = 0.9 \text{ x } (9.79 \text{ x } 2)\text{x } 2\,\pi = 110.76 \text{ kips}$$

Maximum point load considered on slab = 40 kips < 110.76 kips

Hence **SAFE.**

CASE 2: BRIDGE DECK OVERHANG – SINGLE POINT LOAD:-

Mechanism 1

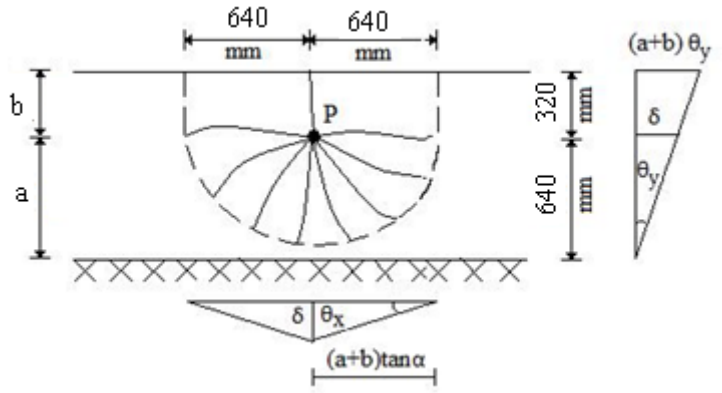

P = Intensity of the point load.

δ = Deflection of slab below point load.

r = Radius of the arc of the yield line pattern.

M, M' = Moment at top and bottom per unit length of slab respectively.

a = Distance of the point load from the fixed end of the overhang = 600 mm

b = Distance of the point load from the free end of the overhang = 300 mm

Equating the external work done to the internal work done,

$$P.\delta = (M + M')(a.\pi)\left(\frac{\delta}{a}\right) + 2.(M + M').(b).\left(\frac{\delta}{a}\right)$$

$$P = \Phi.(M + M')\left(\pi + \frac{2b}{a}\right)$$

Moment calculation on the cantilever portion of the slab,

Top and bottom reinforcement provided is No.4 bars at 6" spacing.

$$M = M' = \frac{0.196}{6}\ x\ 60\ x\ 0.95\ \ x\ (7 - 1.25) = 9.79\ k - in/in$$

$$P = 0.9 \text{ x } (9.79 + 9.79) \left(\pi + \frac{2x320}{640} \right)$$

$$P = 73.01 \text{ kips} > 60\text{kips}$$

Hence **SAFE**.

<u>Mechanism 2</u>:-

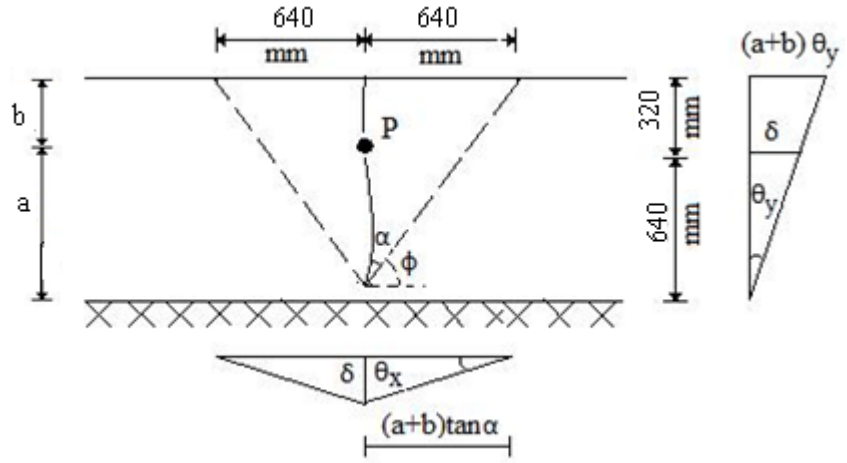

P = Intensity of the point load.

δ = Deflection of slab below point load.

r = Radius of the arc of the yield line pattern.

M, M' = Moment at top and bottom per unit length of slab respectively.

a = Distance of the point load from the fixed end of the overhang = 600 mm

b = Distance of the point load from the free end of the overhang = 300 mm

Equating the external work done to the internal work done,

$$P \,.\, \delta \; = 2[(M + M')(a + b) \left(\frac{\theta_y}{\tan \alpha} \right) + \; M'.\,(a + b).\,(\tan \alpha.\, \theta_y)]$$

$$P \; = (2 + \frac{2b}{a})[(M + M').\cot \alpha + \; M'.\,(\tan \alpha)]$$

The minimum value of P occurs when $\frac{dp}{d\alpha} = 0$

$$\frac{dp}{d\alpha} = (M + M')\text{cosec}^2\alpha + M'(\sec^2\alpha) = 0$$

$$\tan\alpha = \sqrt{\frac{M + M'}{M'}}$$

$$P = \Phi.4\left(1 + \frac{b}{a}\right)(M + M')\sqrt{\frac{M'}{(M+M')}}$$

$$P = 0.9 \text{ x } 4\left(1 + \frac{1}{2}\right)(9.79 + 9.79)\sqrt{\frac{9.79}{(9.79+9.79)}} = 74.79 \text{ kips}$$

$P = 74.79$ Kips > 60 kips

Hence **SAFE**.

CASE 3:- BETWEEN GIRDERS- DOUBLE POINT LOAD

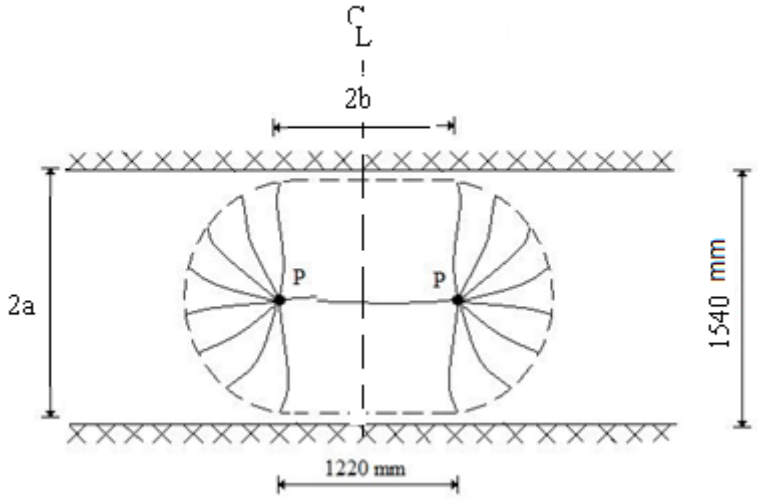

$$P = \Phi.(M + M').\left(\pi + \frac{2b}{a}\right)$$

$$= 0.9 \text{ x } (9.79 + 9.79)\text{x}\left(\pi + \frac{2\text{x}1220}{1540}\right) = 83.31 \text{ kips}$$

Maximum wheel point loads considered on the deck slab = 40 kips < 83.31 kips

Hence **SAFE**.

CHECK FOR PUNCHING SHEAR IN DECK SLAB (TWO LAYER OF REINFORCEMENT):-

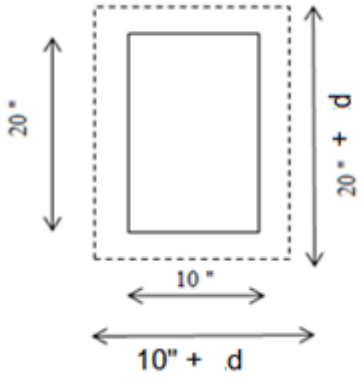

Dimensions of the Critical Section for Punching Shear in Deck Slab

Width of the critical punching area considered = 10 in. (AASHTO Section 3.6.1.2.5)

Depth of the critical punching area considered = 20 in. (AASHTO Section 3.6.1.2.5)

Effective depth of slab, d = 3.5 in.

Width of the critical punching shear area at half the depth of the slab, b' = 10 + 3.5

Hence b= 13.5 in.

Depth of the critical punching shear area at half the depth of the slab, d' = 20 + 3.5

Hence d' = 23.5 in.

The length of critical shear perimeter, b_o is given by,

$b_0 = 2(13.5 + 23.5) = 74$ in.

$\alpha_s = 40$

$\beta c = \frac{20}{10} = 2$

CHECK FOR PUNCHING SHEAR CHECK AS PER AASHTO LRFD BRIDGE DESIGN SPECIFICATIONS:-

Φ, Resistant factor for Shear = 0.9 *(AASHTO Section 5.5.4.2)*

$V_n = \left(0.063 + \frac{0.126}{\beta_c}\right).\sqrt{f'_{c.}}.b_0.d$ *(AASHTO Section 5.13.3.6.3)*

$= \left(0.063 + \frac{0.126}{2}\right) x \sqrt{4}\ x\ 74\ x\ 3.5$

= 65.27 kips

Φ. V_n = 58.74 kips > 40 kips

Hence **SAFE** in Punching Shear.

CHECK FOR PUNCHING SHEAR CHECK AS PER ACI 318:-

Φ. Vc is the smallest of the following :-

a) $\Phi.\ Vc = \Phi.\left(2 + \frac{4}{\beta_c}\right).\sqrt{f'_{c.}}\ b_0.d$ *ACI Equation 11-33*

$= 0.75 \text{ x } (2 + \frac{4}{2}).\sqrt{4000} \text{ x } 74 \text{ x } \frac{3.5}{1000} = 49.14 \text{ kips}$

b) $\Phi.\ V_c = \Phi.\left(2 + \frac{\alpha_s}{b_0}\ d\right).\sqrt{f'_{c.}}\ b_0.d$ *ACI Equation 11-34*

$= 0.75 \text{ x } (2 + \frac{40 \text{x } 3.5}{74}).\sqrt{4000} \text{ x } 74 \text{ x } \frac{3.5}{1000} = 47.81 \text{ kips}$

c) $\Phi.\ V_c = \Phi.\ (4).\sqrt{f'_{c.}}\ b_0.d$ *ACI Equation 11-35*

$$= 0.75 \text{ x } 4 \text{ x } \sqrt{4000} \text{ x } 74 \text{ x } \frac{3.5}{1000} = 49.14 \text{ kips}$$

$\Phi . V_c$ is minimum of above three cases.

$\Phi . V_c$ = 47.81 kips > 40 kips

Hence **SAFE** in Punching Shear.

DESIGN OF GIRDERS

DESIGN OF PRECAST CONCRETE TROUGH GIRDER

							INPUT	
I	**INPUT PARAMETERS**		METRIC UNITS				SI UNITS	
	Characteristic strength of concrete for precast superstructure-girder, f'c	=	6000	psi	=		**6**	ksi
	Characteristic strength of concrete for deck and substructure, f'c	=	4000	psi	=		**4**	ksi
	Coefficient of thermal expansion for concrete, α				=		**0.000006**	/deg F
	Yield strength of steel, fy		60000	psi	=		**60**	ksi
	Unit weight of concrete				=		**150**	pcf
	Span length	=	**140**	ft	=		**40**	m
	Center to center spacing between girders	=	13.12	ft	=		**4**	m
	Width of slab over the trough girder	=	153.54	in.	=		**3900**	mm
	Thickness of slab	=	**7**	in.	=		180	mm
	Cover to CGS	=	**6**	in.	=		152.4	mm
	Diameter of tendon	=	**0.6**	in.				
	Area of one strand of prestressing steel	=	0.217	sq. in.				
	Fpu	=	**270**	ksi				
	fps < 0.7 fpu at transfer	=	189	ksi				
	Effective cover to reinforcement at top	=	**2.75**	in.				
	Effective cover to reinforcement at soffit	=	**1.25**	in.				

DESIGN OF GIRDERS

DESIGN OF PRECAST CONCRETE TROUGH GIRDER

II	**PROPERTIES OF THE GIRDER SECTION**						
	OUTER DIMENSIONS OF TROUGH						
	Width of top of the trough	=	76.25	in.	=	**1936.75**	mm
	Bottom width of trough	=	47.25	in.	=	**1200.15**	mm
	Depth of trough	=	54.00	in.	=	**1371.6**	mm
	INNER DIMENSIONS OF TROUGH						
	Width of top of the trough	=	62.3	in.	=	1581.15	mm
	Bottom width of trough	=	33.3	in.	=	844.55	mm
	Depth of trough	=	47.0	in.	=	1193.8	mm
	Width of the web				=	**180**	mm
	Area of the outer trapezoid				=	2151286.02	mm sq
	Area of the inner trapezoid				=	1447900.33	mm sq
	CG of the outer trapeziod from the bottom of the trough				=	739.48	mm
	CG of the inner trapeziod from the bottom of the trough				=	837.32	mm
	Position of the Neutral Axis from the bottom of the girder	=	21.18	in.	=	538.08	mm

DESIGN OF GIRDERS

DESIGN OF PRECAST CONCRETE TROUGH GIRDER

	y_{top}	=	32.82	in.	=	833.52	mm
	y_{bot}	=	21.18	in.	=	538.08	mm
	Area of the girder	=	1090.25	in^2	=	703385.69	sq mm
	Weight of the girder	=	1135.68	lb/ft			
	Moment of inertia of the outer trapezoid	=	795390.65	in^4	=	3.3107E+11	mm^4
	Moment of inertia of the inner trapezoid	=	400430.48	in^4	=	1.6667E+11	mm^4
	Moment of inertia of the girder section	=	293115.11	in^4	=	1.22E+11	mm^4
	Section Modulus, Sxt	=	8932.13	in^3	=	146371448	mm^3
	Section Modulus, Sxb	=	13836.50	in^3	=	226739553	mm^3
II	**PROPERTIES OF THE COMPOSITE SECTION**						
	Modulus of Elasticity of girder, Eg = 57000.√fc'/1000	=	4415.20	ksi			
	Modulus of Elasticity of deck, Ed= 57000.√fc'/1000	=	3605.00	ksi			
	Modular ratio, n = Eg/Ed	=	1.22				
	Effective width of the slab on top of the trough girder	=	125.37	in.	=	3184.34	mm
	Depth of the slab	=	7.0	in.	=	180	mm

DESIGN OF GIRDERS

DESIGN OF PRECAST CONCRETE TROUGH GIRDER

	CG of the outer trapeziod from the bottom of the trough	=	29.11	in.	=	739.48	mm
	CG of the inner trapeziod from the bottom of the trough	=	32.97	in.	=	837.32	mm
	CG of the slab from the bottom of the trough	=	57.54	in.	=	1461.6	mm
	Position of the neutral axis from the bottom of the girder	=	37.51	in.	=	952.74	mm
	y_{top}	=	23.58	in.	=	598.86	mm
	y_{bot}	=	37.51	in.	=	952.74	mm
	Area of the girder	=	1090.25	in^2	=	703385.69	sq mm
	Area of the slab	=	888.43	in^2	=	573180.6	sq mm
	Area of the composite section	=	1978.68	in^2	=	1276566.29	sq mm
	Weight of the girder	=	1135.68	lb/ft			
	Weight of deck slab	=	925.45	lb/ft			
	Weight of the composite section	=	2061.13	lb/ft			
	Moment of inertia of the outer trapezoid	=	795390.65	in^4	=	3.3107E+11	mm^4
	Moment of inertia of the inner trapezoid	=	400430.48	in^4	=	1.6667E+11	mm^4

DESIGN OF GIRDERS

DESIGN OF PRECAST CONCRETE TROUGH GIRDER

	Moment of inertia of the girder section	=	293115.11	in^4	=	1.22E+11	mm^4
	Moment of inertia of the slab	=	3718.09	in^4	=	1547587619	mm^4
	Moment of inertia of the composite section	=	943976.74	in^4		3.9291E+11	mm^4
	Section Modulus, Sxt = I/ y_{top}	=	40037.8505	in^3	=	656102819	mm^3
	Section Modulus, Sxb = I /y_{bot}	=	25166.3337	in^3	=	412402321	mm^3
III	**PRE-TENSIONING**						
	Load to be considered = 1.2 x self weight	=	1.36	kip/ft			
	Maximum moment in the girder , M = $WL^2/8$	=	3338.89	kip-ft			
	Optimal solution						
	eccentricity, e1a	=	14.19	in.			
	Prestressing Force after losses	=	1121.93	kips			
	Force at transfer, Fi (considering 20% time dependent losses)	=	1402.41	kips			
	Provide eccentricity, e1a	=	**9.61**	in.			
	Force after losses , F1a	=	**1570**	kips			
	Force at transfer, F1ai	=	1891.57	kips			
	Force in a single tendon	=	**41.01**	kips			
	No. of tendons required	=	46.12				
	Provide no. of tendons	=	**48**				

DESIGN OF GIRDERS

DESIGN OF PRECAST CONCRETE TROUGH GIRDER

	Total pretension	=	1968.62	kips			
IV	**POST-TENSIONING**						
	STAGE 1- BALANCING THE GIRDER SELF-WEIGHT						
	Eccentricity at midspan from C.G.C of girder, ec1	=	14.00	in.	=	355.60	mm
	Post-tensioning force,F1 balancing selfweight of girder						
	$F1b.(ec1+e1b)/12 = W_{girder} \times L^2/8$						
	F1b.e1b = F1a.e1a	=	13620.91	kip-in			
	F1b	=	1412.00	Kips			
	e1b	=	9.65	in.			
	Considering 15% time dependent losses + 15% friction losses						
	F1bi	=	1954.32	kips			
	No. of tendons	=	47.65				
	Provide no. of tendons	=	**48**				
	STAGE 2- DECK SLAB BALANCED BY POST-TENSIONED CONTINUITY						
	Additional Post tensioning force balancing the deck load, F2						
	e2	=	**25.5**	in			

DESIGN OF GIRDERS

DESIGN OF PRECAST CONCRETE TROUGH GIRDER

	F2. e2 = W_{deck} . $L^2/8$			
	F2	=	1066.99	kips
	Considering 15% time dependent losses + 15% Friction losses			
	Force at transfer, F2i	=	1476.80	kips
	No. of tendons	=	36.01	
	Provide no. of tendons	=	**36**	

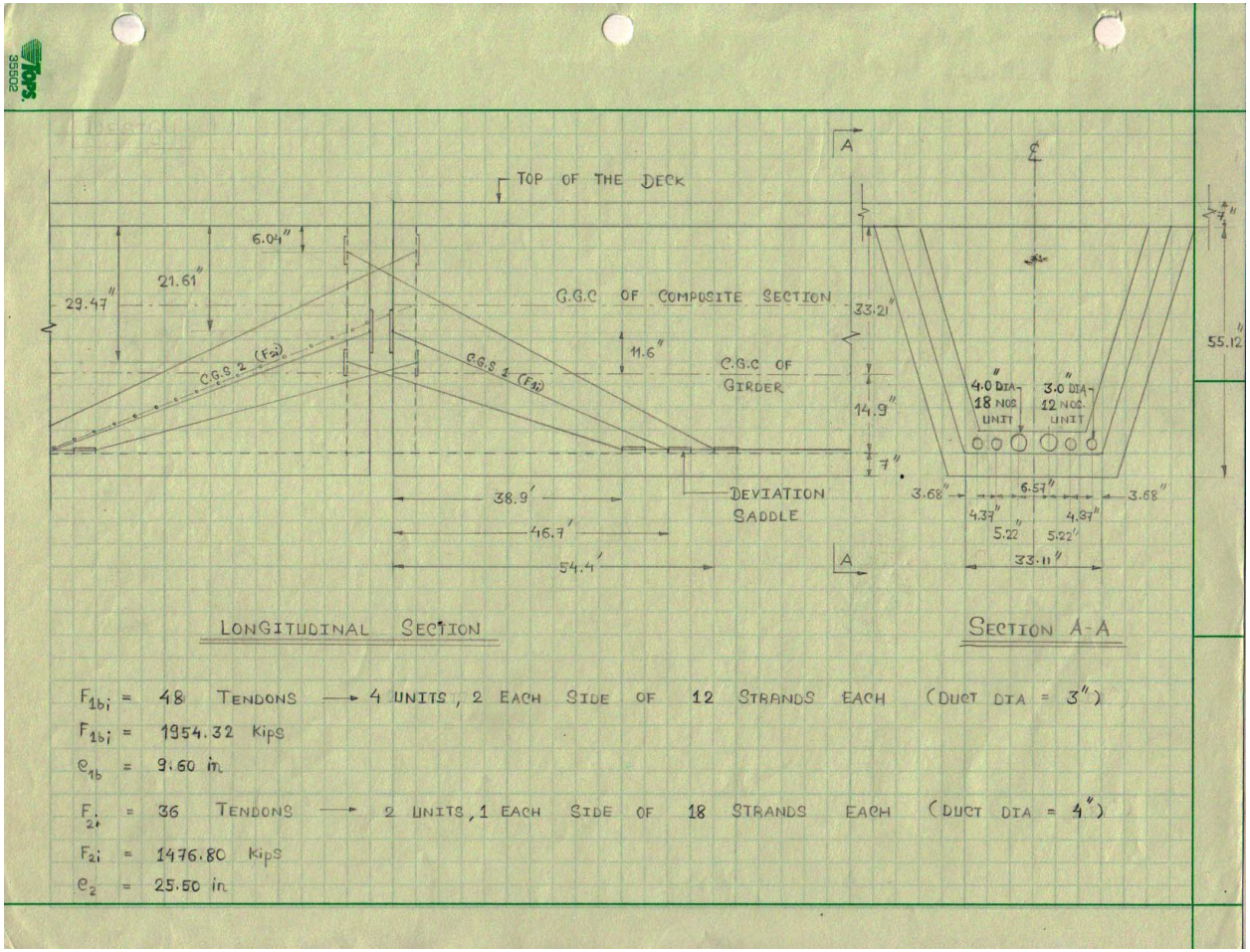

F_{1bi} = 48 TENDONS ⟶ 4 UNITS, 2 EACH SIDE OF 12 STRANDS EACH (DUCT DIA = 3")

F_{1bi} = 1954.32 Kips

e_{1b} = 9.60 in.

F_{2i} = 36 TENDONS ⟶ 2 UNITS, 1 EACH SIDE OF 18 STRANDS EACH (DUCT DIA = 4")

F_{2i} = 1476.80 Kips

e_2 = 25.50 in.

SHEAR DESIGN OF PRECAST CONCRETE TROUGH GIRDER				
	LRFD specifications (AASHTO) based on Modified Compression Field Theory			
			INPUT	
	Characteristic strength of concrete for precast girder, f'c	=	6	ksi
	Yield strength of transverse reinforcement, fy	=	60	ksi
	Modulus of Elasticity of Concrete, Ec	=	4415.2	ksi
	Effective width of the web, bv	=	7	in
	Depth of the composite section, h	=	61	in
	Strength reduction factor for prestressed concrete members, ϕ	=	**0.9**	
	TRANVERSE SHEAR DESIGN AT CRITICAL SECTION			
I	***Effective Shear depth and location***			
	Depth of the resultant Tensile force from top of the deck, dp	=	49.43	in
	Depth of compression block at centre of the end span, a	=	7.59	in
	Effective shear depth, dv is maximum of the following: -			
	i) Distance between resultants of Tensile and Compressive forces, dp-a/2	=	45.63	in
	ii) 0.9dp	=	44.48	in
	iii) 0.72h	=	43.92	in
	Effective shear depth, dv	=	45.63	in
	Angle of inclination of diagonal compressive stress, θ, assume	=	**50**	deg
	Critical section near supports is greater of the following: -			
	i) (0.5).dv.Cotθ	=	1.60	ft
	ii) dv	=	3.80	ft
	Critical section near supports is at a distance	=	3.80	ft
II	***Transverse Shear design at Critical section***			
IIA	***Factored Forces at Critical Section***			
	Factored Shear Force at critical section, Vu	=	458.24	kips
	Factored Moment at critical section, Mu	=	2202.7	kip-ft
	Component of Prestressing force in direction of the shear, Vp	=	1406.3	kips
IIB	***Contribution of Concrete to Nominal Shear Resistance***			
	Area of concrete on flexural tension side below	=	755.16	sqin

SHEAR DESIGN OF PRECAST CONCRETE TROUGH GIRDER				
	(h/2), Ac			
	Strain in reinforcement on the flexural tension side			
	$\varepsilon_x = \frac{\frac{\lvert Mu\rvert}{dv} + 0.5Nu + 0.5\lvert Vu - Vp\rvert cot\theta - Aps.fpo}{2(Es.As + Ep.Aps)} \leq 0.001$	=	-0.0015	
	If the above equation yields a negative value, then following equation should be used			
	$\varepsilon_x = \frac{\frac{\lvert Mu\rvert}{dv} + 0.5Nu + 0.5\lvert Vu - Vp\rvert cot\theta - Aps.fpo}{2(Ec.Ac + Es.As + Ep.Aps)}$	=	-0.0001	
	Shear stress in concrete, vu = $\frac{\lvert Vu - \phi Vp\rvert}{\phi.\ bv.dv}$	=	2.81	ksi
	vu/f'c	=	0.468	
	ε_x x 1000	=	-0.115	
	Using values of β and θ from LRFD Table 5.8.3.4.2-1			
	Θ	=	53.26	deg
	B	=	4.48	
	Nominal Shear strength provided by concrete, Vc			
	Vc = 0.0316 β √f'c $b_v d_v$	=	110.65	kips
	Vu < 0.5 φ(Vc+Vp), Minimum Transverse Shear Reinforcement is required.			
IIC	***Spacing of Transverse reinforcement***			
	Maximum Spacing of Transverse reinforcement, Smax			
	i) If vu < 0.125 f'c, Smax = 0.8 dv ≤ 24 in			
	i) If vu ≥ 0.125 f'c, Smax = 0.4 dv ≤ 12 in			
	Shear stress in concrete at critical section, vu	=	2.81	ksi
	Maximum Spacing of Transverse reinforcement, Smax at support	=	12.00	in
IID	***Minimum Transverse reinforcement***			
	Area of tranverse reinforcement per web: -			
	Av ≥ 0.05.$\frac{bv.S}{fy}$	=	0.006 x S	sqin

SHEAR DESIGN OF PRECAST CONCRETE TROUGH GIRDER				
	Use Stirrups **2** # **5** double-legged			
	Required Spacing of Transverse reinforcement, Sreq	=	12.00	in
	Provide Spacing of Transverse reinforcement, S	=	**12**	in
	Sprov < Sreqd. Hence, OK			
	Area of Transverse reinforcement provided, Av_{prov}	=	0.614	sq.in
	Nominal Shear strength provided by transverse reinforcement, Vs			
	$Vs = \frac{Av.fy.d_v.\cot\theta}{S}$	=	117.46	kips
	Distance from left support upto which this transverse reinforcement is to be provided	=	**40**	ft
	Provide # 5 double-legged stirrups at 12 in c/c upto a distance of 40 ft from support.			
IIE	***Maximum Nominal Shear reinforcement***			
	Vn = 0.25 f'c.bv.dv + Vp			
	Vn = Vc + Vs	=	228.12	kips
	0.25 f'c.bv.dv + Vp	=	1885.4	kips
	Vn < (0.25 f'c.bv.dv + Vp). Hence, OK			
III	***<u>Transverse Shear design at 40 ft from Support</u>***			
IIIA	***Factored Forces at 40 ft***			
	Factored Shear Force at critical section, Vu	=	193.82	kips
	Factored Moment at critical section, Mu	=	12422.77	kip-ft
	Component of Prestressing force in direction of the shear, Vp	=	1165.5	kips
IIIB	***Contribution of Concrete to Nominal Shear Resistance***			
	Area of concrete on flexural tension side, Ac	=	755.16	sqin
	Strain in reinforcement on the flexural tension side			
	$\varepsilon_x = \frac{\frac{\lvert Mu\rvert}{dv} + 0.5Nu + 0.5\lvert Vu - Vp\rvert\cot\theta - Aps.fpo}{2(Es.As + Ep.Aps)} \leq 0.001$			

SHEAR DESIGN OF PRECAST CONCRETE TROUGH GIRDER				
		=	0.0016	
	If the above equation yields a negative value, then following equation should be used $\varepsilon_x = \frac{\frac{\lvert Mu \rvert}{dv} + 0.5Nu + 0.5\lvert Vu - Vp \rvert cot\theta - Aps.fpo}{2(Ec.Ac + Es.As + Ep.Aps)}$	=	0.0001	
	Shear stress in concrete, vu = $\frac{\lvert Vu - \phi Vp \rvert}{\phi . bv.dv}$	=	0.67	ksi
	vu/f'c	=	0.112	
	ε_x x 1000	=	1.636	
	Using values of β and θ from LRFD Table 5.8.3.4.2-1			
	θ	=	27.40	deg
	β	=	2.39	
	Nominal Shear strength provided by concrete, Vc Vc = 0.0316 β √f'c $b_v d_v$	=	59.09	kips
	Vu > 0.5 φ(Vc+Vp), Transverse Shear Reinforcement is required.			
IIIC	***Spacing of Transverse reinforcement*** Maximum Spacing of Transverse reinforcement, Smax i) If vu < 0.125 f'c, Smax = 0.8 dv ≤ 24 in i) If vu ≥ 0.125 f'c, Smax = 0.4 dv ≤ 12 in			
	Shear stress in concrete at critical section, vu	=	0.67	ksi
	Maximum Spacing of Transverse reinforcement, Smax at support	=	24.00	in
IIID	***Minimum Transverse reinforcement*** Area of tranverse reinforcement per web: - Av ≥ 0.05.$\frac{bv.S}{fy}$	=	0.006 x S	sq.in
	Use Stirrups **2** # **5** double-legged			

SHEAR DESIGN OF PRECAST CONCRETE TROUGH GIRDER				
	Required Spacing of Transverse reinforcement, Sreq	=	24.00	in
	Provide Spacing of Transverse reinforcement, S	=	**24**	in
	Sprov < Sreqd. Hence, OK			
	Area of Transverse reinforcement provided, Av_{prov}	=	0.614	sq.in
	Nominal Shear strength provided by transverse reinforcement, Vs			
	$Vs = \frac{Av.fy.d_v.\cot\theta}{S}$	=	58.73	kips
	Provide # 5 double-legged stirrups at 24 in c/c from 40 ft to 100 ft from the left support.			
IIIE	***Maximum Nominal Shear reinforcement***			
	Vn = 0.25 f'c.bv.dv + Vp			
	Vn = Vc + Vs	=	117.82	kips
	0.25 f'c.bv.dv + Vp	=	1165.5	kips
	Vn < (0.25 f'c.bv.dv + Vp). Hence, OK			
IV	***<u>Minimum Longitudinal reinforcement requirement</u>***			
	Factored Shear force at the face of the support, Vu	=	484.56	kips
	Factored Moment at the face of the support, Mu	=	1194.8	kip-ft
	$Aps.fps \geq \frac{Mu}{d_v \varphi_f} + 0.5\,\frac{Nu}{\varphi_c} + \left(\frac{Vu}{\varphi_v} + 0.5Vs - Vp\right)\cot\theta$			
	$\frac{Mu}{d_v \varphi_f} + 0.5\,\frac{Nu}{\varphi_c} + \left(\frac{Vu}{\varphi_v} + 0.5Vs - Vp\right)\cot\theta$	=	815.30	kips
	$Aps.fps$	=	166861	kips
	Aps.fps > (Mu/(dv φf)+0.5 Nu/φc +(Vu/φv +0.5Vs-Vp)cotϑ). Hence, OK			

DESIGN OF SHEAR CONNECTORS FOR PRECAST CONCRETE DECKS				
	Design of Shear Connectors for Precast concrete decks based on Truss Modelling Approach			
			INPUT	
	Characteristic strength of concrete for precast girder, f'c	=	6	ksi
	Yield strength of transverse reinforcement, fy	=	60	ksi
	Modulus of Elasticity of Concrete, Ec	=	4415.20	ksi
	Effective width of the web, bv	=	7	in
	Depth of the composite section, h	=	61	in
	Thickness of slab	=	7	in
	Length of a single slab panel, L_{Panel}	=	**8**	ft
	Strength reduction factor for prestressed concrete members, ϕ	=	**0.9**	
	Co-efficient of friction for sliding shear resistance, μ	=	**0.8**	
	Distribution factor for shear, D.F.	=	**1**	
	Internal lever arm in Girder, jd_{girder}	=	45.63	in
	Internal lever arm Overall, jd_o	=	52.93	in
	Hoop/Stirrup used	=	**5**	#
	Area of Single hoop, A_{sh}	=	0.61	sq.in
	Area of longitudinal mild steel rebar in girder, A_s	=	**3.72**	sq.in
	Area of Prestressing tendons in the girder, A_{sp}	=	26.91	sq.in
	Area of Longitudinal Girder reinforcement, A_{sb}	=	30.63	sq.in
	Area of 2 nos. 1-in CR	=	**1.08**	sq.in
	Area of 2 nos. 1.25-in CR	=	**1.82**	sq.in
	Yield strength of 1-in. CR, $F_{yc,\ 1\text{-}in}$	=	**120**	ksi
	Yield strength of 1-in. CR, $F_{yc,\ 1.25\text{-}in}$	=	**105**	ksi
	END PANEL DESIGN FOR SLIDING SHEAR			
I	***Net Panel Shear demand***			
	At Left End of the Panel			
	Dead load Shear, V_{DL}	=	179.28	kips
	Live load Shear, V_{LL}	=	119.64	kips
	Total Factored Shear, $V_u = 1.25\ V_{DL} + 1.75\ (D.F.)\ (1.33 \times V_{LL})$	=	502.57	kips
	Component of Prestressing force in the direction of applied shear, V_p	=	1406.37	kips
	$V_u - V_p$	=	-903.81	kips

DESIGN OF SHEAR CONNECTORS FOR PRECAST CONCRETE DECKS

At Right End of the Panel

Dead load Shear, V_{DL}	=	161.35	kips
Live load Shear, V_{LL}	=	116.43	kips
Total Factored Shear, $V_u = 1.25\ V_{DL} + 1.75\ (D.F.)\ (1.33 \times V_{LL})$	=	472.68	kips
Component of Prestressing force in the direction of applied shear, V_p	=	1406.37	kips
$V_u - V_p$	=	-933.70	kips
Average shear demand over End Panel, V_{avg}	=	-918.75	kips

II ***Design of Pocket Layout and Connectors***

Number of pockets needed in the end panel

	2 - 1 in CR	*2 - 1.25 in CR*
N_{Pocket}	2.00	2.00

Provide

	2 - 1 in CR	*2 - 1.25 in CR*
N_{pocket}	**2**	**2**

III ***Provide hoops to form Non-contact splice***

Number of hoop groups required to anchor shear connectors in a pocket

	2 - 1 in CR	*2 - 1.25 in CR*
N_{Group}	3.52	5.19

Provide

	2 - 1 in CR	*2 - 1.25 in CR*
N_{group}	**4**	**6**

IV ***Determining Web Shear Capacity***

Use = **2 - 1 in CR**

DESIGN OF SHEAR CONNECTORS FOR PRECAST CONCRETE DECKS				
	Number of pockets, N_{Pocket}	=	2	
	Number of hoop groups, N_{Group}	=	4	
	Expected crack angle, cot θ	=	2.00	
	Shear Capacity of the transverse girder reinforcement, ϕVs	=	251.81	kips
	φVs > Vavg. Hence, OK			

ULTIMATE CAPACITY OF THE TROUGH GIRDER				
	DATA			
			INPUT	
	Characteristic strength of concrete for precast girder, f'cb	=	6	ksi
	Characteristic strength of concrete for deck and substructure, f'cs	=	4	ksi
	Characteristic strength of concrete for precast superstructure, f'c	=	5	ksi
	fpu	=	270	ksi
	fps < 0.7 fpu at transfer	=	189	ksi
	Span of the bridge	=	140	ft
	Width of the diaphragm	=	**5**	ft
	Effective width of the slab on top of the trough girder	=	125.37	in
	Thickness of slab	=	7	in
	Width of the webs	=	**7**	in
	Depth of the girder	=	54.00	in
	Diameter of tendon	=	0.6	in
	Area of one strand of prestressing steel	=	0.217	sq.in
	β1 = 0.85 - 0.05 (f'c - 4)			
	β1s	=	0.85	
	β1b	=	0.75	
	k for Low relaxation strand	=	**0.28**	
	ULTIMATE CAPACITY CALCULATION			
I	***AT 0.3L of Exterior Span*** **Pretension Prestressing tendons (Bonded tendons) - Straight - Bottom Flange**			

ULTIMATE CAPACITY OF THE TROUGH GIRDER			
No. of Tendons	=	**10**	
dp	=	**60.15**	in
bw	=	**47.20**	in
$\rho_{p\ 1a}$	=	0.001	
ρ_{p} . fpu/f'c	=	0.041	
fps_{1a}	=	236.34	ksi
Pretension Prestressing force, F_{1a}	=	512.86	kips
Pretension Prestressing tendons (Bonded tendons) - Straight - Web			
No. of Tendons	=	**20**	
dp	=	**35.30**	in
bw	=	**14.00**	in
$\rho_{p\ 1a}$	=	0.009	
ρ_{p} . fpu/f'c	=	0.474	
fps_{1a}	=	176.10	ksi
Pretension Prestressing force, F_{1a}	=	764.29	kips
Pretension Prestressing tendons (Bonded tendons) - Harped			
No. of Tendons	=	**18**	
dp	=	**54.00**	in
bw	=	**14.00**	in
ρ_{p1b}	=	0.005	
ρ_{p1b} . fpu/f'c	=	0.279	
fps_{1a}	=	214.76	ksi
Pretension Prestressing force, F_{1a}	=	838.84	kips
Post-tension Prestressing tendons (Unbonded tendons)			
No. of Tendons	=	**84**	
dp	=	**52.28**	in
bw	=	**14.00**	in
ρ_{p1b}	=	0.025	
fps_{1a}	=	190.00	ksi

ULTIMATE CAPACITY OF THE TROUGH GIRDER				
	Pretension Prestressing force, F_{1a}	=	3463.32	kips
	For Rectangular section behavior,			
	$c = \frac{Aps.fps + As.fy - As'.fy'}{0.85.f'cs.\beta1s.b + k.Aps.(fps/dp)}$			
	c	=	14.17	in
	a = β1s.c	=	12.05	in
	12.05 > 7 in. Thus, it is a flanged section behavior.			
	For Flanged section behavior,			
	$c' = \frac{[\ Aps.fps - 0.85.hf.(f'cs.bs.\beta1s - f'cb.bw.\beta1b/\beta1s)\ ]}{0.85.f'cb.\beta1b.bw + k.Aps.(fps/dp)}$			
	c'	=	56.15	in
	a' = β1b.c'	=	42.11	in
	42.12 > 7 in. Thus, it is a flanged section behavior.			
	Moment Capacity, ϕMn (+ve)	=	10917.79	kip-ft
III	***At the face of the diaphragm***			
	Pretension Prestressing tendons (Bonded tendons) - Straight - Bottom Flange			
	No. of Tendons	=	**10**	
	dp	=	**2.85**	in
	bw	=	**47.20**	in
	$\rho_{p\ 1a}$	=	0.016	
	ρ_{p} . fpu/f'c	=	0.871	
	fps_{1a}	=	97.52	ksi
	Pretension Prestressing force, F_{1a}	=	211.62	kips
	Pretension Prestressing tendons (Bonded tendons) - Straight - Web			
	No. of Tendons	=	**20**	
	dp	=	**27.70**	in
	bw	=	**14.00**	in
	$\rho_{p\ 1a}$	=	0.011	

ULTIMATE CAPACITY OF THE TROUGH GIRDER			
$\rho_p . fpu/f'c$	=	0.604	
fps_{1a}	=	150.34	ksi
Pretension Prestressing force, F_{1a}	=	652.49	kips
Pretension Prestressing tendons (Bonded tendons) - Harped			
No. of Tendons	=	**18**	
dp	=	**27.40**	in
bw	=	**14.00**	in
ρ_{p1b}	=	0.010	
$\rho_{p1b} . fpu/f'c$	=	0.550	
fps_{1a}	=	161.13	ksi
Pretension Prestressing force, F_{1a}	=	629.37	kips
Post-tension Prestressing tendons (Unbonded tendons)			
No. of Tendons	=	**84**	
dp	=	**35.21**	in
bw	=	**14.00**	in
ρ_{p1b}	=	0.037	
fps_{1a}	=	190.00	ksi
Pretension Prestressing force, F_{1a}	=	3463.32	kips
Reinforcement in the deck slab			
Area of steel provided	=	**0.46**	sq.in/ft
de	=	**58.62**	in
bw	=	**125.37**	in
ρ_s	=	0.001	
fy	=	36.00	ksi
Pretension Prestressing force, F_{1a}	=	173.01	kips
For Rectangular section behavior,			
$c = \frac{Aps.fps + As.fy - As'.fy'}{0.85.f'cs.\beta 1s.b + k.Aps.\frac{(fps}{dp)}}$			

ULTIMATE CAPACITY OF THE TROUGH GIRDER				
	c	=	12.11	in
	a = β1s.c	=	10.29	in
	10.3 > 7 in. Thus, it is a flanged section behavior.			
	For Flanged section behavior,			
	c' = [Aps.fps - 0.85.hf.(f'cs.bs.β1s - f'cb.bw.β1b/β1s)] / [0.85.f'cb.β1b.bw + k.Aps. (fps/dp)]			
	c'	=	31.93	in
	a' = β1b.c'	=	23.95	in
	23.95 > 7 in. Thus, it is a flanged section behavior.			
	Moment Capacity, ϕMn (-ve)	=	9447.75	kip-ft
III	***AT Midspan of Middle Span***			
	Pretension Prestressing tendons (Bonded tendons) - Straight - Bottom Flange			
	No. of Tendons	=	**10**	
	dp	=	**60.15**	in
	bw	=	**47.20**	in
	$\rho_{p\ 1a}$	=	0.001	
	ρ_{p} . fpu/f'c	=	0.041	
	fps_{1a}	=	236.34	ksi
	Pretension Prestressing force, F_{1a}	=	512.86	kips
	Pretension Prestressing tendons (Bonded tendons) - Straight - Web			
	No. of Tendons	=	**20**	
	dp	=	**35.30**	in
	bw	=	**14.00**	in
	$\rho_{p\ 1a}$	=	0.009	
	ρ_{p} . fpu/f'c	=	0.474	
	fps_{1a}	=	176.10	ksi
	Pretension Prestressing force, F_{1a}	=	764.29	kips
	Pretension Prestressing tendons (Bonded			

ULTIMATE CAPACITY OF THE TROUGH GIRDER			
tendons) - Harped			
No. of Tendons	=	**18**	
dp	=	**60.15**	in
bw	=	**47.20**	in
ρ_{p1b}	=	0.001	
ρ_{p1b} . fpu/f'c	=	0.074	
fps_{1a}	=	236.34	ksi
Pretension Prestressing force, F_{1a}	=	923.14	kips
Post-tension Prestressing tendons (Unbonded tendons)			
No. of Tendons	=	**84**	
dp	=	**52.28**	in
bw	=	**14.00**	in
ρ_{p1b}	=	0.025	
fps_{1a}	=	190.00	ksi
Pretension Prestressing force, F_{1a}	=	3463.32	kips
For Rectangular section behavior,			
$c = \frac{Aps.fps + As.fy - As'.fy'}{0.85.f'cs.\beta1s.b + k.Aps.(fps/dp)}$			
c	=	14.39	in
a = β1s.c	=	12.23	in
12.24 > 7 in. Thus, it is a flanged section behavior.			
For Flanged section behavior,			
$c' = \frac{[\ Aps.fps - 0.85.hf.(f'cs.bs.\beta1s - f'cb.bw.\beta1b/\beta1s)\ ]}{0.85.f'cb.\beta1b.bw + k.Aps.(fps/dp)}$			
c'	=	57.65	in
a' = β1b.c'	=	43.24	in
43.24 > 7 in. Thus, it is a flanged section behavior.			
Moment Capacity, ϕMn (+ve)	=	11360.16	kip-ft

ULTIMATE CAPACITY OF THE TROUGH GIRDER

CALCULATION OF λ

For a train of vehicles loaded over a span,

Maximum moment at midspan,

M_{LL}	=	5209.17	kip-ft
Uniformly distributed load, W_{LL}	=	2.13	kip/ft
Uniformly distributed load, W_{DL}	=	2.56	kip/ft
M_1*	=	15641.66	kip-ft
Wu1	=	6.62	kip/ft
M_2*	=	20807.91	kip-ft
Wu2	=	9.13	kip/ft

$\lambda . W_{LL} = Wu1 - 1.25\ W_{DL}$

λ = 1.61

1.61 < 1.75. Hence, Provide additional Mild Steel.

$\lambda . W_{LL} = Wu2 - 1.25\ W_{DL}$

λ = 2.79

2.79 > 1.75. Hence, Safe.

Additional Capacity required

Additional Moment at supports,

ΔM	=	465.82	kip-ft
Additional steel required in the deck at the supports	=	0.29	sq.in
	=	0.002	sq.in/in

Use # **4** bars

Number of $Bars_{reqd}$ = 3

Number of $Bars_{prov}$ = **4**

Add 4 Nos. # 4 bars spaced equally in the deck slab at supports.

AASHTO TYPE IV I- GIRDER: Two Stage Post-tensioning

DESIGN OF PRECAST CONCRETE AASHTO TYPE IV I-GIRDER								
							INPUT	
I	**INPUT PARAMETERS**		METRIC UNITS				SI UNITS	
-	-							
	Characteristic strength of concrete for precast superstructure-girder, f'c	=	6000	psi	=	**6**	ksi
	Characteristic strength of concrete for deck and substructure, f'c	=	4000	psi	=	**4**	ksi
	Coefficient of thermal expansion for concrete, α				=	**6E-06**	/deg F
	Yield strength of steel, fy		60000	psi	=	**60**	ksi
	Unit weight of concrete				=	**150**	pcf
	Span length	=	132	ft	=	**40**	m
	Center to center spacing between girders	=	6	ft	=	**1.83**	m
	Width of slab over the I girder	=	76.77	in.	=	**1950**	mm
	Thickness of slab	=	7	in.	=	180	mm
	Cover to CGS	=	**6**	in.	=	152.4	mm
	Diameter of tendon	=	**0.6**	in.			
	Area of one strand of prestressing steel	=	0.217	sq. in.			
	fpu	=	**270**	ksi			
	fps < 0.7 fpu at transfer	=	189	ksi			
	Effective cover to reinforcement at top	=	**2.75**	in.			
	Effective cover to reinforcement at soffit	=	**1.25**	in.			
II	**PROPERTIES OF THE GIRDER SECTION**							
	DIMENSIONS OF I - GIRDER							
	Width of top flange	=	20	in.				
	Width of bottom flange	=	26	in.				
	Depth of the I - Girder	=	54	in.				
	Depth of the straight portion of the top flange	=	8	in.				
	Depth of the slanting portion of the top flange	=	6	in.				
	Depth of the straight portion of the bottom flange	=	8	in.				

DESIGN OF PRECAST CONCRETE AASHTO TYPE IV I-GIRDER				
	Depth of the slanting portion of the bottom flange	=	9	in.
	Width of the web	=	8	in.
	Position of the Neutral Axis from the bottom of the girder	=	24.73	in.
	y_{top}	=	29.27	in.
	y_{bot}	=	24.73	
	Area of the girder	=	789	in^2
	Weight of the girder	=	821.88	lb/ft
	Moment of inertia of the girder section	=	260740.8	in^4
	Section Modulus, Sxt	=	8908.1	in^3
	Section Modulus, Sxb	=	10543.53	in^3
II	**PROPERTIES OF THE COMPOSITE SECTION**			
	Modulus of Elasticity of girder, Eg = 57000.√fc'/1000	=	4415.2	ksi
	Modulus of Elasticity of deck, Ed= 57000.√fc'/1000	=	3605	ksi
	Modular ratio, n = Eg/Ed	=	1.22	
	Effective width of the slab on top of the girder	=	62.68	in.
	Depth of the slab	=	7.1	in.
	CG of the Girder section from the bottom flange	=	24.73	in.
	CG of the slab from the bottom flange	=	57.54	in.
	Position of the neutral axis from the bottom of the girder	=	36.55	in.
	y_{top}	=	24.54	in.
	y_{bot}	=	36.55	in.
	Area of the girder	=	789	in^2
	Area of the slab	=	444.22	in^2
	Area of the composite section	=	1233.22	in^2

DESIGN OF PRECAST CONCRETE AASHTO TYPE IV I-GIRDER				
	Weight of the girder	=	821.88	lb/ft
	Weight of deck slab	=	462.72	lb/ft
	Weight of the composite section	=	1284.6	lb/ft
	Moment of inertia of the girder section	=	260740.8	in^4
	Moment of inertia of the slab	=	1859.05	in^4
	Moment of inertia of the composite section	=	568608.7	in^4
	Section Modulus, Sxt = I/ y_{top}	=	23173.52	in^3
	Section Modulus, Sxb = I /y_{bot}	=	15557.18	in^3
III	**PRE-TENSIONING**			
	Load to be considered = 1.2 x self weight	=	0.99	kip/ft
	Maximum moment in the girder , M = $WL^2/8$	=	2148.05	kip-ft
	Optimal solution			
	eccentricity, e_{1a}		**17.4**	
	Prestressing Force after losses	=	**678.41**	kips
	Force at transfer, F_{1ai} (considering 20% time dependent losses)		848.01	kips
	Provide eccentricity, e_{1a}	=	**17**	in.
	Force after losses , F_{1a}	=	**689**	kips
	Force at transfer, F_{1ai}	=	861.25	kips
	Force in a single tendon	=	**41.01**	kips
	No. of tendons required	=	**21**	
	Provide no. of tendons	=	**22**	
	Total pretension	=	902.29	kips
IV	**POST-TENSIONING**			
	STAGE 1- BALANCING THE GIRDER SELF-WEIGHT			
	Eccentricity at midspan from C.G.C of girder, (e_{c1} + e_{1b})	=	18.5	in.
	Post-tensioning force,F_{1b} balancing selfweight of girder			
	$F_{1b}.(e_{c1}+e_{1b})/12 = W_{girder}$ x $L^2/8$			

DESIGN OF PRECAST CONCRETE AASHTO TYPE IV I-GIRDER				
	$F_{1b}.e_{1b} = F_{1a}.e_{1a}$	=	11713	kips
	F_{1b}		1161.11	Kips
	e_{1b}		10.1	in.
	Considering 15% time dependent losses + 15% friction losses			
	F_{1bi}		1607.07	kips
	No. of tendons	=	39.18	
	Provide no. of tendons	=	**43**	
	Total $F_{1b}i$		1763.56	kips
	STAGE 2- DECK SLAB BALANCED BY POST-TENSIONED CONTINUITY - END SPAN			
	Additional Post tensioning force balancing the deck load, F_{2a}			
	e_{2a}		**37.5**	in
	$F_{2a}. e_{2a} = W_{deck} . L^2/8$			
	F_{2a}		322.5	kips
	Considering 15% time dependent losses + 15% Friction losses			
	Force at transfer, F_{2ai}	=	446.37	kips
	No. of tendons	=	10.88	
	Provide no. of tendons	=	**12**	
	Total $F_{2a}i$	=	492.16	kips
	STAGE 2- DECK SLAB BALANCED BY POST-TENSIONED CONTINUITY - MIDDLE SPAN			
	Eccentricity at center of the midspan, ec_{2b} (considering F_{2a})	=	30.4	in.
	Eccentricity at center of the midspan, ec_{2b}	=	**49.5**	in.
	Post-tensioning force,F_{2b} balancing selfweight of girder and deck			
	$F_{2b}.ec_{2b} = F_{2a}.ec_{2a}$			
	F_{2b}	=	198.15	Kips
	Considering 15% time dependent losses + 15% friction losses			
	$F_{2b}i$		274.25	kips
	No. of tendons	=	6.69	
	Provide no. of tendons	=	**7**	
	Total $F_{2b}i$		287.09	kips

SIDE ELEVATION OF I-GIRDER SHOWING CABLE PROFILE

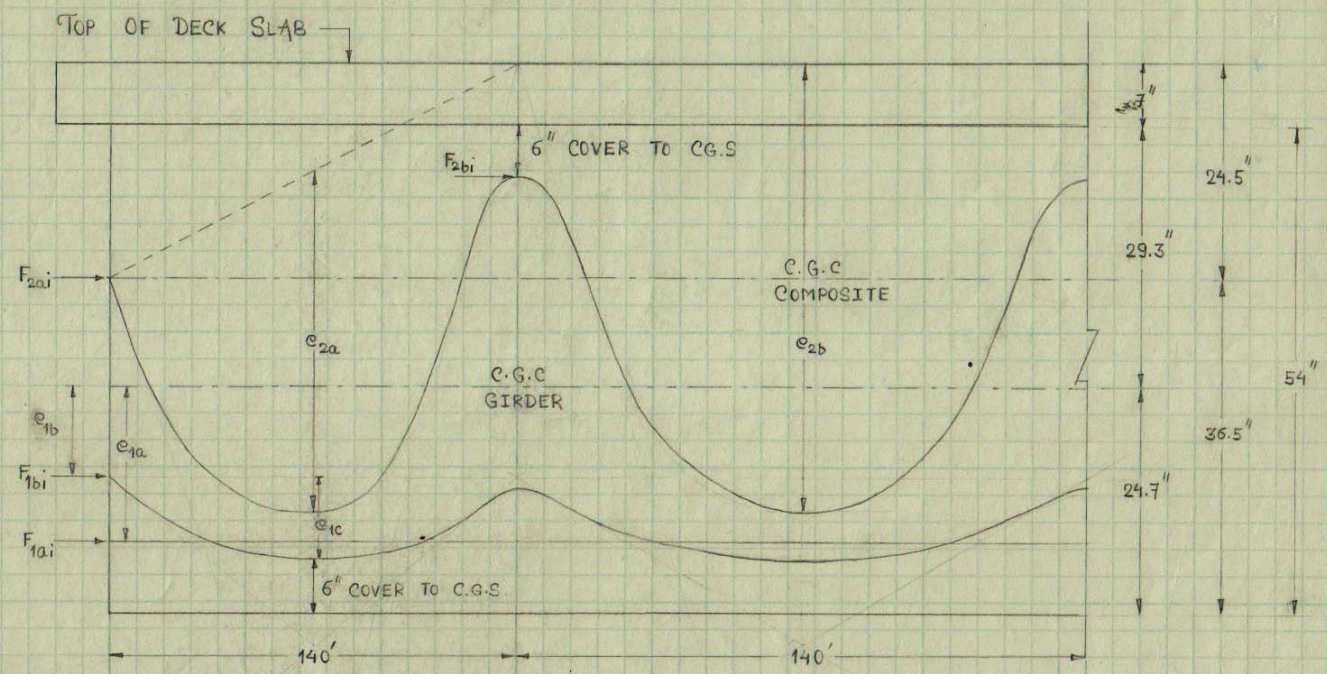

PRETENSIONING :- FORCE F_{1ai} = 902.5 kips, e_{1a} = 17", TENDONS = 0.6" dia, 22 Nos.

POST-TENSIONING :- STAGE 1 → FORCE F_{1bi} = 1763.5 kips, e_{1b} = 10", e_{1c} = 8.5", TENDONS = 0.6" dia, 43 Nos. [1 DUCT-6

STAGE 2 → FORCE F_{2ai} = 492 kips, e_{2a} = 37.5", TENDONS = 0.6" dia, 12 Nos. [1 DUCT - 3" dia

FORCE F_{2bi} = 287 kips, e_{2b} = 49.5", TENDONS = 0.6" dia, 7 Nos. [1 DUCT - 2.5" di

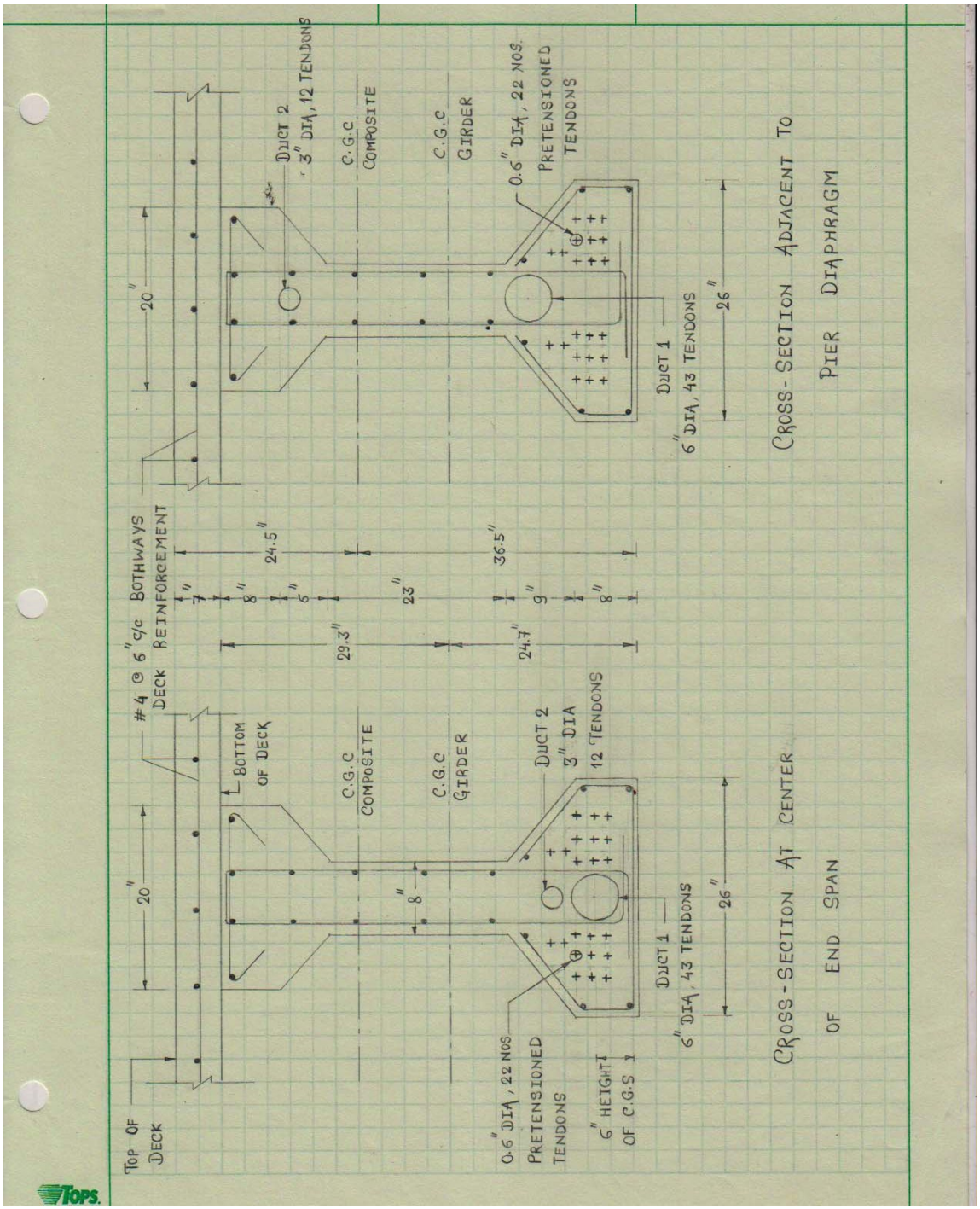
TOP OF DECK
#4 @ 6" c/c BOTHWAYS DECK REINFORCEMENT
20"
BOTTOM OF DECK
C.G.C COMPOSITE
C.G.C GIRDER
8"
6" HEIGHT OF C.G.S
0.6" DIA, 22 NOS. PRETENSIONED TENDONS
DUCT 2 3" DIA 12 TENDONS
DUCT 1 6" DIA, 43 TENDONS
26"
29.3"
24.7"
24.5"
36.5"
23"
7"
8"
6"
9"
CROSS-SECTION AT CENTER OF END SPAN
CROSS-SECTION ADJACENT TO PIER DIAPHRAGM

ULTIMATE CAPACITY OF THE AASHTO TYPE IV GIRDER				
	DATA			
			INPUT	
	Characteristic strength of concrete for precast girder, f'cb	=	6	ksi
	Characteristic strength of concrete for deck and substructure, f'cs	=	4	ksi
	Characteristic strength of concrete for precast superstructure, f'c	=	5	ksi
	fpu	=	270	ksi
	fps < 0.7 fpu at transfer	=	189	ksi
	Span of the bridge	=	140	ft
	Width of the diaphragm	=	**5**	ft
	Effective width of the slab on top of the I girder	=	76.77	in
	Thickness of slab	=	7	in
	Width of the webs	=	**8**	in
	Depth of the girder	=	54	in
	Diameter of tendon	=	0.6	in
	Area of one strand of prestressing steel	=	0.217	sq.in
	β1 = 0.85 - 0.05 (f'c - 4)			
	β1s	=	0.85	
	β1b	=	0.75	
	k for Low relaxation strand	=	**0.28**	
	ULTIMATE CAPACITY CALCULATION			
I	***AT 0.3L of Exterior Span***			
	Pretension Prestressing tendons (Bonded tendons)			
	No. of Tendons	=	**22**	
	dp	=	**53.27**	in
	bw	=	**20**	in
	$\rho_{p\ 1a}$	=	0.004	
	ρ_{p} . fpu/f'c	=	0.242	
	fps_{1a}	=	222.09	ksi
	Pretension Prestressing force, F_{1a}	=	1060.26	kips
	Stage 1 - Post-tension Prestressing tendons (Bonded tendons)			
	No. of Tendons	=	**43**	
	dp	=	**54.07**	in
	bw	=	**26**	in
	ρ_{p1b}	=	0.007	
	ρ_{p1b} . fpu/f'c	=	0.358	

ULTIMATE CAPACITY OF THE AASHTO TYPE IV GIRDER				
	fps_{1b}	=	199.03	ksi
	Post-tension Prestressing force, F_{1b}	=	1857.18	kips
	Stage 2 - Post-tension Prestressing tendons (Bonded tendons)			
	No. of Tendons	=	**12**	
	dp	=	**45.2**	in
	bw	=	**9**	in
	ρ_{p2}	=	0.006	
	ρ_{p2} . fpu/f'c	=	0.346	
	fps_2	=	201.56	ksi
	Post-tension Prestressing force, F_2	=	524.86	kips
	For Rectangular section behavior,			
	$c = \frac{Aps.fps + As.fy - As'.fy'}{0.85.f'cs.\beta 1s.b + k.Aps.(fps/dp)}$			
	c	=	14.32	in
	$a = \beta 1s.c$	=	12.18	in
	12.18 > 7 in. Thus, it is a flanged section behavior.			
	For Flanged section behavior,			
	$c' = \frac{[\ Aps.fps - 0.85.hf.(f'cs.bs.\beta 1s - f'cb.bw.\beta 1b/\beta 1s)\ ]}{0.85.f'cb.\beta 1b.bw + k.Aps.(fps/dp)}$			
	c'	=	43.33	in
	$a' = \beta 1b.c'$	=	32.5	in
	32.5 > 7 in. Thus, it is a flanged section behavior.			
	Moment Capacity, φMn (+ve)	=	10690.83	kip-ft
III	***At the face of the diaphragm***			
	Stage 2 - Post-tension Prestressing tendons (Bonded tendons)			
	No. of Tendons	=	**7**	
	dp	=	**39.8**	in
	bw	=	**18**	in
	ρ_{p2}	=	0.002	
	ρ_{p2} . fpu/f'c	=	0.114	
	fps_2	=	236.34	ksi
	Post-tension Prestressing force, F_2	=	359	kips
	Reinforcement in the deck slab			
	Area of steel provided	=	**0.46**	sq.in/ft
	de	=	**57.5**	in
	bw	=	**62.68**	in

ULTIMATE CAPACITY OF THE AASHTO TYPE IV GIRDER				
	ρ_s	=	0.001	
	fy	=	36	ksi
	Pretension Prestressing force, F	=	105.94	kips
	For Rectangular section behavior,			
	$c = \frac{Aps.fps + As.fy - As'.fy'}{0.85.f'cs.\beta 1s.b + k.Aps.(fps/dp)}$			
	c	=	2.07	in
	$a = \beta 1s.c$	=	1.76	in
	1.77 < 7 in. Thus, it is a rectangular section behavior.			
	Moment Capacity, φMn (-ve)	=	1664.22	kip-ft
III	***AT Midspan of Middle Span***			
	Pretension Prestressing tendons (Bonded tendons)			
	No. of Tendons	=	**22**	
	dp	=	**53.27**	in
	bw	=	**20**	in
	$\rho_{p\ 1a}$	=	0.004	
	ρ_{p1a} . fpu/f'c	=	0.242	
	fps_{1a}	=	222.09	ksi
	Pretension Prestressing force, F_{1a}	=	1060.26	kips
	Stage 1 - Post-tension Prestressing tendons (Bonded tendons)			
	No. of Tendons	=	**43**	
	dp	=	**54.77**	
	bw	=	**26**	
	ρ_{p1b}	=	0.007	
	ρ_{p1b} . fpu/f'c	=	0.354	
	fps_{1b}	=	199.94	ksi
	Post-tension Prestressing force, F_{1b}	=	1865.64	kips
	Stage 2 - Post-tension Prestressing tendons (Bonded tendons)			
	No. of Tendons	=	**7**	
	dp	=	**45.2**	
	bw	=	**9**	
	ρ_{p2}	=	0.004	
	ρ_{p2} . fpu/f'c	=	0.202	
	fps_2	=	230.08	ksi

ULTIMATE CAPACITY OF THE AASHTO TYPE IV GIRDER				
	Post-tension Prestressing force, F_2	=	349.49	kips
	For Rectangular section behavior,			
	$c = \frac{Aps.fps + As.fy - As'.fy'}{0.85.f'cs.\beta1s.b + k.Aps.(fps/dp)}$			
	c	=	13.7	in
	$a = \beta1s.c$	=	11.64	in
	11.65 > 7 in. Thus, it is a flanged section behavior.			
	For Flanged section behavior,			
	$c' = \frac{[\ Aps.fps - 0.85.hf.(f'cs.bs.\beta1s - f'cb.bw.\beta1b/\beta1s)\ ]}{0.85.f'cb.\beta1b.bw + k.Aps.(fps/dp)}$			
	c'	=	40.9	in
	$a' = \beta1b.c'$	=	30.68	in
	30.68 > 7 in. Thus, it is a flanged section behavior.			
	Moment Capacity, φMn (+ve)	=	10635.21	kip-ft
	CALCULATION OF λ			
	For a train of vehicles loaded over a span,			
	Maximum moment at midspan, M_{LL}	=	5209.17	kip-ft
	Distribution Factor	=	**0.92**	
	Uniformly distributed load, W_{LL}	=	1.96	kip/ft
	Uniformly distributed load, W_{DL}	=	1.7	kip/ft
	M_1*	=	11522.94	kip-ft
	Wu1	=	4.88	kip/ft
	M_2*	=	12299.43	kip-ft
	Wu2	=	5.4	kip/ft
	$\lambda . W_{LL} = Wu1 - 1.25\ W_{DL}$			
	λ	=	1.41	
	1.41 < 1.75. Hence, Provide additional Mild Steel.			
	$\lambda . W_{LL} = Wu2 - 1.25\ W_{DL}$			
	λ	=	1.67	
	1.67 < 1.75. Hence, Provide additional Mild Steel.			
	Additional Capacity required			
	Additional Moment at supports, ΔM	=	1633.98	kip-ft
	Additional steel required in the deck at the supports	=	1.021	sq.in

ULTIMATE CAPACITY OF THE AASHTO TYPE IV GIRDER			
	=	0.013	sq.in/in
Add # 5 bars at 22 in c/c spacing in the deck slab at supports.			

AASHTO TYPE IV I- GIRDER: Single Stage Post-tensioning

DESIGN OF PRECAST CONCRETE AASHTO TYPE IV I-GIRDER						
I	**INPUT PARAMETERS**		METRIC UNITS		**INPUT SI UNITS**	
	Characteristic strength of concrete for precast superstructure-girder, f'c	=	6000	psi	= **6**	ksi
	Characteristic strength of concrete for deck and substructure, f'c	=	4000	psi	= **4**	ksi
	Coefficient of thermal expansion for concrete, α				= **6E-06**	/deg F
	Yield strength of steel, fy		60000	psi	= **60**	ksi
	Unit weight of concrete				= **150**	pcf
	Span length	=	**140**	ft	= **40**	m
	Center to center spacing between girders	=	6.00	ft	= **1.83**	m
	Width of slab over the I girder	=	76.77	in.	= **1950**	mm
	Thickness of slab	=	**7.0**	in.	= **180**	mm
	Cover to CGS	=	**6**	in.	= 152.4	mm
	Diameter of tendon	=	**0.6**	in.		
	Area of one strand of prestressing steel	=	0.217	sq. in.		
	fpu	=	**270**	ksi		
	fps < 0.7 fpu at transfer	=	189	ksi		
	Effective cover to reinforcement at top	=	**2.75**	in.		
	Effective cover to reinforcement at soffit	=	**1.25**	in.		
II	**PROPERTIES OF THE GIRDER SECTION**					

DESIGN OF PRECAST CONCRETE AASHTO TYPE IV I-GIRDER								
	DIMENSIONS OF I - GIRDER							
	Width of top flange	=	20.0	in.	=	**508**	mm
	Width of bottom flange	=	26.0	in.	=	**660.4**	mm
	Depth of the I - Girder	=	54.00	in.	=	**1371.6**	mm
	Depth of the straight portion of the top flange	=	8.0	in.	=	**203.2**	mm
	Depth of the slanting portion of the top flange	=	6.0	in.	=	**152.4**	mm
	Depth of the straight portion of the bottom flange	=	8.0	in.	=	**203.2**	mm
	Depth of the slanting portion of the bottom flange	=	9.0	in.	=	**228.6**	mm
	Width of the web	=	8.0	in.	=	**203.2**	mm
	Position of the Neutral Axis from the bottom of the girder	=	24.73	in.	=	**628.14**	mm
	y_{top}	=	29.27	in.	=	743.46	mm
	y_{bot}	=	24.73	in.	=	628.14	mm
	Area of the girder	=	789.00	in^2	=	**509031**	sq mm
	Weight of the girder	=	821.88	lb/ft			
	Moment of inertia of the girder section	=	260740.76	in^4	=	**1.1E+11**	mm^4
	Section Modulus, Sxt	=	8908.10	in^3	=	1.5E+08	mm^3
	Section Modulus, Sxb	=	10543.53	in^3	=	1.7E+08	mm^3
II	**PROPERTIES OF THE COMPOSITE SECTION**							
	Modulus of Elasticity of girder, Eg = 57000.√fc'/1000	=	4415.20	ksi			
	Modulus of Elasticity of deck, Ed= 57000.√fc'/1000	=	3605.00	ksi			
	Modular ratio, n = Eg/Ed	=	1.22				
	Effective width of the slab on top of the girder	=	62.68	in.	=	1592.17	mm
	Depth of the slab	=	7.0	in.	=	180	mm

DESIGN OF PRECAST CONCRETE AASHTO TYPE IV I-GIRDER								
	CG of the Girder section from the bottom flange	=	24.73	in.	=	628.14	mm
	CG of the slab from the bottom flange	=	57.54	in.	=	1461.6	mm
	Position of the neutral axis from the bottom of the girder	=	36.55	in.	=	928.36	mm
	y_{top}	=	24.54	in.	=	623.24	mm
	y_{bot}	=	36.55	in.	=	928.36	mm
	Area of the girder	=	789.00	in^2	=	509031	sq mm
	Area of the slab	=	438.79	in^2	=	286590	sq mm
	Area of the composite section	=	1227.79	in^2	=	795622	sq mm
	Weight of the girder	=	821.88	lb/ft			
	Weight of deck slab	=	457.07	lb/ft			
	Weight of the composite section	=	1278.94	lb/ft			
	Weight of the upstand	=	**500**	lb/ft			
	Moment of inertia of the girder section	=	260740.76	in^4	=	1.1E+11	mm^4
	Moment of inertia of the slab	=	1859.05	in^4	=	7.7E+08	mm^4
	Moment of inertia of the composite section	=	568608.70	in^4		2.4E+11	mm^4
	Section Modulus, Sxt = I/ y_{top}	=	23173.52	in^3	=	3.8E+08	mm^3
	Section Modulus, Sxb = I /y_{bot}	=	15557.18	in^3	=	2.5E+08	mm^3
III	**PRE-TENSIONING**						
	Load to be considered = 1.2 x self weight	=	0.99	kip/ft			
	Maximum moment in the girder , M = $WL^2/8$	=	2416.31	kip-ft			
	Optimal solution						
	eccentricity, e_1	=	16.42	in.			

DESIGN OF PRECAST CONCRETE AASHTO TYPE IV I-GIRDER							
	Prestressing Force after losses	=	808.90	kips			
	Force at transfer, F_{1i} (considering 20% time dependent losses)	=	1011.12	kips			
	Provide eccentricity, e_1	=	16.40	in.			
	Force after losses , F_1	=	817.00	kips			
	Force at transfer, F_{1i}	=	1021.25	kips			
	Force in a single tendon	=	**41.01**	kips			
	No. of tendons required	=	**24.90**				
	Provide no. of tendons	=	**25**				
	Total pretension	=	1025.33	kips			
IV	**POST-TENSIONING** **BALANCING THE TOTAL DEAD - WEIGHT - END SPAN**						
	Eccentricity at center of the end span, ec_{2a}	=	46.50	in.	=	1181.10	mm
	Post-tensioning force,F_{2a} balancing selfweight of girder and deck						
	$F_{2a}.(ec_{2a})/12 = W_{(girder+deck)} \times L^2/8$						
	$F_{2a}.e_{2a} = F_1.e_1$	=	13398.8	kip-in			
	F_{2a}	=	1124.75	Kips			
	e_{2a}	=	11.9	in.			
	Considering 15% time dependent losses + 15% friction losses						
	$F_{2a}i$	=	1556.75	kips			
	No. of tendons	=	35.96				
	Provide no. of tendons	=	**36**				
	Total $F_{2a}i$	=	1476.47	kips			
	BALANCING THE TOTAL DEAD - WEIGHT - MIDDLE SPAN						
	Eccentricity at center of the midspan, ec_{2b} (considering F_{2a})	=	39.50	in.			
	Eccentricity at center of the midspan, ec_{2b}	=	**53.5**	in.	=	1358.90	mm
	Post-tensioning force,F_{2b} balancing selfweight of girder and deck						
	$F_{2b}.ec_{2b} = F_{2a}.ec_{2a}$						
	F_{2b}	=	830.42	Kips			

DESIGN OF PRECAST CONCRETE AASHTO TYPE IV I-GIRDER				
	Considering 15% time dependent losses + 15% friction losses			
	$F_{2b}i$	=	1149.38	kips
	No. of tendons	=	28.02	
	Provide no. of tendons	=	**28**	
	Total $F_{2b}i$	=	1148.36	kips

	PRESTRESSING FORCES			
	Diameter of tendon	**=**	0.6	in
	Area of one strand of prestressing steel, Aps	**=**	0.217	in^2
	fpu	**=**	270	ksi
	fps < 0.7 fpu at transfer	**=**	189	ksi
	Force in a single tendon	**=**	41.01	kips
I	**Straight Tendons**			
	0.6 in diameter 25 Nos. unit			
	Number of units	=	**1**	
	No. of tendons in one unit	=	**25**	
	Total number of tendons	=	25	
	Total prestressing force in tendons	=	820.26	kips
	Angle of the inclined tendons w.r.t horizontal plane	=	**0**	deg
	Component of prestressing force in direction of applied shear	=	**0.00**	kips
II	**Tendons in a Profile**			
	0.6 in diameter 12 Nos. unit			
	Number of units	=	**3**	
	No. of tendons in one unit	=	**12**	
	Total number of tendons	=	36	
	Total prestressing force in tendons	=	1181.17	kips
	Angle of the inclined tendons w.r.t horizontal plane	=	**35**	deg
	Component of prestressing force in direction of applied shear	=	**677.49**	kips

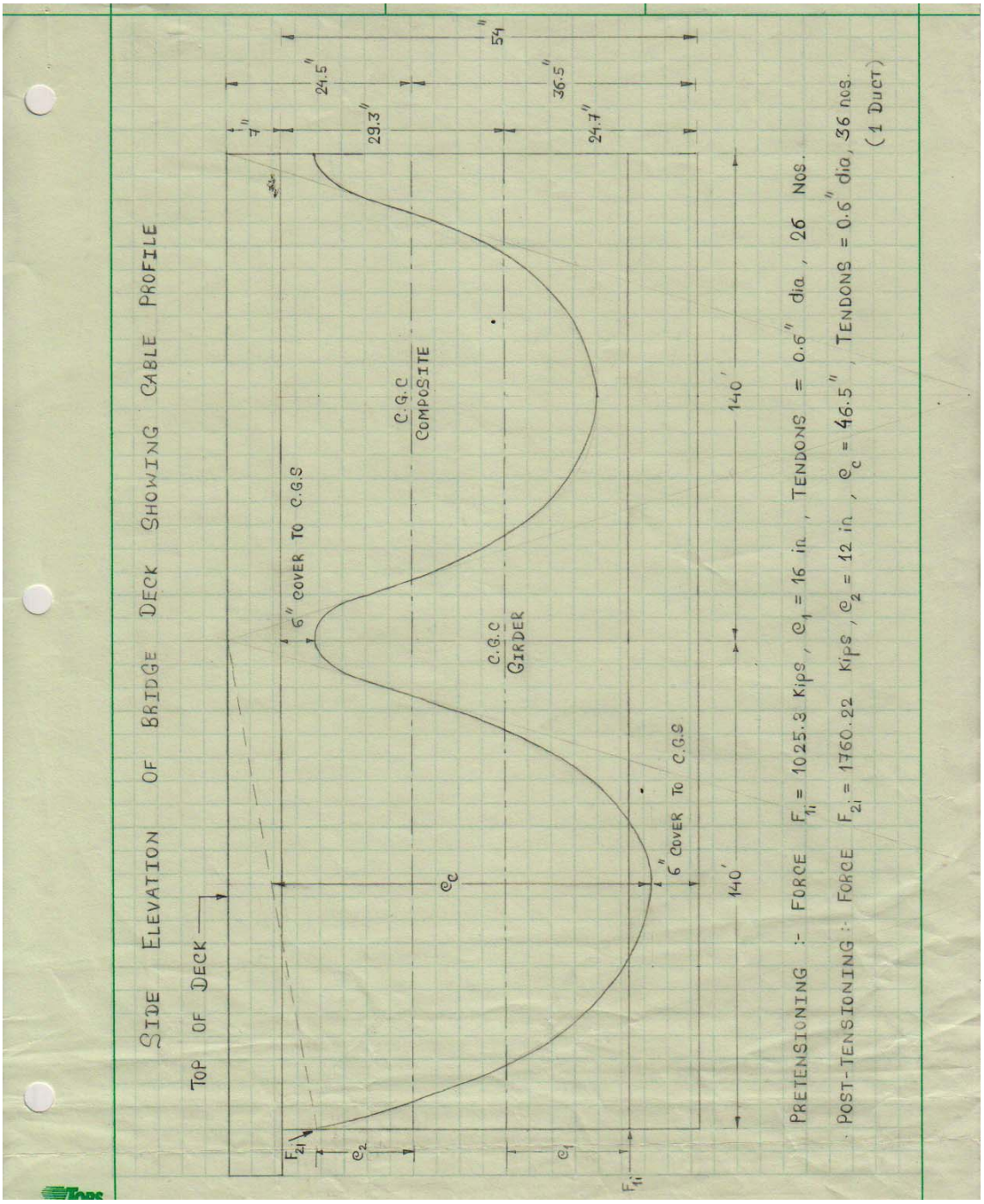
SIDE ELEVATION OF BRIDGE DECK SHOWING CABLE PROFILE
TOP OF DECK
6" COVER TO C.G.S
C.G.C COMPOSITE
C.G.C GIRDER
6" COVER TO C.G.S
140'
140'
1"
7"
24.5"
29.3"
54"
36.5"
24.7"
e_c
e_1
e_2
F_{1i}
F_{2i}
PRETENSIONING :- FORCE F_{1i} = 1025.3 Kips, e_1 = 16 in., TENDONS = 0.6" dia., 26 Nos.
POST-TENSIONING :- FORCE F_{2i} = 1760.22 Kips, e_2 = 12 in., e_c = 46.5", TENDONS = 0.6" dia, 36 nos.
(1 Duct)

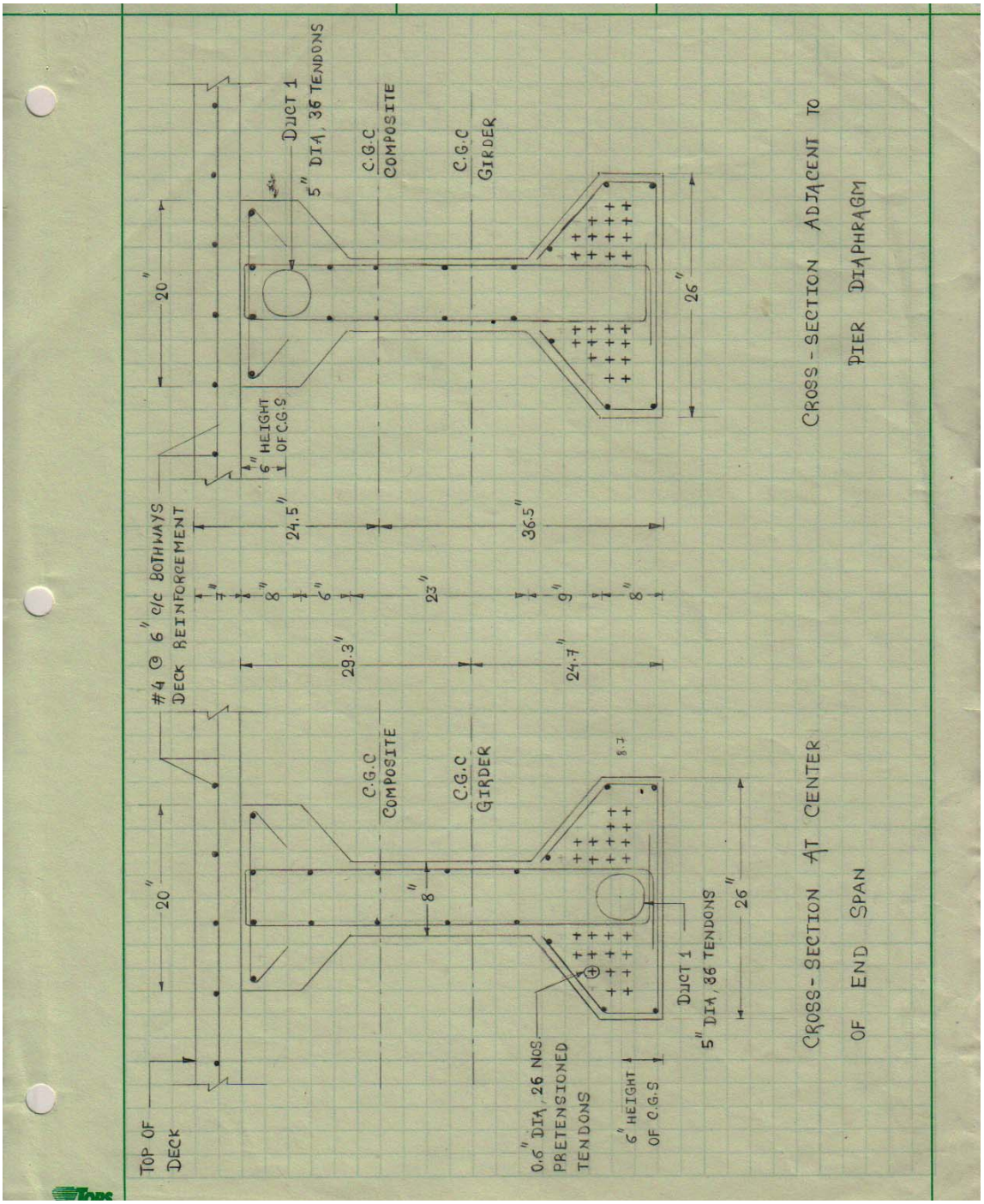
TOP OF DECK
20"
#4 @ 6" c/c BOTHWAYS DECK REINFORCEMENT
20"
DUCT 1
5" DIA, 36 TENDONS
6" HEIGHT OF C.G.S
C.G.C COMPOSITE
C.G.C GIRDER
24.5"
36.5"
29.3"
24.7"
8"
23"
9"
26"
CROSS-SECTION ADJACENT TO PIER DIAPHRAGM
C.G.C COMPOSITE
C.G.C GIRDER
8"
0.6" DIA, 26 NOS. PRETENSIONED TENDONS
6" HEIGHT OF C.G.S
DUCT 1
5" DIA, 86 TENDONS
26"
CROSS-SECTION AT CENTER OF END SPAN

SHEAR DESIGN OF PRECAST CONCRETE I-GIRDER				
	LRFD specifications (AASHTO) based on Modified Compression Field Theory			
			INPUT	
	Characteristic strength of concrete for precast girder, f'c	=	6	ksi
	Yield strength of transverse reinforcement, fy	=	60	ksi
	Modulus of Elasticity of Concrete, Ec	=	4415.20	ksi
	Effective width of the web, bv	=	**8**	in
	Depth of the composite section, h	=	61	in
	Strength reduction factor for prestressed concrete members, ϕ	=	**0.9**	
	TRANVERSE SHEAR DESIGN			
I	***Effective Shear depth and location***			
	Depth of the resultant Tensile force from top of the deck, dp	=	52.67	in
	Depth of compression block at centre of the end span, a	=	**5.02**	in
	Effective shear depth, dv is maximum of the following: -			
	i) Distance between resultants of Tensile and Compressive forces, dp-a/2	=	50.16	in
	ii) 0.9dp	=	47.40	in
	iii) 0.72h	=	43.92	in
	Effective shear depth, dv	=	50.16	in
	Angle of inclination of diagonal compressive stress, θ, ***assume***	=	**23.4**	deg
	Critical section near supports is greater of the following: -			
	i) (0.5).dv.Cotθ	=	4.83	ft
	ii) dv	=	4.18	ft
	Critical section near supports is at a distance	=	4.83	ft

SHEAR DESIGN OF PRECAST CONCRETE I-GIRDER				
II	***<u>Transverse Shear design at Critical section</u>***			
IIA	***Factored Forces at Critical Section***			
	Factored Shear Force at critical section, Vu	=	326.78	kips
	Factored Moment at critical section, Mu	=	1984.74	kip-ft
	Component of Prestressing force in direction of the shear, Vp	=	677.49	kips
IIB	***Contribution of Concrete to Nominal Shear Resistance***			
	Area of concrete on flexural tension side below (h/2), Ac	=	469.00	sq.in
	Strain in reinforcement on the flexural tension side			
	$\varepsilon_x = \frac{\frac{\lvert Mu\rvert}{dv} + 0.5Nu + 0.5\lvert Vu - Vp\rvert cot\theta - Aps.fpo}{2(Es.As + Ep.Aps)} \leq 0.001$		-0.0004698	
	If the above equation yields a negative value, then following equation should be used			
	$\varepsilon_x = \frac{\frac{\lvert Mu\rvert}{dv} + 0.5Nu + 0.5\lvert Vu - Vp\rvert cot\theta - Aps.fpo}{2(Ec.Ac + Es.As + Ep.Aps)}$	–	-3.264E-05	
	Shear stress in concrete, vu = $\frac{\lvert Vu - \phi Vp\rvert}{\phi . bv.dv}$	=	0.78	ksi
	vu/f'c	=	0.131	
	ε_x x 1000	=	-0.033	
	Using values of β and θ from LRFD Table 5.8.3.4.2-1			
	θ	=	23.4	deg
	β	=	2.88	
	Nominal Shear strength provided by concrete, Vc Vc = 0.0316 β √f'c $b_v d_v$	=	89.48	kips

SHEAR DESIGN OF PRECAST CONCRETE I-GIRDER				
	Vu < 0.5 φ(Vc+Vp), Minimum Transverse Shear Reinforcement is required.			
IIC	***Spacing of Transverse reinforcement*** Maximum Spacing of Transverse reinforcement, Smax			
IID	i) If vu < 0.125 f'c, Smax = 0.8 dv ≤ 24 in i) If vu ≥ 0.125 f'c, Smax = 0.4 dv ≤ 12 in Shear stress in concrete at critical section, vu	=	0.78	ksi
	Maximum Spacing of Transverse reinforcement, Smax at support	=	12.00	in
	Minimum Transverse reinforcement Area of tranverse reinforcement per web: - $Av \geq 0.05 \frac{bv.S}{fy}$	=	0.007 x S	sq.in
	Use Stirrups **1** # **5** double-legged			
	Required Spacing of Transverse reinforcement, Sreq	=	12.00	in
	Provide Spacing of Transverse reinforcement, Sprov	=	**12**	in
	Sprov < Sreqd. ***Hence, OK***			
	Area of Transverse reinforcement provided, Av_{prov}	=	0.614	sq.in
	Nominal Shear strength provided by transverse reinforcement, Vs $Vs = \frac{Av.fy.d_v.\cot\theta}{S}$	=	355.62	kips
	Distance from left support upto which this transverse reinforcement is to be provided	=	**40**	ft
	Provide # 5 double-legged stirrups at 12 in c/c upto a distance of 40 ft from support.			

SHEAR DESIGN OF PRECAST CONCRETE I-GIRDER				
IIE	***Maximum Nominal Shear reinforcement***			
	Vn = 0.25 f'c.bv.dv + Vp			
	Vn = Vc + Vs	=	445.09	kips
	0.25 f'c.bv.dv + Vp	=	1279.41	kips
	Vn < (0.25 f'c.bv.dv + Vp). Hence, OK			
III	***<u>Transverse Shear design at 25 ft from Support</u>***			
IIIA	***Factored Forces at 25 ft***			
	Factored Shear Force at critical section, Vu	=	234.54	kips
	Factored Moment at critical section, Mu	=	7679.99	kip-ft
	Angle of the inclined tendons w.r.t horizontal plane	=	**33.42**	
	Component of Prestressing force in direction of the shear, Vp	=	650.56	kips
IIIB	***Contribution of Concrete to Nominal Shear Resistance***			
	Area of concrete on flexural tension side below (h/2), Ac	=	469.00	sq.in
	Strain in reinforcement on the flexural tension side			
	$\varepsilon_x = \frac{\frac{\lvert Mu\rvert}{dv} + 0.5Nu + 0.5\lvert Vu - Vp\rvert cot\theta - Aps.fpo}{2(Es.As + Ep.Aps)} \leq 0.001$		-0.0002436	
	If the above equation yields a negative value, then following equation should be used			
	$\varepsilon_x = \frac{\frac{\lvert Mu\rvert}{dv} + 0.5Nu + 0.5\lvert Vu - Vp\rvert cot\theta - Aps.fpo}{2(Ec.Ac + Es.As + Ep.Aps)}$		-3.754E-05	
	Shear stress in concrete, vu = $\frac{\lvert Vu - \phi Vp\rvert}{\phi . bv.dv}$	=	0.97	ksi

SHEAR DESIGN OF PRECAST CONCRETE I-GIRDER				
	vu/f'c	=	0.162	
	ε_x x 1000	=	-0.038	
	β	=	2.881	
	Nominal Shear strength provided by concrete, Vc Vc = 0.0316 β √f'c $b_v d_v$ ***Vu > 0.5 φ(Vc+Vp), Transverse Shear Reinforcement is required.***	=	89.48	kips
IIIC	***Spacing of Transverse reinforcement*** Maximum Spacing of Transverse reinforcement, Smax i) If vu < 0.125 f'c, Smax = 0.8 dv ≤ 24 in i) If vu ≥ 0.125 f'c, Smax = 0.4 dv ≤ 12 in			
	Shear stress in concrete at critical section, vu	=	0.97	ksi
	Maximum Spacing of Transverse reinforcement, Smax	=	12.00	in
IIID	***Minimum Transverse reinforcement*** Area of tranverse reinforcement per web: -			
	$Av \geq 0.05 \frac{bv.S}{fy}$	=	0.007 x S	sq.in
	Use Stirrups **1** # **5** double-legged			
	Required Spacing of Transverse reinforcement, Sreq	=	12.00	in
	Provide Spacing of Transverse reinforcement, Sprov ***Sprov < Sreqd.*** ***Hence, OK***	=	**12**	in
	Area of Transverse reinforcement provided, Av_{prov}	=	0.614	sq.in
	Nominal Shear strength provided by transverse reinforcement, Vs			

SHEAR DESIGN OF PRECAST CONCRETE I-GIRDER				
	Vs = $\frac{Av.fy.d_v.\cot\theta}{S}$	=	355.62	kips
	Provide # 5 double-legged stirrups at 12 in c/c from 40 ft to 100 ft from the left support.			
IIIE	***Maximum Nominal Shear reinforcement***			
	Vn = 0.25 f'c.bv.dv + Vp			
	Vn = Vc + Vs	=	445.09	kips
	0.25 f'c.bv.dv + Vp	=	650.56	kips
	Vn < (0.25 f'c.bv.dv + Vp). Hence, OK			
IV	***<u>Minimum Longitudinal reinforcement requirement</u>***			
	Factored Shear force at the face of the support, Vu	=	416.12	kips
	Factored Moment at the face of the support, Mu	=	1194.89	kip-ft
	$Aps.fps \geq \frac{Mu}{d_v\varphi_f} + 0.5\,\frac{Nu}{\varphi_c} + \left(\frac{Vu}{\varphi_v} + 0.5Vs - Vp\right)\cot\theta$			
	$\left\lvert \frac{Mu}{d_v\varphi_f} + 0.5\,\frac{Nu}{\varphi_c} + \left(\frac{Vu}{\varphi_v} + 0.5Vs - Vp\right)\cot\theta \right\rvert$	=	1765.18	kips
	$\lvert Aps.fps \rvert$	=	3527.12	kips
	Aps.fps > (Mu/(dv φf)+0.5 Nu/φc +(Vu/φv +0.5Vs-Vp)cotϑ). Hence, OK			

DESIGN OF SHEAR CONNECTORS FOR PRECAST CONCRETE DECKS				
	Design of Shear Connectors for Precast concrete decks based on Truss Modelling Approach			
			INPUT	
	Characteristic strength of concrete for precast girder, f'c	=	6	ksi
	Yield strength of transverse reinforcement, fy	=	60	ksi
	Modulus of Elasticity of Concrete, Ec	=	4415.20	ksi
	Effective width of the web, bv	=	7	in
	Depth of the composite section, h	=	61	in
	Thickness of slab	=	7	in
	Length of a single slab panel, L_{Panel}	=	**8**	ft
	Strength reduction factor for prestressed concrete members, ϕ	=	**0.9**	
	Co-efficient of friction for sliding shear resistance, μ	=	**0.8**	
	Distribution factor for shear, D.F.	=	**1**	
	Internal lever arm in Girder, jd_{girder}	=	50.16	in
	Internal lever arm Overall, jd_o	=	56.17	in
	Hoop/Stirrup used	=	**5**	#
	Area of Single hoop, A_{sh}	=	0.61	sq.in
	Area of longitudinal mild steel rebar in girder, A_s	=	**3.72**	sq.in
	Area of Prestressing tendons in the girder, A_{sp}	=	13.24	sq.in
	Area of Longitudinal Girder reinforcement, A_{sb}	=	16.96	sq.in
	Area of 2 nos. 1-in CR	=	**1.08**	sq.in
	Area of 2 nos. 1.25-in CR	=	**1.82**	sq.in
	Yield strength of 1-in. CR, $F_{yc,\ 1\text{-}in}$	=	**120**	ksi
	Yield strength of 1-in. CR, $F_{yc,\ 1.25\text{-}in}$	=	**105**	ksi

DESIGN OF SHEAR CONNECTORS FOR PRECAST CONCRETE DECKS								
I	**END PANEL DESIGN FOR SLIDING SHEAR**							
	Net Panel Shear demand							
	At Left End of the Panel							
	Dead load Shear, V_{DL}				=	124.53	kips	
	Live load Shear, V_{LL}				=	119.64	kips	
	Total Factored Shear, $V_u = 1.25\ V_{DL} + 1.75\ (D.F.)\ (1.33 \times V_{LL})$				=	434.13	kips	
	Component of Prestressing force in the direction of applied shear,							
	V_p				=	677.49	kips	
	$V_u - V_p$				=	-243.37	kips	
	At Right End of the Panel							
	Dead load Shear, V_{DL}				=	112.07	kips	
	Live load Shear, V_{LL}				=	116.43	kips	
	Total Factored Shear, $V_u = 1.25\ V_{DL} + 1.75\ (D.F.)\ (1.33 \times V_{LL})$				=	411.08	kips	
	Component of Prestressing force in the direction of applied shear,							
	V_p				=	677.49	kips	
	$V_u - V_p$				=	-266.41	kips	
	Average shear demand over End Panel, V_{avg}				=	-254.89	kips	
II	***Design of Pocket Layout and Connectors***							
	Number of pockets needed in the end panel							
		2 - 1 in CR	*2 - 1.25 in CR*	Provide		*2 - 1 in CR*	*2 - 1.25 in CR*	
	N_{Pocket}	2.00	2.00		N_{pocket}	**2**	**2**	
III	***Provide hoops to form Non-contact splice***							

DESIGN OF SHEAR CONNECTORS FOR PRECAST CONCRETE DECKS

IV

Number of hoop groups required to anchor shear connectors in a pocket

	2 - 1 in CR	*2 - 1.25 in CR*
N_{Group}	3.52	5.19

Provide

	2 - 1 in CR	*2 - 1.25 in CR*
N_{group}	**4**	**6**

Determining Web Shear Capacity

Use	=	**2 - 1 in CR**
Number of pockets, N_{Pocket}	=	2
Number of hoop groups, N_{Group}	=	4
Expected crack angle, cot θ	=	1.68
Shear Capacity of the transverse girder reinforcement, ϕVs	=	233.19 kips

φVs > Vavg. Hence, OK

ULTIMATE CAPACITY OF THE AASHTO TYPE IV I-GIRDER

DATA

		INPUT	
Characteristic strength of concrete for precast girder, f'cb	=	6	ksi
Characteristic strength of concrete for deck and substructure, f'cs	=	4	ksi
Characteristic strength of concrete for precast superstructure, f'c	=	5	ksi
fpu	=	270	ksi
fps < 0.7 fpu at transfer	=	189	ksi
Span of the bridge	=	140	ft
Width of the diaphragm	=	**5**	ft
Effective width of the slab on top of the I girder	=	76.77	in
Thickness of slab	=	7	in

ULTIMATE CAPACITY OF THE AASHTO TYPE IV I-GIRDER				
	Width of the webs	=	**8**	in
	Depth of the girder	=	54	in
	Diameter of tendon	=	0.6	in
	Area of one strand of prestressing steel	=	0.217	sq.in
	β1 = 0.85 - 0.05 (f'c - 4)			
	β1s	=	0.85	
	β1b	=	0.75	
	k for Low relaxation strand	=	**0.28**	
	ULTIMATE CAPACITY CALCULATION			
I	***AT 0.3L of Exterior Span***			
	Pretension Prestressing tendons (Bonded tendons)			
	No. of Tendons	=	**25**	
	dp	=	**52.30**	in
	bw	=	**20.00**	in
	$\rho_{p\,1a}$	=	0.005	
	ρ_{p} . fpu/f'c	=	0.280	
	fps_{1a}	=	214.55	ksi
	Pretension Prestressing force, F_{1a}	=	1163.92	kips
	Post-tension Prestressing tendons (Bonded tendons)			
	No. of Tendons	=	**36**	
	dp	=	**54.90**	in
	bw	=	**26.00**	in
	ρ_{p2}	=	0.006	
	ρ_{p2} . fpu/f'c	=	0.304	
	fps_2	=	209.86	ksi
	Post-tension Prestressing force, F_2	=	1684.95	kips
	For Rectangular section behavior,			

ULTIMATE CAPACITY OF THE AASHTO TYPE IV I-GIRDER				
	$c = \frac{Aps.fps + As.fy - As'.fy'}{0.85.f'cs.\beta1s.b + k.Aps.(fps/dp)}$			
	c	=	12.04	in
	a = β1s.c	=	10.23	in
	10.24 > 7 in. Thus, it is a flanged section behavior.			
	For Flanged section behavior,			
	$c' = \frac{[\ Aps.fps - 0.85.hf.(f'cs.bs.\beta1s - f'cb.bw.\beta1b/\beta1s)\ ]}{0.85.f'cb.\beta1b.bw + k.Aps.(fps/dp)}$			
	c'	=	34.07	in
	a' = β1b.c'	=	25.56	in
	25.56 > 7 in. Thus, it is a flanged section behavior.			
	Moment Capacity, ϕMn (+ve)	=	9984.18	kip-ft
III	***At the face of the diaphragm***			
	Post-tension Prestressing tendons (Bonded tendons)			
	No. of Tendons	=	**36**	
	dp	=	**47.40**	in
	bw	=	**18.00**	in
	ρ_{p2}	=	0.008	
	ρ_{p2} . fpu/f'c	=	0.426	
	fps_2	=	185.70	ksi
	Post-tension Prestressing force, F_2	=	1249.20	kips
	Reinforcement in the deck slab			
	Area of steel provided	=	**0.46**	sq.in/ft
	de	=	**57.50**	in
	bw	=	**62.68**	in
	ρ_s	=	0.001	
	fy	=	36.00	ksi
	Pretension Prestressing force, F	=	105.94	kips

ULTIMATE CAPACITY OF THE AASHTO TYPE IV I-GIRDER				
	For Rectangular section behavior,			
	c = Aps.fps + As.fy - As'.fy' / 0.85.f'cs.β1s.b + k.Aps. (fps/dp)			
	c	=	5.91	in
	a = β1s.c	=	5.02	in
	5.03 < 7 in. Thus, it is a rectangular section behavior.			
	Moment Capacity, ϕMn (-ve)	=	5158.29	kip-ft
III	***AT Midspan of Middle Span***			
	Pretension Prestressing tendons (Bonded tendons)			
	No. of Tendons	=	**25**	
	dp	=	**52.30**	in
	bw	=	**20.00**	in
	$\rho_{p\,1a}$	=	0.005	
	ρ_{p1a} . fpu/f'c	=	0.280	
	fps_{1a}	=	214.55	ksi
	Pretension Prestressing force, F_{1a}	=	1163.92	kips
	Stage 2 - Post-tension Prestressing tendons (Bonded tendons)			
	No. of Tendons	=	**36**	
	dp	=	**54.90**	
	bw	=	**26.00**	
	ρ_{p2}	=	0.005	
	ρ_{p2} . fpu/f'c	=	0.254	
	fps_2	=	219.61	ksi
	Post-tension Prestressing force, F_2	=	1477.32	kips
	For Rectangular section behavior,			
	c = Aps.fps + As.fy - As'.fy' / 0.85.f'cs.β1s.b + k.Aps. (fps/dp)			
	c	=	11.21	in
	a = β1s.c	=	9.53	in
	9.53 > 7 in. Thus, it is a flanged section behavior.			

ULTIMATE CAPACITY OF THE AASHTO TYPE IV I-GIRDER			
For Flanged section behavior,			
c' = [Aps.fps - 0.85.hf.(f'cs.bs.β1s - f'cb.bw.β1b/β1s)] / (0.85.f'cb.β1b.bw + k.Aps.(fps/dp))			
c'	=	30.21	in
a' = β1b.c'	=	22.66	in
22.66 > 7 in. Thus, it is a flanged section behavior.			
Moment Capacity, ϕMn (+ve)	=	9547.70	kip-ft
CALCULATION OF λ			
For a train of vehicles loaded over a span,			
Maximum moment at midspan, M_{LL}	=	5209.17	kip-ft
Distribution Factor	=	**0.92**	
Uniformly distributed load, W_{LL}	=	1.96	kip/ft
Uniformly distributed load, W_{DL}	=	1.78	kip/ft
M_1*	=	12563.33	kip-ft
Wu1	=	5.32	kip/ft
M_2*	=	14705.99	kip-ft
Wu2	=	6.46	kip/ft
λ. W_{LL} = Wu1 - 1.25 W_{DL}			
λ	=	1.58	
1.58 < 1.75. Hence, Provide additional Mild Steel.			
λ. W_{LL} = Wu2 - 1.25 W_{DL}			
λ	=	2.16	
2.16 > 1.75. Hence, Safe.			

ULTIMATE CAPACITY OF THE AASHTO TYPE IV I-GIRDER				
	Additional Capacity required			
	Additional Moment at supports, ΔM	=	827.99	kip-ft
	Additional steel required in the deck at the supports	=	0.52	sq.in
		=	0.007	sq.in/in
	Use # **5** bars			
	$Spacing_{reqd}$ = 45 in			
	$Spacing_{prov}$ = **24** in			
	Add # 5 bars at 24 in c/c spacing in the deck slab at supports.			

DESIGN OF SUBSTRUCTURE

Load Calculations:

WEIGHT CALCULATION FOR PIER DESIGN - SINGLE PIER			
			INPUT
Unit wt. of concrete	=	0.15	kcf
GIRDER WEIGHT ON EACH PIER			
no. of girders	=	2	
weight of girder per feet	=	1.17	kip/ft
Span of the girder	=	140	ft
Total weight of girders on each pier	=	328.76	kips
WEIGHT OF UPSTAND			
weight of upstand	=	0.5	kip/ft
Span of the girder	=	140	ft
Total weight of girders on each pier	=	70.00	kips
DECK SLAB WEIGHT ON EACH PIER			
Thickness of deck slab	=	7	in.
total width of deck slab	=	25.6	ft.
length of deck slab	=	140	ft.
Total weight of deck slab on each pier	=	313.48	kips
SELF WEIGHT OF PIERS			
Dia. of piers	=	5	ft
height of pier columns	=	16	ft
total weight of piers	=	47.12	kips
WEIGHT OF PIERCAP ON EACH PIER			
Top width of the trapezoidal pier cap	=	22	ft
bottom width	=	18.6	ft
Depth of the pier cap	=	1.8	ft
cross sectional width of the pier cap	=	5	

WEIGHT CALCULATION FOR PIER DESIGN - SINGLE PIER			
Weight of pier cap	=	27.41	kips
WEIGHT OF FWS ON EACH PIER			
weight of future wearing surface	=	30	psf
total weight of FWS	=	107.48	kips
WEIGHT OF parapet wall			
Top width	=	9.5	in.
Bottom width	=	14	in.
Height of wall	=	2	ft
Length of wall	=	140	ft
Weight of wall	=	0	kips
Total tributary weight of superstructure on each pier,W	=	894.25	kips
Maximum weight on end pier= 1.5 x times the weight of each span	=	1341.374	kips

DAMAGE AVOIDANCE DESIGN- TWIN PIER									
	DESIGN PARAMETERS				**INPUT PARAMETERS**			**REFERENCES**
	Compressive strength of concrete, fc'	=	6	ksi	**IMPORTANT VALUES**			
	Yield Strength of reinforcement,fy	=	60	ksi				
	Depth of slab	=	**7**	in.				
	Depth of girder	=	**54**	in.				
	spacing of girders	=	13.12	ft	=	**4000**	mm	
	no. of girders	=	**2**		=			
	overhang width	=	3.28	ft	=	**1000**	mm	
	Total width of deck	=	19.69	ft	=	6000	mm	
	Height of pier	=	**16**	ft	=	4876.8	mm	
	Depth of pier cap beam	=	**5**	ft	=	1524	mm	
	Height to seismic center of mass, H	=	23.25	ft	=	7086.6	mm	
II	**INITIAL SIZING PARAMETERS**							
	Diameter of pier,D	=	**4**	ft	=	1219.2	mm	
	Area of the pier,A	=	**1809.56**	in^2				
	Width of shoe block, B	=	5.00	ft				
	Height of shoe block, h	=	**3**	ft		half of width		
	1. ASSUMPTION OF DECK DISPLACEMENT							

DAMAGE AVOIDANCE DESIGN- TWIN PIER					
	Initial column drift, Δ	=	**1.1625**	ft OK <0.05H	
	2. ESTIMATION OF DAMPING				
	ξo (intrinsic damping)	=	**5**		
	ξrock = 2x(width of shoe block)/(π x ht.of shoe block)	=	6.22		
	ξhyst	=	**0**		
	ξeff = ξo + ξrock + ξhyst	=	11.22		
	Damping response factor $B_{\xi} = \sqrt{(5 + \xi eff)/10}$	=	1.27		
III	**3. CALCULATION OF BASE SHEAR CAPACITY**				
	Value of accelaration due to gravity, g	=	32.17	ft/sec^2	
	Fv. S1	=	**0.6**		
	Required base shear capacity ,Cd = $gx(FvS1/B\xi)^2/(4\pi^2\Delta)$	=	**0.16**		

DAMAGE AVOIDANCE DESIGN- TWIN PIER							
IV	**4. DESIGN OVERTURNING MOMENT**						
	Weight of bridge on each pier , Wy	=	**773.28**	kips	=	3439.72	kN
	Demand , Mo = H . Fx = H x Cd x Wy	=	**33575.70**	kip-in			
	Base Width of shoe, B	=	5.00	ft			
	No. of DYWIDAG prestressing steel bars	=	**4**				
	Dia.of bar	=	**1.25**	in.			
	Nominal diameter of DYWIDAG bar	=	**1.125**	in.			
	Area of prestressing strand, Ap	=	0.994	sq.in.			
	Ultimate Strength of prestressing steel	=	**160**	ksi			
	Additional Axial force due to Prestressing tendons, Pp	=	**445.32**	kips			
	Resisting moment, (Wy + P).B/2	=	**36558.00**	kip-in	**OK**		
	Moment resisted by prestressing, P.B/2	=	13359.62	kip-in			
	Moment to be resisted by longitudinal reinforcing bars		**23198.37**	kip-in			
	Axial load due to live load	=	**222.60**	kips			
	Force to be resisted by longitudinal reinforcing bars	=	**327.96**	kips			

DAMAGE AVOIDANCE DESIGN- TWIN PIER					
	Total Factored axial load, 1.25 DL+1.75LL	=	799.50	kips	
	Pu/fc'.Ag	=	0.07		
	Mu/fc'.Ag.h	=	0.06		
	Provide % of steel	=	**0.013**		
	Mu/fc'.Ag.h	=	**0.06**		
	Moment to be resisted by longitudinal reinforcing bars	=	31269.15	kip-in	
	Required area of steel, Ast(req) = ρt .Ag	=	23.52	in^2	
	Bar size designation no. to be used	=	**10**		
	Dia. of bars	=	1.25	in.	
	Area of one bar	=	1.227	in^2	
	Required no. of bars	=	19.17		
	No. of bars Provided	=	**24**		
	Area of Steel Provided, Ast(prov)	=	29.45	in^2	**ok**
	Center to center spacing between bars	=	6.56	in.	
	Percentage of steel provided,ρt	=	1.63	%	
	Provide 24 - No. 10 bars				
	<u>Check for Maximum and Minimum reinforcement requirements as per AASHTO-S.5.7.4.2-1</u>				

DAMAGE AVOIDANCE DESIGN- TWIN PIER								
	Maximum area of non prestressed longitudinal reinforcement for non-composite compression componenets shall be :							
	As/Ag + Aps.fpu/Ag.fy <0.08 and Aps.fpe/Ag.fc' <= 0.30							
	Provided As/Ag + Aps.fpu/Ag.fy	=	**0.02**		**OK**			AASHTO-S.5.7.4.2-1
	Aps.fpe/Ag.fc'	=	**0.04**		**OK**			AASHTO-S.5.7.4.2-2
	Minimum area of nonprestressed longitudinal reinforcement for non composite compression components shall be:							
	As.fy/Ag.fc' +Aps.fpu/Ag.fc' > = 0.135	=	**0.221**		**OK**			AASHTO-S.5.7.4.2-3
V	**PRESTRESSING BAR CALCULATION**							- -
	Calculation of force at uplift, Pup							
	Percent ratio of prestress in threaded bars	=	**50**		=	**0.500**		
	Uplift force, Pup = Wy + 0.5 P	=	995.94	kip	=	4430.16	kN	
	Fup = Pup x e / H	=	85.67	kip				

DAMAGE AVOIDANCE DESIGN- TWIN PIER							
	Calculation of displacement at uplift, Δup						
	I col	=	260576.26	in^4			
	Ec	=	4415.20	ksi			
	Assume EIeff = 0.6 E Ig	=	690297943.34	k-sq in			
	Lateral displacement on uplift , Δup =(Fup x L^3)/3EIeff	=	**0.07**	ft.	=	0.006	in.
	drift %	=	**0.32**	%			
	μ = Δ/Δup	=	**15.53**				
	E	=	29007.545				
	Maximum displacement due to elongation of tendons at yield,Δpmax = FL/EA = 0.5.Pp.H /EA	=	0.54	in.			
	Δmax=Δpmax . H./(B/2)	=	5.01	in.	=	0.13	m
VI	**RE-ESTIMATION OF DAMPING**						
	ξo (intrinsic damping)	=	0.05				
	ξrock = 2x(width of shoe block)/(π x ht.of shoe block)	=	0.06				
	ξhyst = 0.08 X (1-1/μ)	=	0.07				
	ξeff = ξo + ξrock + ξhyst	=	0.19				

DAMAGE AVOIDANCE DESIGN- TWIN PIER							
	Damping response factor $B_{\xi} = \sqrt{(5 + \xi eff)/10}$	=	0.720				
	nearly same as before						
VII	**FUSE BAR CALCULATION**						-
	Additional fuse bar dia.		1.25	in.			-
	Nominal diameter of fuse bar		1.125	in.			
	Area of prestressing strand, Ap		0.994	sq.in.			
	Ultimate strength of PS, fpu	=	42	ksi			
	No. of bars to be used	=	4				
	total force in fuse bars	=	167.00	kips			
	Distance of fuse bars from centre line of column,e	=	2	ft			
	Total moment resisted by prestress bars and fuse bars (Wy+P)B/2 +FY(e+B/2)	=	45575.74	kip-ft	OK SINCE >Mo =	33575.70	kip-in

DAMAGE AVOIDANCE DESIGN OF SINGLE PIER									
	DESIGN PARAMETERS				**INPUT PARAMETERS**			**REFERENCES**
	Compressive strength of concrete, fc'	=	6	ksi	**IMPORTANT VALUES**			
	Yield Strength of reinforcement,fy	=	60	ksi				
	Depth of slab	=	**7**	in.				
	Depth of girder	=	**54**	in.				
	spacing of girders	=	13.12	ft	=	**4000**	mm	
	no. of girders	=	**2**		=			
	overhang width	=	3.28	ft	=	**1000**	mm	
	Total width of deck	=	19.69	ft	=	6000	mm	
	Height of pier	=	**16**	ft	=	4876.8	mm	
	Depth of pier cap beam	=	**5**	ft	=	1524	mm	
	Height to seismic center of mass, H	=	23.25	ft	=	7086.6	mm	
	Clear cover to ties	=	**1.5**	in				
	UnFactored axial load of column, Pu	=	**1348.27**	kips				
	Factored Live load intensity	=	**1.26**	kip/ft				
	Unfactored single load-live load intensity		**0.95**	kip/ft				
	Unfactored train of vehicles-live load intensity	=	**1.59**	kip/ft				
	Max. Axial load on column due to live load on each pier	=	**2.39**	kips				
II	**INITIAL SIZING PARAMETERS**							
	Diameter of pier,D	=	**5**	ft	=	1524	mm	

DAMAGE AVOIDANCE DESIGN OF SINGLE PIER						
	Area of the pier,Ag	=	**2827.43**	in^2		
	Width of shoe block, B	=	6.00	ft		
	Height of shoe block, h	=	**3**	ft		half of width
	1. ASSUMPTION OF DECK DISPLACEMENT					
	Initial column drift, Δ	=	**1.1625**	ft	OK	<0.05H
	2. ESTIMATION OF DAMPING					
	ξo (intrinsic damping)	=	**5**			
	ξrock = 2x(width of shoe block)/(π x ht.of shoe block)	=	8.95			
	ξhyst	=	**0**			
	ξeff = ξo + ξrock + ξhyst	=	13.95			
	Damping response factor $B_{\xi} = \sqrt{(5 + \xi eff)/10}$	=	1.38			
III	**3. CALCULATION OF BASE SHEAR CAPACITY**					
	Value of accelaration due to gravity, g	=	32.17	ft/sec^2		
	Fv. S1	=	**0.6**			
	Required base shear capacity ,Cd = gx(FvS1/Bξ)^2/(4π^{2}Δ)	=	**0.13**			

DAMAGE AVOIDANCE DESIGN OF SINGLE PIER								
IV	**4. DESIGN OVERTURNING MOMENT**							
	Weight of bridge on each pier , Wy	=	**1341.37**	kips	=	5966.73	kN	
	Demand , Mo = H . Fx = H x Cd x Wy	=	**49835.99**	kip-in				
	Base Width of shoe, B	=	6.00	ft				
	No. of DYWIDAG prestressing steel bars	=	**4**					
	Dia.of bar	=	**1.5**	in.				
	Nominal diameter of DYWIDAG bar	=	**1.350**	in.				
	Area of prestressing strand, Ap	=	1.431	sq.in.				
	Ultimate Strength of prestressing steel	=	**160**	ksi				
	Additional Axial force due to Prestressing tendons, Pp	=	**641.26**	kips				
	Resisting moment, (Wy + P).B/2	=	**71374.88**	kip-in	**OK**			
	Moment resisted by prestressing, P.B/2	=	23085.43	kip-in				
	Moment to be resisted by longitudinal reinforcing bars		**48289.45**	kip-in				
	Axial load due to live load	=	**222.60**	kips				

DAMAGE AVOIDANCE DESIGN OF SINGLE PIER					
	Force to be resisted by longitudinal reinforcing bars	=	**700.11**	kips	
	Total Factored axial load, 1.25 DL+1.75LL	=	1264.69	kips	
	Pu/fc'.Ag	=	0.07		
	Mu/fc'.Ag.h	=	0.06		
	Provide % of steel	=	**0.011**		
	Mu/fc'.Ag.h	=	**0.06**		
	Moment to be resisted by longitudinal reinforcing bars	=	61072.56	kip-in	
	Moment resisted by prestressing tendons	=	23085.43	kip-in	
	total moment resisted by columns, Mn	=	**84157.99**	kip-in	
	Required area of steel, Ast(req) = ρt .Ag	=	31.10	in^2	
	Bar size designation no. to be used	=	**10**		
	Dia. of bars	=	1.25	in.	
	Area of one bar	=	1.227	in^2	
	Required no. of bars	=	25.34		
	No. of bars Provided	=	**28**		
	Area of Steel Provided, Ast(prov)	=	34.36	in^2	**ok**
	Center to center spacing between bars	=	6.98	in.	
	Percentage of steel provided,ρt	=	1.22	%	

DAMAGE AVOIDANCE DESIGN OF SINGLE PIER					
	Provide 28 - No. 10 bars				
	<u>Check for Maximum and Minimum reinforcement requirements as per AASHTO-S.5.7.4.2-1</u> Maximum area of non prestressed longitudinal reinforcement for non-composite compression componenets shall be : As/Ag + Aps.fpu/Ag.fy <0.08 and Aps.fpe/Ag.fc' <= 0.30				
	Provided As/Ag + Aps.fpu/Ag.fy	=	**0.02**	**OK**	AASHTO-S.5.7.4.2-1
	Aps.fpe/Ag.fc'	=	**0.03**	**OK**	AASHTO-S.5.7.4.2-2
	Minimum area of nonprestressed longitudinal reinforcement for non-composite compression components shall be:				
	As.fy/Ag.fc' +Aps.fpu/Ag.fc' > = 0.135	=	**0.159**	**OK**	AASHTO-S.5.7.4.2-3
V	**PRESTRESSING BAR CALCULATION**				-
	<u>Calculation of force at uplift, Pup</u>				-
	Percent ratio of prestress in threaded bars	=	**50**	= **0.500**	
	Uplift force, Pup = Wy + 0.5 P	=	1564 kip		

DAMAGE AVOIDANCE DESIGN OF SINGLE PIER							
	Fup = Pup x e / H	=	168.81	kip			
	Calculation of displacement at uplift, Δup						
	I col	=	636172.51	in^4			
	Ec	=	4415.20	ksi			
	Assume EIeff = 0.6 E Ig	=	702207380.51	k-sq in			
	Lateral displacement on uplift , Δup =(Fup x L^3)/3EIeff	=	**0.14**	ft.	=	0.005	in.
	drift %	=	**0.62**	%			
	μ = Δ/Δup	=	**8.05**				
	E	=	29007.545				
	Maximum displacement due to elongation of tendons at yield,Δpmax = FL/EA = 0.5.Pp.H /EA	=	0.54	in.			
	Δmax=Δpmax . H./(B/2)	=	4.17	in.			
VI	**RE-ESTIMATION OF DAMPING**						
	ξo (intrinsic damping)	=	5				
	ξrock = 2x(width of shoe block)/(π x ht.of shoe block)	=	8.95				
	ξhyst = 0.08 X (1-1/μ)	=	7.01				
	ξeff = ξo + ξrock + ξhyst	=	20.96				

DAMAGE AVOIDANCE DESIGN OF SINGLE PIER							
	Damping response factor $B_{\xi} = \sqrt{(5 + \xi eff)/10}$	=	1.611				
VII	**FUSE BAR CALCULATION**						- -
	Additional fuse bar dia.		1.25	in.			
	Nominal diameter of fuse bar		1.125	in.			
	Area of prestressing strand, Ap		0.994	sq.in.			
	Ultimate strength of PS, fpu	=	42	ksi			
	No. of bars to be used	=	4				
	Total force in fuse bars	=	167.00	kips			
	Distance of fuse bars from centre line of column,e	=	2.5	ft			
	Total moment resisted by prestress bars and fuse bars (Wy+P)B/2 +FY(e+B/2)	=	75342.69	kip-IN.	OK SINCE >Mo =	49835.9	kip-in
	DESIGN OF SHEAR REINFORCEMENT						
I	**PLASTIC HINGE ZONE CONFINEMENT**						
	Diameter of core outside to outside of spirals, Dc	=	**57.0**	in.			
	Area of Core, $Ac = \pi.Dc^2/4$	=	2551.8	sq.in			
(1)	$\rho s = 0.45 [(Ag/Ach)-1]fc'/fy$	=	0.0049				ACI-10.9.3-Eqn. 10-5

DAMAGE AVOIDANCE DESIGN OF SINGLE PIER					
	Provide spiral reinforcement volumetric ratio, ρs (max)	=	**0.012**		AASHTO-5.10.11.4.1d
	Required spacing of spirals= 4.Asp/(ρs.Dc)	=	1.79	in.	
	Maximum spacing in confinement zone :-				
	Spacing is not greater than the following:-				
(1)	1/4 th minimum member dimension	=	15.0	in.	
(2)	4 in.	=	4.0	in.	
	Hence maximum spacing in confining zone	=	**4.00**	in.	
	Spacing of spirals provided,S	=	**3**		
	Bar size designation no. to be used	=	**5**		
	Dia. of bars	=	0.625	in	
	Area of spiral reinforcement of bar, Asp	=	0.31	in^2	
	ρs, provided = 4.Asp/(S.Dc)	=	**0.007**		
	Spiral reinforcement requirements as per ACI-7.10				
	Volume of spiral reinf	=	0.004861		ACI 7.10.4.2
	Minimum Diameter of spiral to be used	=	**0.625**	in.	ACI 7.10.4.2
	Maximum c/c pitch spacing of spirals, $s = \pi.Dsp^2.fy/(0.45Dc.fc'[(Ag/Ac)-1])$	=	4.43	in.	ACI 7.10.4.3

DAMAGE AVOIDANCE DESIGN OF SINGLE PIER						
	Maximum clear spacing between spirals	=	**3.00**	in.	**(Detailing requirements)**	ACI 7.10.4.3
	Hence maximum pitch between spirals as per ACI	=	3.625	in.		
	Minimum spacing of spirals	=	**1**	in.		ACI 7.10.4.3
	Provided spacing	=	**3**	in.		
	Area of spiral reinforcement provided, Asp(prov)	=				
	Use No. 5 at 3 in. c/c spacing					
	Provided Pitch	=	**3.6**	in.		
II	**LENGTH OF CONFINEMENT ZONE**					
	Length of confining zone adjacent to each end of column:-					ACI-21.4.4.4
	Largest of :					
	1 . dia. Of column	=	60	in.		
	2. one-sixth of clear ht of column	=	46	in.		
	3. 18 inch	=	18	in.		

DAMAGE AVOIDANCE DESIGN OF SINGLE PIER					
	Length of confining zone adjacent to each end of column,l_0	=	**60**	in.	
		=	**5**	ft.	
III	**SHEAR CAPACITY IN PLASTIC HINGE ZONE** **Computation of Base Shear**				
	Modulus of Elasticity,E = 57000.√fc'/1000	=	4415.20	ksi	
	Moment of Inertia of Column, Ic	=	636172.5	in^4	
	EI eff = 0.25EIc	=	7.02E+08	$kip\text{-}in^2$	
	Stiffness of Cantilever bridge pier,k = $3EIc/L^3$	=	1219110.04		
	Base Shear Coefficient, Cd as calculated above	=	0.13		
	Base Shear on column, V = Cd x W	=	**178.62**	kips	
	Shear force on column	=	178.62	kips	
	Factor for shear force	=	**1.25**	kips	
	Factored Shear force on column, Vu	=	223.28	kips	
	Shear strength provided by concrete for non prestressed members subjected to axial compression, $Vc = 2[1+ Nu/2000Ag].\sqrt{fc'}.b_w.d$	=	557.834	kips	ACI-11.3.1.2
	ϕ	=	**0.75**		

DAMAGE AVOIDANCE DESIGN OF SINGLE PIER						
	ϕ. Vc	=	418.38	kips	**Check as below**	
	0.5 x ϕ. Vc	=	209.19	kips	**Minimum shear reinforcement required as per ACI-11.5.6.1**	
	Effective depth = d = Dc/2+Dr/π	=	45.85	in.		
	Maximum permissible spacing for the chosen bar no. of ties, s(max) = d/2	=	**22.92**	in.		ACI-11.5.5.1-
	Spacing provided	=	**3.00**	in.	**OK < Max. Permissible spacing**	
	Total shear strength with the provided spirals					
	ϕ. Vs = ϕ. Av.fy.d/s	=	**0.00**	kips		
	ϕ. Vc + ϕ. Vs	=	418.38	kips	**OK > Vu**	
	REINFORCEMENT OTHER THAN CONFINING ZONE					
	Maximum Spacing of spirals is the minimum of:					ACI-21.4.4.2
(1)	0.25 xD	=	15	in.		

DAMAGE AVOIDANCE DESIGN OF SINGLE PIER					
(2)	6 x dia. of longitudinal bar	=	7.5	in.	ACI 21.4.4.6
(3)	So = 4 + (14-hx)/3	=	4.00	in.	ACI 21.4.2.2-Eqn. 21.5
(4)	Clear cover to longitudinal bars	=	3	in.	
(5)	6 in.	=	6	in.	
	Required maximum spacing of spirals	=	**3.0**	in.	
(1)	6 x dia. of longitudinal bar	=	**7.5**	in.	ACI 21.4.4.6
(2)	6 in.	=	**6.0**	in.	ACI 21.4.4.6
	Required maximum spacing of spirals	**=**	**6.0**	**in.**	
III	**SHEAR CAPACITY IN NON-PLASTIC ZONE**				
	Shear force on column	=	178.62	kips	
	Factor for shear force	=	**1.25**	kips	
	Factored Shear force on column, Vu	=	223.28	kips	
	Shear strength provided by concrete for non prestressed members subjected to axial compression,	=	557.834		ACI-11.3.1.2
	$Vc = 2[1+ Nu/2000Ag].\sqrt{fc'}.b_w.d$			kips	
	ϕ	=	**0.75**		

DAMAGE AVOIDANCE DESIGN OF SINGLE PIER						
	ϕ. Vc	=	418.38	kips	**Check as below**	
	0.5 x ϕ. Vc	=	209.19	kips	**Minimum shear reinforcement required as per ACI-11.5.6.1**	
	Effective depth = d = Dc/2+Dr/π	=	45.85	in.		
	Maximum permissible spacing for the chosen bar no. of ties, s(max) = d/2	=	**22.92**	in.		ACI-11.5.5.1
	Spacing provided	=	**5.00**	in.	**OK < Max. Permissible spacing**	
	Total shear strength with the provided spirals ϕ. Vs = ϕ. Asp.fy.d/s	=	**126.59**	kips		
	ϕ. Vc + ϕ. Vs	=	544.97	kips	**OK > Vu**	

CONVENTIONAL DESIGN OF SINGLE PIER						
						REFERENCES
I	**INPUT DATA**				**INPUT PARAMETERS**	
					IMPORTANT VALUES	
	Compressive strength of concrete, fc'	=	**6**	ksi		
	Yield Strength of reinforcement,fy	=	60	ksi		
	Clear cover to ties	=	**1.5**	in		
	Cover to longitudinal bars	=	2.125	in		
	Span of the bridge	=	**140.00**	ft.		
	UnFactored axial load of column, Pu	=	**1341.37**	kips		
	Factored Live load intensity	=	**1.26**	kip/ft		
	Unfactored single load-live load intensity		**0.95**	kip/ft		
	Unfactored train of vehicles-live load intensity	=	**1.59**	kip/ft		
	Max. Axial load on column due to live load on each pier	=	**222.60**	kips		
	Height of pier columns,L	=	16	ft		
	Seismic parameters					
	Site Coefficient, S	=	**1**		(Soil Profile Type-II)	AASHTO-Table-3.10.5.1-1
	Peak ground accelaration(PGA),A	=	**0.6**			
	Response Reduction/Modification Factor, R	=	**3**		(For single Columns)	AASHTO-Table-3.10.7.1
	Accelaration due to gravity,g	=	**32.17**	ft/sec^2		

CONVENTIONAL DESIGN OF SINGLE PIER						
	Type of Column		**SPIRAL**			
II	**DESIGN CALCULATIONS**					
(A)	**SIZING OF THE PIER**					
	Gross cross sectional area of the column , Ag(trial) ≥ Pu / (0.1 x fc')	>	**2235.62**	sq.in		ACI 21.4
	Diameter of column , D	=	**5**	ft		
	Gross area of section provided, Ag	=	**2827.43**	sq in	**SECTION OK**	
(B)	**DESIGN OF LONGITUDINAL REINFORCEMENT**					
	Computation of Base Shear					
	Modulus of Elasticity,E = 57000.√fc'/1000	=	4415.20	ksi		
	Moment of Inertia of Column, Ic	=	636172.5	in^4		
	EI eff = 0.25EIc	=	7.02E+08	$kip\text{-}in^2$		
	Stiffness of Cantilever bridge pier,k = $3EIc/L^3$	=	297.63			
	Time Period, T = 2π.√(w/(g.k))	=	**0.68**	secs		
	Base Shear Coefficient, Cd = SA/RT	=	0.29			
	Base Shear on column, V = Cd x W	=	**395.17**	kips		

CONVENTIONAL DESIGN OF SINGLE PIER						
	Check for Effects of Slenderness					
	Unsupported length of the compression member , L	=	16.00	ft		
	Radius of Gyration, r = 0.25 D	=	1.25	ft		
	Effective Length factor , k	=	**2.1**		(Cantilever Column)	
	Slenderness Ratio, KL/r	=	**26.88**		Slender column,slenderness effect needs to be considered.	
	Modulus of Elasticity of concrete, Ec = 57000. √fc'	=	4.42E+03	ksi		ACI-8.5.1, S5.4.2.4
	Moment of Inertia of gross concrete section about the centroidal axis, Ig = $\pi.r^4/4$	=	6.36E+05	in^4		
	Ratio of factored dead load to the total factored axial load,βd	=	**0.86**			
	Column Flexural Stiffness is greater of :					
(a)	EI = [0.2 Ec.Ig + Es.Is]/(1+βd)	=	3.02E+08	$kip\text{-}in^2$		ACI-EQ.-10-11, AASHTO-S5.7.4.3-1
(b)	EI = [0.4 Ec.Ig]/(1+βd)	=	6.04E+08	$kip\text{-}in^2$		ACI-EQ.-10-12, AASHTO-

						S5.7.4.3-2
	Hence Column Flexural Stiffness	=	6.04E+08	kip-in^2		
	Computation of Moment Magnification					
	Unfactored Axial load for critical case, P	=	1341.37	kips		
	Euler Critical Buckling Load, Pc = π^2.EI/(KL)^2	=	36669.9 7	kips		
	ϕ	=	**0.75**			ACI 10-12,AASHTO-S5.5.4.2
	Parameter of the effect of moment curvature, Cm	=	**1**		For members not braced for sidesway	S4.5.3.2.2b-3
	Moment magnification factor, δ = Cm / (1 - (Pu/ϕ.Pc))	=	**1.051**			ACI 10-9, AASHTO S4.5.3.2.2b-3
	P' = δ x P	=	**1410.15**	kips		
	M' = δ x M	=	**79762.6** **6**	kip-in		
	Using Interaction diagrams,					
	g	=	0.888			
	e=M/P	=	56.6	in.		
	e/h	=	**0.94**			

CONVENTIONAL DESIGN OF SINGLE PIER					
	Pn/fc'.Ag	=	**0.083**		
	Mn/fc'.Ag.h	=	**0.078**		
	Ratio of the distance between the centers of the outside layers of bars to the overall depth of the column, γ	=	**0.89**		
	ρt computed from interaction charts	=	**0.01**		
	Required area of steel, Ast(req) = ρt .Ag	=	**28.27**	sq.in	
	Required no. of bars	=	**22.32**		**Provide 32 No. 10 bars**
	Bar size designation no. to be used	=	**10**		
	Dia. of bars	=	1.270	in	
	No. of bars Provided	=	**32**		**OK**
	Area of Steel Provided, Ast(prov)	=	40.54	sq in	**OK**
	Center to center spacing between bars	=	**6.1**	in.	
	Percentage of steel provided,ρt	=	**1.43**	%	
	Check for limits of reinforcement in compression memebers as per AASHTO-S.5.7.4.2				**AASHTO-S.5.7.4.2**
	Maximum area of non prestressed longitudinal reinforcement for non-composite compression componenets shall be :				
	As/Ag <0.08				S.5.7.4.2-1
	Provided As/Ag	=	**0.01**		**OK**

CONVENTIONAL DESIGN OF SINGLE PIER					
	Minimum area of nonprestressed longitudinal reinforcement for non composite compression components shall be:				
	As.fy/Ag.fc' > = 0.135	=	**0.143**		**OK**
	Check for maximum axial load and moment capacity of the section				
	Strength reduction factor,ϕ	=	**0.7**		**(For Spiral Columns)**
	Axial load capacity for spiral columns, ϕ.Pn = 0.85. ϕ [(0.85 fc')(Ag- Ast)+fy(Ast)]	=	**9903.99**	kips	
	Factored axial load on column , 1.25D + 1.75 L	=	**2152.24**	kips	**OK**
	Moment on column, (1.25 times)	=	**99703.33**	kip-in	
	Check for provided reinforcement for factored load				
	ϕ.Pn/Ag.f'c	=	**0.13**		
	ϕ.Mn/Ag.h.f'c	=	**0.10**		
	Required percentage of Steel	=	**1.4**		
	Provided % of steel	=	**1.43**	%	**ok**

ACI Eq. 10-1
ACI 10.3.6.1,10.3.6.2
AASHTO TABLE-3.4.1,2

CONVENTIONAL DESIGN OF SINGLE PIER					
	Check for Stresses				
	Total axial load on column, Dead+live,Pt	=	**1632.75**	kips	
	Section Modulus, Sx= $\pi D^3/32$	=	**21205.7 5**	in^3	
	Stress due to axial load, Pt/A	=	0.58	ksi	
	Stress due to moment, M/Sx	=	3.76	ksi	
	Total final stress in the section,Pt/A+ M/Sx	=	**4.34**	ksi	
	Maximum compressive stress, fcu =0.85 fc'	=	**5.1**	ksi	
	DESIGN OF SHEAR REINFORCEMENT				
I	**PLASTIC HINGE ZONE CONFINEMENT**				
	Diameter of core outside to outside of spirals, Dc	=	**57.0**	in.	
	Area of Core, Ach = $\pi.Dc^2/4$	=	2551.8	sq.in	
(1)	ρs = 0.45 [(Ag/Ach)-1]fc'/fy	=	0.0049		ACI-10.9.3-Eqn. 10-5
(2)	ρs = 0.12 fc'/fy (in region of plastic hinges)	=	0.012		ACI-21.4.4.1(a)

CONVENTIONAL DESIGN OF SINGLE PIER						
	Provide spiral reinforcement volumetric ratio, ρs (max)	=	**0.012**			AASHTO-5.10.11.4.1d
	Required spacing of spirals= 4.Asp/(ρs.Dc)	=	1.79	in.		
	Maximum spacing in confinement zone :-					
	Spacing is not greater than the following:-					
(1)	1/4 th minimum member dimension	=	15.0	in.		
(2)	4 in.	=	4.0	in.		
	Hence maximum spacing in confining zone	=	**4.00**	in.		
	Spacing of spirals provided,S	=	**3**			
	Bar size designation no. to be used	=	**5**			
	Dia. of bars	=	0.625	in		
	Area of spiral reinforcement of bar	=	0.31	in^2		
	ρs, provided = 4.Asp/(S.Dc)	=	**0.007**			
	Spiral reinforcement requirements as per ACI-7.10					
			0.00486			
	Volume of spiral reinf	=	1			ACI 7.10.4.2
	Minimum Diameter of spiral to be used	=	**0.625**	in.		ACI 7.10.4.2
	Maximum c/c pitch spacing of spirals, $s = \pi.Dsp^2.fy/(0.45Dc.fc'[(Ag/Ac)-1])$	=	4.43	in.		ACI 7.10.4.3
	Maximum clear spacing between spirals	=	**3.00**	in.	**(Detailing requirements)**	ACI 7.10.4.3
	Hence maximum pitch between spirals as per ACI	=	3.625	in.		

CONVENTIONAL DESIGN OF SINGLE PIER					
	Minimum spacing of spirals	=	**1**	in.	ACI 7.10.4.3
	Provided spacing	=	**3**	in.	
	Area of spiral reinforcement provided, Asp(prov)	=			
	Use No. 5 at 3 in. c/c spacing				
	Provided Pitch	=	**3.6**	in.	
II	**LENGTH OF CONFINEMENT ZONE**				
	Length of confining zone adjacent to each end of column:-				ACI-21.4.4.4
	Largest of :				
	1 . dia. Of column	=	72	in.	
	2. one-sixth of clear ht of column	=	32	in.	
	3. 18 inch	=	18	in.	
	Length of confining zone adjacent to each end of column,l_0	=	**72**	in.	
		=	**6**	ft.	
III	**SHEAR CAPACITY IN PLASTIC HINGE ZONE**				
	Shear force on column	=	395.17	kips	
	Factor for shear force	=	**1.25**	kips	

CONVENTIONAL DESIGN OF SINGLE PIER					
	Factored Shear force on column, Vu	=	493.96	kips	
	Shear strength provided by concrete for non prestressed members subjected to axial compression, $Vc = 2[1+ Nu/2000Ag].\sqrt{fc'}.b_w.d$	=	557.922	kips	ACI-11.3.1.2
	ϕ	=	**0.75**		
	ϕ. Vc	=	418.44	kips	**Shear reinforcement must be provided to carry excess shear**
	0.5 x ϕ. Vc	=	209.22	kips	**Minimum shear reinforcement required as per ACI-11.5.6.1**
	Effective depth = d = Dc/2+Dr/π	=	45.84	in.	
	Maximum permissible spacing for the chosen bar no. of ties, s(max) = d/2	=	**22.92**	in.	ACI-11.5.5.1
	Spacing provided	=	**3.00**	in.	**OK < Max. Permissible spacing**
	Total shear strength with the provided spirals ϕ. Vs = ϕ. Av.fy.d/s	=	**210.96**	kips	
	ϕ. Vc + ϕ. Vs	=	629.40	kips	**OK > Vu**
	<u>REINFORCEMENT OTHER THAN CONFINING ZONE</u>				

CONVENTIONAL DESIGN OF SINGLE PIER					
	Maximum Spacing of spirals is the minimum of:				ACI-21.4.4.2
(1)	0.25 xD	=	15	in.	
(2)	6 x dia. of longitudinal bar	=	7.62	in.	ACI 21.4.4.6
(3)	So = 4 + (14-hx)/3	=	4.00	in.	ACI 21.4.2.2-Eqn. 21.5
(4)	Clear cover to longitudinal bars	=	3	in.	
(5)	6 in.	=	6	in.	
	Required maximum spacing of spirals	=	**3.0**	in.	
(1)	6 x dia. of longitudinal bar	=	**7.62**	in.	ACI 21.4.4.6
(2)	6 in.	=	**6.0**	in.	ACI 21.4.4.6
	Required maximum spacing of spirals	**=**	**6.0**	**in.**	
III	**SHEAR CAPACITY IN NON-PLASTIC ZONE**				
	Shear force on column	=	395.17	kips	
	Factor for shear force	=	**1.25**	kips	
	Factored Shear force on column, Vu	=	493.96	kips	
	Shear strength provided by concrete for non prestressed members subjected to axial compression, $Vc = 2[1+ Nu/2000Ag].\sqrt{fc'}.b_w.d$	=	557.922	kips	ACI-11.3.1.2
	ϕ	=	**0.75**		

CONVENTIONAL DESIGN OF SINGLE PIER						
	ϕ. Vc	=	418.44	kips	**Shear reinforcement must be provided to carry excess shear**	
	0.5 x ϕ. Vc	=	209.22	kips	**Minimum shear reinforcement required as per ACI-11.5.6.1**	
	Effective depth = d = Dc/2+Dr/π	=	45.84	in.		
	Maximum permissible spacing for the chosen bar no. of ties, s(max) = d/2	=	**22.92**	in.		ACI-11.5.5.1
	Spacing provided	=	**5.00**	in.	**OK < Max. Permissible spacing**	
	Total shear strength with the provided spirals ϕ. Vs = ϕ. Av.fy.d/s	=	**126.58**	kips		
	ϕ. Vc + ϕ. Vs	=	545.02	kips	**OK > Vu**	

VITA

Name:	Anagha Sureshkumar Parkar
Address:	Texas A&M University
	Zachry Department of Civil Engineering
	3136 TAMU
	College Station, Texas 77843-3136
	USA
Email Address:	anaghaparkar@yahoo.com

Education: B.E., Civil Engineering, Mumbai University, 2006

M.S., Civil Engineering, Texas A&M University, 2011